TECHNICAL REPORT

UXO Characterization in Challenging Survey Environments Using the MPV
Former Camp George West, Colorado

MR-201228

OCTOBER 2013

This document has been cleared for public release

ESTCP

REPORT DOCUMENTATION PAGE

Form Approved
OMB No. 0704-0188

The public reporting burden for this collection of information is estimated to average 1 hour per response, including the time for reviewing instructions, searching existing data sources, gathering and maintaining the data needed, and completing and reviewing the collection of information. Send comments regarding this burden estimate or any other aspect of this collection of information, including suggestions for reducing the burden, to the Department of Defense, Executive Services and Communications Directorate (0704-0188). Respondents should be aware that notwithstanding any other provision of law, no person shall be subject to any penalty for failing to comply with a collection of information if it does not display a currently valid OMB control number.
PLEASE DO NOT RETURN YOUR FORM TO THE ABOVE ORGANIZATION.

1. REPORT DATE *(DD-MM-YYYY)*	2. REPORT TYPE	3. DATES COVERED *(From - To)*
10-10-2013	Technical Report	October 2012-September 2013

4. TITLE AND SUBTITLE
Demonstration report for the MPV study at former Camp George West, Colorado.
ESTCP MR-201158: Man-Portable Vector (MPV) EMI Sensor for UXO Contamination Assessment at Munitions Sites.

5a. CONTRACT NUMBER
W912HQ-12-C-0076

5b. GRANT NUMBER

5c. PROGRAM ELEMENT NUMBER

6. AUTHOR(S)
Nicolas Lhomme, Kevin Kingdon and Laurens Beran.
Black Tusk Geophysics, Inc.

5d. PROJECT NUMBER

5e. TASK NUMBER

5f. WORK UNIT NUMBER

7. PERFORMING ORGANIZATION NAME(S) AND ADDRESS(ES)
Black Tusk Geophysics, Inc.
401-1755 West Broadway
Vancouver, BC, V6J 4S5 Canada

8. PERFORMING ORGANIZATION REPORT NUMBER

9. SPONSORING/MONITORING AGENCY NAME(S) AND ADDRESS(ES)
Environmental Security Technology Certification Program
4800 Mark Center Drive, Suite 17D08
Alexandria, VA 22350-3605

10. SPONSOR/MONITOR'S ACRONYM(S)

11. SPONSOR/MONITOR'S REPORT NUMBER(S)

12. DISTRIBUTION/AVAILABILITY STATEMENT
Approved for public release; distribution is unlimited

13. SUPPLEMENTARY NOTES

14. ABSTRACT

This report documents the ESTCP live-site demonstration conducted with the Man-Portable Vector (MPV) sensor at former Camp George West in October 2012. The MPV technology was deployed on the side hills of Green Mountain near Denver, Colorado. The objective was to map metallic contamination and identify 75 mm projectiles up to a maximum burial depth of two feet, relying solely on the MPV technology. The site required a portable system due to steep slope and a rough surface with boulders, ruts and cacti. The survey consisted of a detection sweep to cover the two-acre area of interest, followed with cued interrogation of 500 detected anomalies. Classification was independently applied to the dynamic and cued data. The site conditions, large target size and high-quality data allowed for all 75 mm projectiles to be recovered while rejecting most of clutter with both dynamic and cued data. These results suggest that the MPV could be used for full-site characterization and that, under favorable conditions, dynamic data could be sufficient to classify some of the field anomalies without need for cued interrogations, potentially reducing costs.

15. SUBJECT TERMS
Man Portable Vector Sensor, Electromagnetic Induction Sensor, UXO, George West, Live-Site Demonstration, Classification, Geophysical Inversion, steep terrain

16. SECURITY CLASSIFICATION OF:			17. LIMITATION OF ABSTRACT	18. NUMBER OF PAGES	19a. NAME OF RESPONSIBLE PERSON
a. REPORT	b. ABSTRACT	c. THIS PAGE			Dr. Herb Nelson
UU	UU	Uu	UU	74	19b. TELEPHONE NUMBER *(Include area code)* 571-372-6400

Table of Contents

List of Figures iii
List of Tables iv
Acronyms v
EXECUTIVE SUMMARY vii
1.0 INTRODUCTION 1
2.0 TECHNOLOGY 2
2.1 MPV TECHNOLOGY DESCRIPTION 2
2.2 MPV TECHNOLOGY DEVELOPMENT 4
2.3 ADVANTAGES AND LIMITATIONS OF THE MPV TECHNOLOGY 4
3.0 PERFORMANCE OBJECTIVES 6
3.1 OBJECTIVE: SPATIAL COVERAGE FOR DETECTION 7
3.2 OBJECTIVE: REPEATABILITY OF INSTRUMENT VERIFICATION TESTS 7
3.3 OBJECTIVE: CUED INTERROGATION OF ANOMALIES 8
3.4 OBJECTIVE: DETECTION OF ALL TARGETS OF INTEREST 8
3.5 OBJECTIVE: PRODUCTION RATE 8
3.6 OBJECTIVE: MAXIMIZE CORRECT CLASSIFICATION OF TOI 9
3.7 OBJECTIVE: MAXIMIZE CORRECT CLASSIFICATION OF NON-TOI 9
3.8 OBJECTIVE: SPECIFICATION OF NO-DIG THRESHOLD 10
3.9 OBJECTIVE: MINIMUM NUMBER OF UNCLASSIFIABLE ANOMALIES 10
3.10 OBJECTIVE: CORRECT ESTIMATION OF LOCATION AND DEPTH 11
4.0 SITE DESCRIPTION 12
4.1 SITE SELECTION 12
4.2 BRIEF SITE HISTORY 13
4.3 MUNITIONS CONTAMINATION 13
4.4 SITE CONFIGURATION 13
5.0 TEST DESIGN 15
5.1 DEMONSTRATION SCHEDULE 15
5.2 SYSTEM SPECIFICATION 16
5.3 CALIBRATION ACTIVITIES 16
5.4 DATA COLLECTION PROCEDURES 17
6.0 DATA ANALYSIS 21
6.1 PREPROCESSING 21
6.2 TARGET SELECTION FOR DETECTION 21
6.3 PARAMETER ESTIMATION 23

6.4 TRAINING 24
6.5 CLASSIFICATION 24
7.0 PERFORMANCE ASSESSMENT 26
7.1 Repeatability on Instrument Verification Strip 26
7.2 Acquisition of cued anomalies 27
7.3 Detection of all targets of interest 28
7.4 False detections 29
7.5 Classification with dynamic data 32
7.6 Classification with static data 34
7.7 Estimation of target location and depth 34
7.8 Production rate 36
8.0 COST ASSESSMENT 37
8.1 COST MODEL 37
8.2 COST DRIVERS 39
8.3 COST BENEFIT 39
9.0 MANAGEMENT AND STAFFING 40
10.0 REFERENCES 41
APPENDICES 42
Appendix A: Health and Safety Plan (HASP) 42
Appendix B: Points of Contact 44
Appendix C: Detection range with MPV survey 45
Appendix D: Classification memorandum for dynamic data 50
Appendix E: Classification with cued interrogation data 58

List of Figures

Figure 4: MPV detection survey at George West near ravine (West side boundary). 1
Figure 1: The MPV as deployed at Camp George West, CO in October 2012. 2
Figure 2: Aerial photograph of the demonstration site. 12
Figure 3: False color image of the anomaly density interpolated from the EM61 transect surveys over the ten-acre initial area and the two-acre area chosen for the Classification demonstration (red color suggests higher target density than green background level). 13
Figure 5: Cued interrogation of anomalies on the side of Green Mountain. 14
Figure 6: Station spacing in detection survey (spacing<0.1 m for 66% points and <0.15 m for 94%). 18
Figure 7: Detection survey across (A) and along (B) slope. 18
Figure 8: Cued survey pattern with five points centered on expected target location. 19
Figure 9: Typical target response when the MPV head is placed directly above a buried target. 20
Figure 10: Detection map using the Z-component on all receiver cubes with the 0.5 ms time channel. 22
Figure 11: Target detection analytic process based on simulation and site-specific data. 23
Figure 12: Format of prioritized anomaly list to be submitted to ESTCP Program Office. 25
Figure 13: Detection on IVS lane for Z-component data at 0.5 ms. 26
Figure 14: Detection on IVS lane for X-component (A) and Y-component (B) data. 26
Figure 15: Polarizabilities on IVS lane for cued (A,C, E) and dynamic data (B,D, F). 27
Figure 16: Positional accuracy of cued acquisition of field anomalies. 28
Figure 17: Detection and cued data around close targets GW-2032 and GW-12032. 29
Figure 18: Detection map for zone 6, where many false alarms occurred along the hiking path (NNW to S). 30
Figure 19: Location and size of excavated items in zone 6 of George West. Most of the empty holes (cross markers) are concentrated along the hiking path that crosses in the NNW to S direction in the W part. 31
Figure 20: Noisy late-time data can cause false detections (GW-6117). 31
Figure 21: ROC curve for dynamic data analysis. 32
Figure 22: Gridded Y-component data reveals GW-3274 target and secondary GW-13274 at 0.4 m to SE. 33
Figure 23: Polarizabilities for GW-3274 (left) and GW-13274 (right) as predicted by multi-target inversion. 33
Figure 24: Predictability of target location and depth with cued data. 34
Figure 25: Target location for detection, cued and dynamic inversion and validation. 35
Figure 26: Graphical summary of the daily data-collection activities and production rate. 36
Figure 27: Project management hierarchy for Camp George West demonstration. 40
Figure 28: Location of medical facilities: St. Anthony Hospital in Lakewood, CO. 43
Figure 29: SNR cross section map for different target offset and depth relative to MPV receiver. 45
Figure 30: SNR contour lines for 37 mm target in vertical orientation. 46
Figure 31: Detection contour for 105 mm projectile in horizontal (A) and vertical (B) position. 46
Figure 32: Detection contour in quiet background for 105mm (A) and 37 mm (B) in horizontal position. Depth of investigation is increased. 46
Figure 33: Predicted total response for 37 mm (A) and 75 mm (B) projectiles placed in horizontal position. Here the total response is the sum of the signal amplitude on all receivers at 1.4 ms... 47

Figure 34: Surface anomaly for a dynamic survey above a 75 mm target at 0.7 m depth in vertical position..... 47
Figure 35: Variability of background response using sensor total response (A) or maximum total field (B)..... 48
Figure 36: Signal amplitude as a function of depth for a 75 mm projectile in horizontal orientation. 49
Figure 37: Distribution of target size and decay parameters relative to reference UXOs. 50
Figure 38: Decision statistic based on "recognized UXO" (red dots). 53
Figure 39: Classification of target GW-1. The first two polarizability curves L1-L2 match with medium ISO. 54
Figure 40: Full inversion QC display for Target GW-1 54
Figure 41: Target GW-4038 would relate to a 75 mm projectile according to the L1 and L2 parameters 55
Figure 42: Target GW-6123 does fit a 75 mm projectile using the L1 and L2 parameters. 55
Figure 43: Inversion and classification parameters for target GW-6121. 56
Figure 44: Model parameters for GW-6121. 56
Figure 45: Decision statistic for dynamic stage 2. 57
Figure 46: Cued data classification - Training data requests for potential 75mm projectiles. 59
Figure 47: Cued data classification - Training data requests for potential medium ISOs. 60
Figure 48: Cued data classification - Training data requests for potential 60mm mortar. 61
Figure 49: Training data requests for an unknown cluster. 62
Figure 50: Analysis of training data requests revealed two partial 75mm TOI. 63
Figure 51: Polarizability decay curves in ranked dig list for digs 50-98. 64
Figure 52: Partial (A) and final (B) ROC curve for classification with cued data. 65

List of Tables

Table 1: Performance Objectives. 6
Table 2: Demonstration steps. 15
Table 3: Cost model for MPV demonstration at Camp George West. 37
Table 4: Points of Contact for the MPV Demonstration. 44
Table 5: Training data request. 51
Table 6: Targets included in the initial reference library. 58

Acronyms

BUD	Berkeley UXO Discriminator
CFR	Code of Federal Regulations
cm	Centimeter
CO	Colorado
CGW	Camp George West
CRREL	Cold Regions Research and Engineering Laboratory (ERDC)
DAQ	Data Acquisition System
DGM	Digital Geophysical Mapping
EMI	Electromagnetic Induction
ERDC	Engineering Research and Development Center
ESTCP	Environmental Security Technology Certification Program
FAR	False Alarm Rate
GPS	Global Positioning System
GW	George West
IDA	Institute for Defense Analyses
IVS	Instrument Verification Strip
ISO	Industry Standard Objects
ISO2	Small Industry Standard Objects (second generation)
ISOmed	Medium Size Industry Standard Objects
m	Meter
mm	Millimeter
MPV	Man Portable Vector
ms	millisecond
MR	Munitions Response
NH	New Hampshire
PI	Principal Investigator
POC	Points of Contact
ROC	Receiver-Operator Characteristic
RTK	Real-time Kinematic
s	Second
SERDP	Strategic Environmental Research and Development Program
SNR	Signal to Noise Ratio
SR	Spencer Range
SVM	Support Vector Machine
TEMTADS	Time Domain Electromagnetic Towed Array Detection System
UXO	Unexploded Ordnance
YPG	Yuma Proving Ground

ACKNOWLEDGEMENTS

The MPV demonstration at former Camp George West was funded by the Environmental Security Technology Certification Program, project MR-201158. Initial development and testing of the MPV technology was done by Kevin O'Neil and Benjamin Barrowes from the Engineering Research and Development Center (ERDC) at the Cold Regions Research and Engineering Laboratory (CRREL) in Dartmouth, New Hampshire and with David George of G&G Sciences, and supported by the Strategic Environmental Research and Development Program (SERDP) project MM-1443. The George West study was conducted with the second-generation MPV, a lighter and ruggedized sensor that was also fabricated by D. George as part of the ESTCP project MR-201005 (PI Nicolas Lhomme). This study is the fourth field deployment of the MPV technology.

The field deployment involved Jon Jacobson, Kevin Kingdon, Tom Ladd and the PI Lhomme (all with Sky Research at the time; Kingdon and Lhomme are now with Black Tusk Geophysics, Inc.). Most of the data analysis was performed by Lhomme, with Jacobson assisting in reviewing inversion results for the cued interrogation data set and Kingdon applying classification to cued data. Data processing and analysis was mostly accomplished with the UXOLab software package, a suite of MatLab-based programs for digital geophysical mapping, target picking, inversion of single and multiple sources and classification. The software has been jointly developed with the University of British Columbia and funded under ERDC, SERDP and ESTCP projects. Most of this report was written by Lhomme, with contributions from Kingdon for the cued data classification report and review by Laurens Beran.

EXECUTIVE SUMMARY

This report documents data collection and analysis for the ESTCP live-site demonstration conducted with the Man-Portable Vector (MPV) sensor at former Camp George West in October 2012. The MPV technology was deployed on the side hills of Green Mountain, adjacent to a residential area near Denver, Colorado. The goal of this study was to map metallic contamination and identify 75 mm projectiles up to a maximum burial depth of two feet.

The MPV is an electromagnetic induction (EMI) sensor designed for munitions detection and classification. Its handheld form factor provides enhanced portability and ruggedness relative to vehicular-based systems. The sensor head is a 50-centimeter diameter disk that includes a vertical transmitter and an array of five three-component receivers. The MPV can be utilized for detection mapping and subsequent classification of detected anomalies. Anomalies can also be reacquired in a stationary, cued mode to maximize data quality for classification. The MPV uses standard GPS technology for positioning in open field areas. Under thick canopy GPS can no longer provide the necessary accuracy. A dedicated positioning system was therefore developed for local positioning. The system locates the center of the MPV by measuring the transmitted electromagnetic fields with a pair of stationary external receivers. The beacon method has been proved to be sufficiently accurate for classification.

This study is the fourth demonstration of the MPV with the ESTCP. The technology was first validated at the Army Yuma Proving Ground UXO Standardized Test Site in Arizona in October 2010, where detection and classification were tested. It was subsequently demonstrated in live site conditions in open field and trees at the former Camp Beale, California in June 2011 and at Spencer Range, Tennessee in June 2012. Targets of interest were correctly classified in 100% and 99%, respectively, while rejecting over 80% of the clutter. The Spencer study also included collection of dynamic data in open field for a detection and classification study.

The George West demonstration relied solely on the MPV technology. The sensor was first deployed in a detection sweep to cover the two-acre area of interest. The site required a portable system due to steep slope and a rough surface with boulders, ruts and cacti. Potential targets were selected from a detection map at a detection threshold that was derived by simulating the worst case scenarios for detection and validating with test pit measurements. Approximately 500 anomalies were retained for cued, static interrogation. The field deployment was completed after three days of detection surveying and four days of cued interrogation. Two field personnel were required to operate and carry the sensor, with one additional person laying out survey lines, and one data processor for quality control. Classification was independently applied to the dynamic and cued data. The site conditions, large target size and high quality data allowed for all 75 mm projectiles to be recovered while rejecting most of the clutter with both dynamic and cued data (one target was missed in the dynamic data set due to mislabeling). These results suggest that the MPV could be used for full-site characterization and that, under favorable conditions, dynamic data could be sufficient to classify some of the field anomalies without need for cued interrogations, thereby potentially reducing data collection and analysis costs.

The MPV has now been successfully demonstrated for data collection, detection and classification in mountainous terrain, moderately dense forest and flat open field. The next sites could test denser vegetation, smaller target size, magnetic soils or rougher surface conditions. The MPV is scheduled for further testing in 2013 as part of the ESTCP ongoing live-site demonstration program.

1.0 INTRODUCTION

The demonstration at Camp George West (CGW) is one in the series of the Environmental Security Technology Certification Program (ESTCP) demonstrations of classification technologies for Munitions Response (MR). This particular project proposes to demonstrate detection and classification at a site where steep terrain, vegetation and boulders preclude access by wheel-based sensor platforms (Figure 1). The study was entirely based on a remediation survey with the Man Portable Vector (MPV), a handheld electromagnetic induction (EMI) sensor with detection and classification capabilities. The MPV technology was used first to survey the entire site in full coverage mode to map the metallic contamination at the site. Detected anomalies were then reacquired for further characterization with high quality data. Detection and classification algorithms were applied to guide site remediation.

Figure 1: MPV detection survey at George West near ravine (West side boundary).

2.0 TECHNOLOGY

The MPV technology is based on electromagnetic induction sensing using one transmitter coil and multiple vector receivers in a handheld form factor. The sensor presented in this study is the second-generation prototype MPV.

2.1 MPV TECHNOLOGY DESCRIPTION

2.1.1 Electromagnetic sensor

The MPV is a handheld wide-band, time-domain, EMI sensor. The sensor head is composed of a single transmitter coil and an array of five receiver units that measure all three components of the EM field (Figure 2). This second-generation MPV is specifically designed to (1) be man portable and therefore easy to deploy, maneuver and adapt to a survey environment, and (2) acquire data that is suitable for discriminating unexploded ordnance (UXO) from non-UXO targets. The MPV head is a 50-centimeter (cm) diameter transparent disk. The transmitter coil is wound around the disk and intermittently illuminates the subsurface. Five receiver units (cubes) measure the three orthogonal components of the transient secondary EM field decay with three air-induction 8-cm square coils. Having multiple receivers generally improves the recovery of target parameters for classification (Gasperikova et al., 2007).

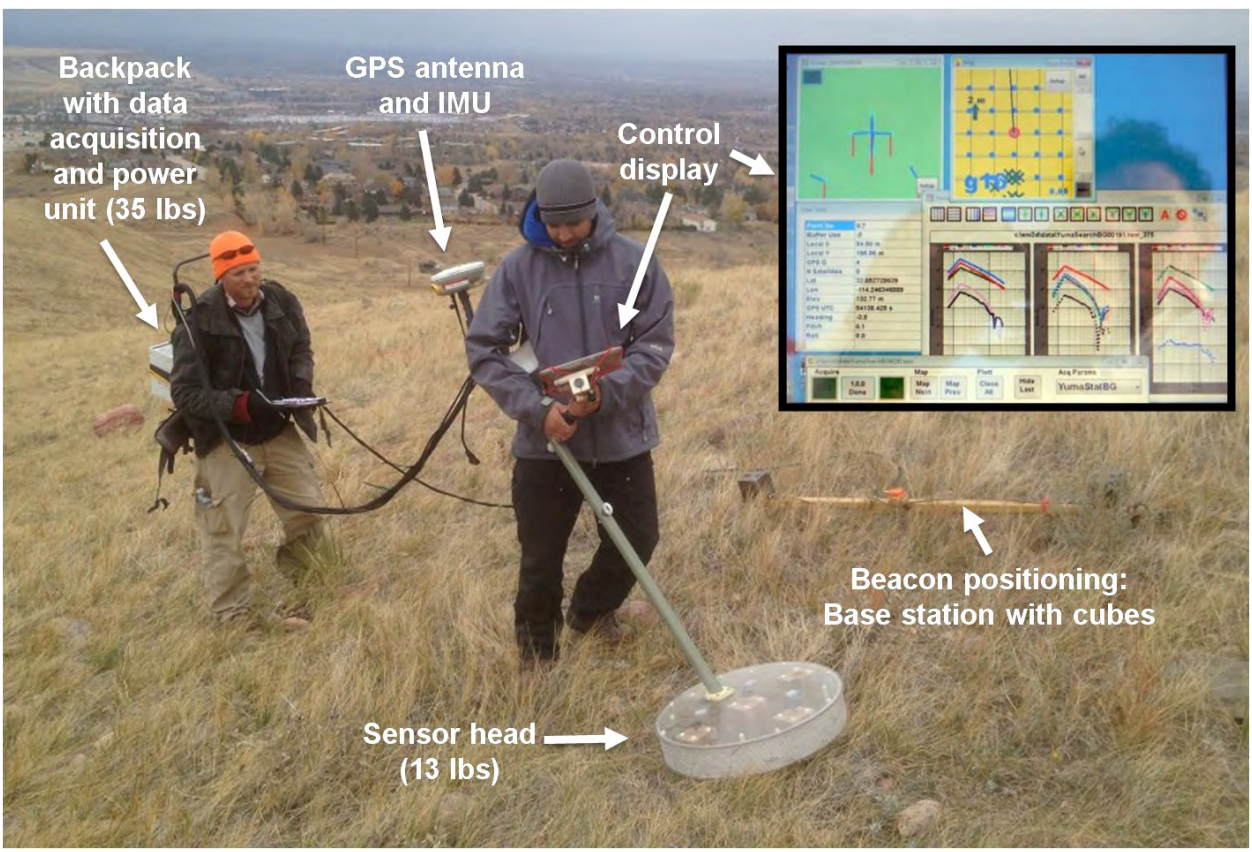

Figure 2: The MPV as deployed at Camp George West, CO in October 2012.
The sensor head is made of a transparent disk that contains a circular transmitter wound around the side and five 3D receiver cubes. A touch-screen display controls survey parameters and acquisition events (right inset). The data acquisition system and batteries are mounted on a backpack frame caried by the second operator. Positioning can be achieved with GPS (only in open field) or a beacon boom (cued interrogation).

The MPV is a programmable instrument. The duration of the excitation and time decay recording can be adjusted to accommodate the specific needs of target detection and classification. The detection survey consists of a full-coverage sweep where dynamic data are collected for digital geophysical mapping (DGM). Fast EMI transmit-receive cycles are applied so that the sensor can continuously move (e.g., 1 millisecond [ms] time decay, similar to the Geonics EM-61). The quality of detection data may not always be sufficient for target classification. In such case a target is reacquired in cued interrogation, where data quality is maximized. The sensor is stationary and the recorded signal is stacked to reduce noise. Longer EMI cycles are applied to fully characterize target time decay rates (e.g., 25 milliseconds (ms), similar to Geonics EM-63). This late-time information has been shown to improve distinction between intact ordnance and thinner walled shrapnel and cultural debris (Billings et al., 2007).

The MPV is a handheld sensor. The sensor head weighs 13 pounds and the backpack-mounted data acquisition (DAQ) weighs approximately 35 pounds. Existing sensors with multiple time channel measurement capabilities (e.g., Berkeley UXO Discriminator [BUD], Geonics EM63, Time Domain EM Towed Array Detection System [TEMTADS]) are required to be mounted on a cart platform due to the size and weight of the multiple coils of wire required for the transmitters and receivers.

The MPV user interface has real-time data monitoring capabilities. The recorded data can be displayed to verify data quality and detect potential disturbances caused by the presence of magnetic soil or a damaged receiver. The past and present sensor location is displayed on a map along with preset survey points to verify spatial coverage and global location. A target detection and location tool indicates the origin of measured EMI fields with arrows (the so-called “dancing arrows” in the top left corner of control display, Figure 2 inset). These features assist the field operator in efficient data collection, so that detection and discrimination data can be collected in a single survey, thus limiting the need to revisit an anomaly for further characterization.

2.1.1 Geolocation

The sensor requires positioning for detection and classification, though with different spatial accuracy requirements. Therefore a field survey with the MPV can utilize two complementary positioning systems. Detection mapping has decimeter accuracy requirements and can be performed with a GPS or a spool-mounted cotton thread and optical encoder. Classification is based on geophysical inversion of multiple soundings and generally requires centimeter-level sensor positioning when surveying a target (Bell, 2005). Designed to extend UXO classification to difficult survey environments, the MPV technology is augmented with a local positioning system that remains accurate in steep terrain and under thick tree canopy, where GPS cannot guarantee high accuracy. The beacon positioning system (San Filippo et al., 2007; Lhomme et al., 2011) locates the origin of the MPV transmitter with a pair of EMI receivers rigidly attached to a portable beam that serves as a base station (Figure 2). The horizontal and vertical location of the center of the MPV head and its roll and pitch can be predicted from the beacon measurements. The heading is provided by a 3-axis attitude sensor (XSens MTi) that also records roll and pitch, which in turn can be compared with the predicted roll and pitch for quality control. Field trials showed 1-2 cm and 1-2 degrees accuracy for position and roll-pitch – similar to GPS and attitude sensors – out to distances of 3-4 meters (m) away from the beacon boom.

2.2 MPV TECHNOLOGY DEVELOPMENT

The project was initiated in 2005 under the Strategic Environmental Research and Development Program (SERDP) MM-1443. The project was led by Drs. Kevin O'Neill and Benjamin Barrowes with the Cold Regions Research and Engineering Laboratory of the Engineering Research and Development Center (CRREL, ERDC) in Dartmouth, New Hampshire (NH). The first MPV prototype was built in 2005-2006 with David George of G&G Sciences, Grand Junction, Colorado (CO). It was tested in 2007 at ERDC in a laboratory setting. Data analysis showed that stable target parameters could be retrieved and used for UXO classification.

The SERDP project was first extended in 2008 to continue testing. Field trials were done on a test plot to assess static and dynamic acquisition mode over buried targets. Stable target parameters were recovered. Effect of magnetic soil on EMI sensors was investigated. Adverse soil effects could be defeated owing to the MPV's array structure. The original positioning system – ArcSecond laser ranger – proved to be impractical for field application due to line-of-sight requirement for all three rovers and tedious calibration. The SERDP project was extended with BTG personnel involvement in 2009 to test an alternative positioning system based on the beacon concept and prepare modifications of the original MPV prototype for extensive field deployments. The sensor head was redesigned with lighter materials and a smaller head diameter to reduce weight and improve maneuverability while maintaining expected classification performance (Lhomme, 2011b). Receivers were brought inside the transmitter coil to reduce fragility; transparent material was employed to make the ground visible through the unit. Fabrication of the new head and replacement of the DAQ began under the SERDP funding extension.

Funding was obtained in 2010 under ESCTP MR-201005 to continue developing the MPV and conduct field demonstrations. The MPV fabrication was completed. The MPV was successfully demonstrated at YPG UXO test site in October 2010 and at former Camp Beale in June 2011. High detection and classification rates – comparable to existing EMI sensors designed for UXO classification – were achieved.

2.3 ADVANTAGES AND LIMITATIONS OF THE MPV TECHNOLOGY

The MPV is the only available handheld sensor that can acquire multi-static, multi-component data on a wide and programmable time range. The MPV offers several additional key benefits:

- Hand-held form factor: The MPV can be deployed at sites where terrain and vegetation preclude use of heavier, cart-based systems. Portability can improve productivity in rough terrain. The system is easy packable and transportable;
- Five receivers simultaneously record three orthogonal components of EM field with near-perfect relative positioning among receivers. Multi-component, multi-axis design reduces number of soundings for target characterization and relaxes positional accuracy (Grzegorczyk et al., 2009). Tests with low-noise test-stand MPV (first generation) data showed that UXO could be identified with as few as 5 soundings (Barrowes et al., 2007). This was confirmed at YPG and Camp Beale.
- Magnetic soil can be detected and defeated: The geometric arrangement of receivers and the wide-band time range offer potential for identifying and neutralizing the effect of magnetic soil through techniques developed in SERDP MM-1414 and MM-1573.

- Fully programmable through field display: Graphical field-user interface controls acquisition parameters such as transmitter waveform characteristics, duration of excitation, number of measurement cycles, stacking and recorded time channels.
- Highly stable EMI components: Responses are directly predictable using standard EMI theory. Field tests verified that MPV components had imperceptible measurement drift and were largely insensitive to survey conditions.
- Small target characterization: Small items have localized, rapidly-varying spatial response. Voltage in an air induction receiver coil is an average of a target scattered field through the face of the loop. Therefore, large receivers tend to "smear out" secondary fields. The MPV's 8 cm square coils are well suited for detecting and sampling signals from small targets.

Portability has limitations: with a single transmitter, multiple soundings must be collected to characterize a target. Therefore the MPV requires (1) an accurate positioning system for cued interrogation and (2) manual operation to move the sensor, which reduces productivity relative to a multi-transmitter platform for which a single sounding is often sufficient.

3.0 PERFORMANCE OBJECTIVES

This project includes data collection in dynamic detection and cued interrogation, data analysis and user feedback for evaluation of the MPV technology. The specific objectives for each stage are detailed in Table 1.

Table 1: Performance Objectives.

Performance Objective	Metric	Data Required	Success Criteria	Results
Data Collection Objectives				
Spatial coverage in detection survey	Extended footprint coverage	• Mapped survey data	98% coverage	99%
Repeatability of Instrument Verification Strip (IVS) survey	Amplitude of EM anomaly Amplitude of polarizabilities	• Twice-daily IVS survey data	Factor 3 on detection amplitude and target polarizability	Detection: Amplitude within factor 1.2 Cued: Size within factor 1.1
Cued interrogation of anomalies	Instrument position	• Cued data	100% of anomalies where center of cued pattern is located within 0.5 m of anomaly pick	100% of anomalies were correctly reacquired
Detection of all targets of interest (TOI)	Percent detected of seeded anomalies	• Location of seeded items • Anomaly list	100% of seeded items detected within 0.6 m halo	100% of seeds were detected
Production rate	Acreage and number of cued anomalies; Pre-processing time	• Log of field work and data pre-processing time	0.8 acre/day in survey mode 100 anomalies/ day in cued mode Pre-processing time <3 min per target	0.7 acre per day 135 anomalies 2.5 min processing
Analysis and Classification Objectives				
Maximize correct classification	Number of TOI retained	• Ranked dig list • Scoring reports by IDA	Approach correctly identifies the presence of 95% of TOI	Dynamic: 98% Static: 100%
Maximize correct classification of non TOI	False alarm rate (FAR)	• Ranked dig list • Scoring reports by IDA	Reduction of clutter digs by 75%	Dynamic: 85% Static: 92%
Specification of no-dig threshold	Probability of correct classification of TOI and FAR at operating point	• Demonstrator threshold • IDA score	Specified threshold to meet above criteria	Criteria based on decision statistic Success

Minimize number of unclassifiable anomalies	Number of "Can't Analyze" in classification	• Ranked dig list	Reliable classification parameters for at least 95% of dig list	100% of anomalies analyzed for dynamic and cued data
Correct location and depth of TOI	Accuracy of estimated target parameters for seed items	• Results of intrusive investigation • Predicted location	$\sigma Z < 0.10$ m σN and $\sigma E < 0.15$ m	$\sigma Z < 0.04$ m $\sigma N+\sigma E < 0.07$ m

3.1 OBJECTIVE: SPATIAL COVERAGE FOR DETECTION

Dynamic detection survey should cover a maximum of the area of interest so that all detectable targets are illuminated. Targets are detectable if the transmitted field is sufficiently strong to reach the target and if the measured target response is sufficiently strong in return to exceed a given threshold. Simulations suggest that there is negligible loss of detectability when a target is located 10 cm to the side of the MPV (Appendix C).

3.1.1 Metric

The survey footprint is compared with dynamic survey surface area. In practice the geographical coordinates of MPV receivers are binned in 20-cm square cells. The ratio of the number of non-empty cells and the number of cells in survey area provides the rate of coverage.

3.1.2 Data requirements

The geographic coordinates of the survey perimeter and the survey track are utilized.

3.1.3 Success criteria and result

The survey achieved 99% coverage for an objective of 98%.

3.2 OBJECTIVE: REPEATABILITY OF INSTRUMENT VERIFICATION TESTS

Reliability of survey data depends on the stability of survey equipment. This objective concerns twice-daily verification on a test strip where metallic targets will be buried. The IVS is surveyed in detection mode during the detection survey. The IVS targets are surveyed in cued interrogation during the entire demonstration.

3.2.1 Metrics

The amplitude of the MPV data over a target and the magnitude of the polarizability components span multiple orders of magnitude. The metric for detection relates to the amplitude of the maximum target response, defined as the norm of the total field on a cube at 0.5 ms. The metric for cued interrogation is the target size, here defined as the norm of the polarizability components also for the 0.5 ms time channel.

3.2.2 Data requirements

The IVS survey data were recorded and analyzed.

3.2.3 Success criteria and result

The objective was that target response amplitude and size remained within a factor 3 of their mean value. For dynamic data the response was within better than a factor 2 (1.2 in general). The size factor for cued data was within a factor 1.5 (within 1.1 in general; details in Section 7.1).

3.3 OBJECTIVE: CUED INTERROGATION OF ANOMALIES

The reliability of cued data depends on acceptable instrument positioning during data collection in relation to actual anomaly location. Because the cued survey was brief, just 4 days, the demonstrator directly verified that flags had been acquired within an acceptable distance.

3.3.1 Metric

The metric for this objective is the percentage of anomaly peaks that are located within the acceptable distance to the center of the cued interrogation survey of each anomaly.

3.3.2 Data requirements

The detection list contains the peak anomaly locations, as identified by detection survey. Location of the cued survey was recorded by GPS.

3.3.3 Success criteria and result

The objective was to center the survey pattern within the 50cm distance of the actual anomaly location for 100% of the cued anomalies. The objective was attained, with 98% of the acquisitions within 20 cm, a mean offset of less than 1 cm and a standard deviation of 6 cm (details in Section 7.2). Less than 3% of the anomalies needed to be recollected to extend the spatial coverage or include neighboring anomalies which signal may interfere.

3.4 OBJECTIVE: DETECTION OF ALL TARGETS OF INTEREST

Target detection depends on signal intensity, spatial coverage and the target picking method.

3.4.1 Metric

The metric for this objective is the percentage of seed items that are detected using the specified anomaly detection threshold.

3.4.2 Data requirements

The demonstrator submitted a detection list that was compared to seeded items locations.

3.4.3 Success criteria and result

The objective was to detect 100% of the seeded items within a halo of 0.6 m. All seeds were accounted for. One seed was detected in a large halo near that threshold. However, the seed was not missed by the field crew, who identified it as a secondary target during cued interrogation of GW-2032 and accordingly collected sufficient data to characterize that anomaly before notification by the Program Office of a potential miss (Details in 7.3).

3.5 OBJECTIVE: PRODUCTION RATE

This objective concerns data collection and pre-processing time.

3.5.1 Metric

This objective is measured by the mean daily acreage for dynamic survey and number of targets for cued interrogations, and the mean pre-processing time per anomaly.

3.5.2 Data requirements

Acreage, number of interrogations and pre-processing time were recorded every day.

3.5.3 Success criteria and result

The expected mean daily survey rates were 0.8 acre and 100 anomalies, and pre-processing time of less than 3 minutes per anomaly. Actual mean rates were 0.7 acre and 135 anomalies per day, and 2.5 minutes pre-processing per anomaly.

3.6 OBJECTIVE: MAXIMIZE CORRECT CLASSIFICATION OF TOI

This is one of the two primary measures of the effectiveness of the classification approach. This objective concerns the component of the classification problem that involves correct classification of TOI. Detection (dynamic) and cued (static) data were independently analyzed to produce prioritized dig lists.

3.6.1 Metric

The metric for this objective is the number of items on the anomaly list for a particular sensor that can be correctly classified as TOI by each classification approach.

3.6.2 Data requirements

Each demonstrator prepared a ranked anomaly list for the targets on the sensor anomaly list. IDA personnel used their scoring algorithms to assess the results.

3.6.3 Success criteria and result

The objective was met if 95% of the TOI are correctly labeled as TOI on the ranked anomaly list. The dynamic dig list achieved 98% correct classification and the static list 100%.

3.7 OBJECTIVE: MAXIMIZE CORRECT CLASSIFICATION OF NON-TOI

This is the second of the two primary measures of the effectiveness of the classification approach. This objective concerns the component of the classification problem that involves false alarm reduction.

3.7.1 Metric

The metric for this objective is the number of items on the sensor dig list that can be correctly classified as non-TOI by each classification approach.

3.7.2 Data requirements

Each demonstrator prepared a ranked anomaly list for the targets on the sensor anomaly list. IDA personnel used their scoring algorithms to assess the results.

3.7.3 Success criteria and result

The objective was met if more than 75% of the non-TOI items were correctly labeled as non-TOI while retaining at least 95% of the TOI on the dig list. We were able to reject 85% of the clutter using dynamic data and 92% with static data.

3.8 OBJECTIVE: SPECIFICATION OF NO-DIG THRESHOLD

In a retrospect it is possible to tell the true classification capabilities of a classification procedure based solely on the ranked anomaly list, whereas in a real-world scenario all targets may not be dug so the success of the approach will depend on the ability of an analyst to accurately specify their dig/no-dig threshold.

3.8.1 Metric

The probability of correct classification of TOI, P_{class}, and number of false alarms, N_{fa}, at the demonstrator-specified threshold are the metrics for this objective.

3.8.2 Data requirements

The demonstrator prepared a ranked anomaly list with a dig/no-dig threshold indicated. IDA personnel used their scoring algorithms to assess the results.

3.8.3 Success criteria and result

The objective is met if more than 75% of the non-TOI items can be correctly labeled as non-TOI while retaining 95% of the TOI at the demonstrator-specified threshold. The demonstrator used the decision statistic metric to define stop-dig thresholds in their cascading classification algorithms (see sections 7.5 and 7.6). The objective was met for both dynamic-based and cued-based classification, with retaining 98% and 100% of TOI and rejecting 85% and 92%, respectively.

3.9 OBJECTIVE: MINIMUM NUMBER OF UNCLASSIFIABLE ANOMALIES

Anomalies for which reliable parameters cannot be estimated cannot be classified by the classifier. These anomalies must be placed in the dig category and reduce the effectiveness of the classification process.

3.9.1 Metric

The metric is the number of anomalies that cannot be analyzed by our method.

3.9.2 Data requirements

The submitted dig list specified those anomalies for which parameters could not be reliably estimated.

3.9.3 Success criteria and result

The objective was to be able to classify at least 95% of the cued anomalies. Data quality allowed for 100% anomalies to be analyzed for both the cued data and dynamic data.

3.10 OBJECTIVE: CORRECT ESTIMATION OF LOCATION AND DEPTH

Correct target classification relies on the capability to extract valid target parameters. Accurate TOI location is also important for safe and efficient site remediation.

3.10.1 Metric

The metric is the difference between observed and predicted depth and geographic location.

3.10.2 Data requirements

Target location and depth were recorded and compared to ground-truth validation measurements. This objective requires accurate ground truth.

3.10.3 Success criteria and result

The depth of TOI should generally be predicted within 0.10 m and geographic location within 0.15 m. The standard deviations for the differences between measured and predicted depths and locations were 0.04 m and 0.07 m for TOI. Note that non-TOI are generally well predicted too with 0.10 m for depth and 0.11 m for location error. Graphical results are presented in Section 7.7.

4.0 SITE DESCRIPTION

The site description material reproduced here is taken from a section of the ESTCP Demonstration Plan, which itself borrows from the stakeholder review draft of the Colorado Site Inspection Report, Army National Guard Munitions Response Sites. More details can be obtained in the report. Camp George West is located in Jefferson County, Colorado, in Lakewood. The demonstration will be conducted in a portion of the Non-Department of Defense Owned, Non-Operational Defense Site (NDNODS) Camp George West Artillery Range located primarily on the northern and eastern faces of Green Mountain. An aerial photo of the demonstration area is shown in Figure 3.

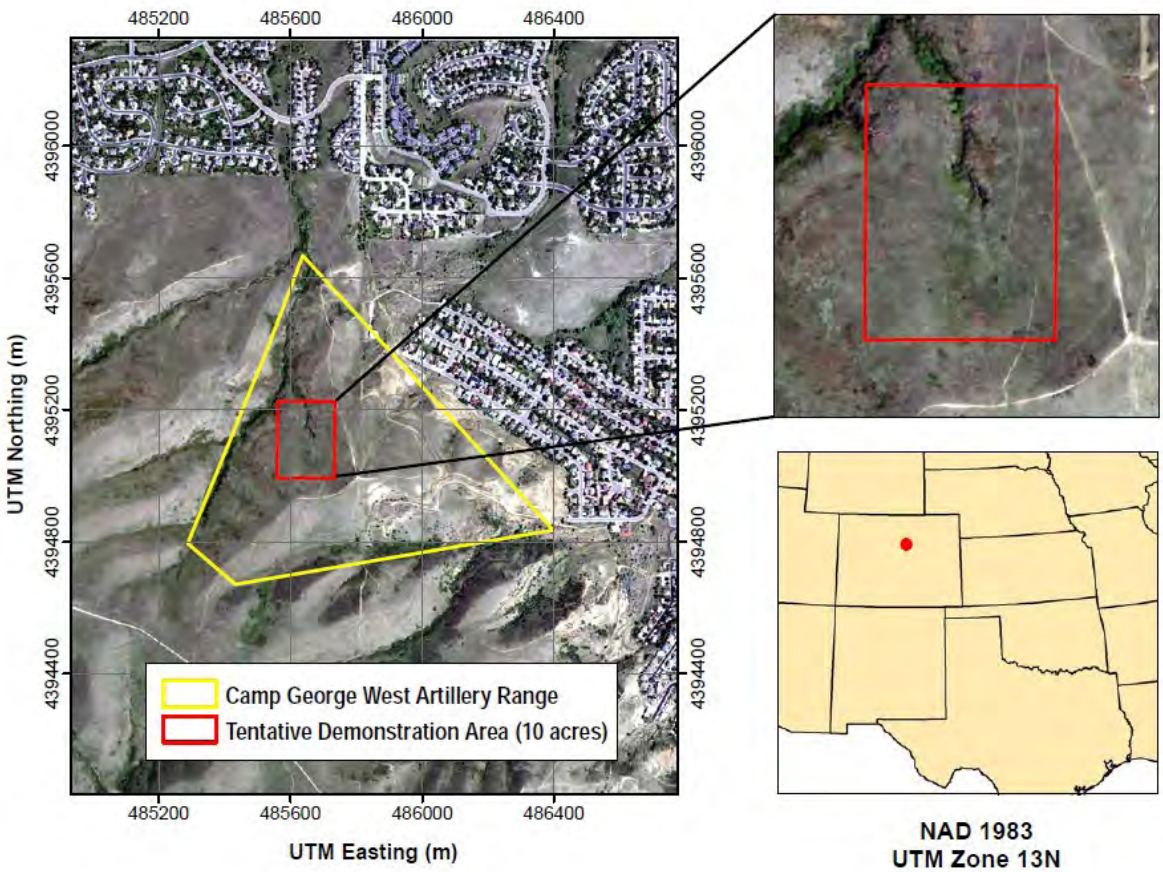

Figure 3: Aerial photograph of the demonstration site.

4.1 SITE SELECTION

This site was chosen as one in a series of sites for demonstration of the classification process. Sites including this one provide opportunities to demonstrate the capabilities and limitations of the classification process on a variety of site conditions. Further information about ESTCP's classification program can be found at http://www.serdp-estcp.org/Featured-Initiatives/Munitions-Response-Initiatives/Classification-Applied-to-Munitions-Response. This site was selected for the program because of its terrain and an opportunity to involve a stakeholder community including state regulators and the Colorado Army National Guard (ARNG) in the classification pilot program.

4.2 BRIEF SITE HISTORY

The 135-acre Camp George West Artillery Range Munitions Response Site (MRS) was used by the Colorado ARNG for artillery training from 1930 to 1945 as an impact area for 75-mm high explosive (HE) projectiles. Other portions of the artillery range, including firing points, forward observer position(s), and surface danger zones are not precisely known. The MRS (impact area) is currently owned by the city of Lakewood.

4.3 MUNITIONS CONTAMINATION

The only known munitions type is the 75 mm projectile.

4.4 SITE CONFIGURATION

The two-acre area chosen for the demonstration site is shown in Figure 4. The results of the initial EM61 transect survey is shown as false color and the demonstration area is shown as a white rectangle. Photographs of the demonstration area in Figure 1 and Figure 5 show the rugged terrain. Survey coordinates were made available by the ESTCP Program Office.

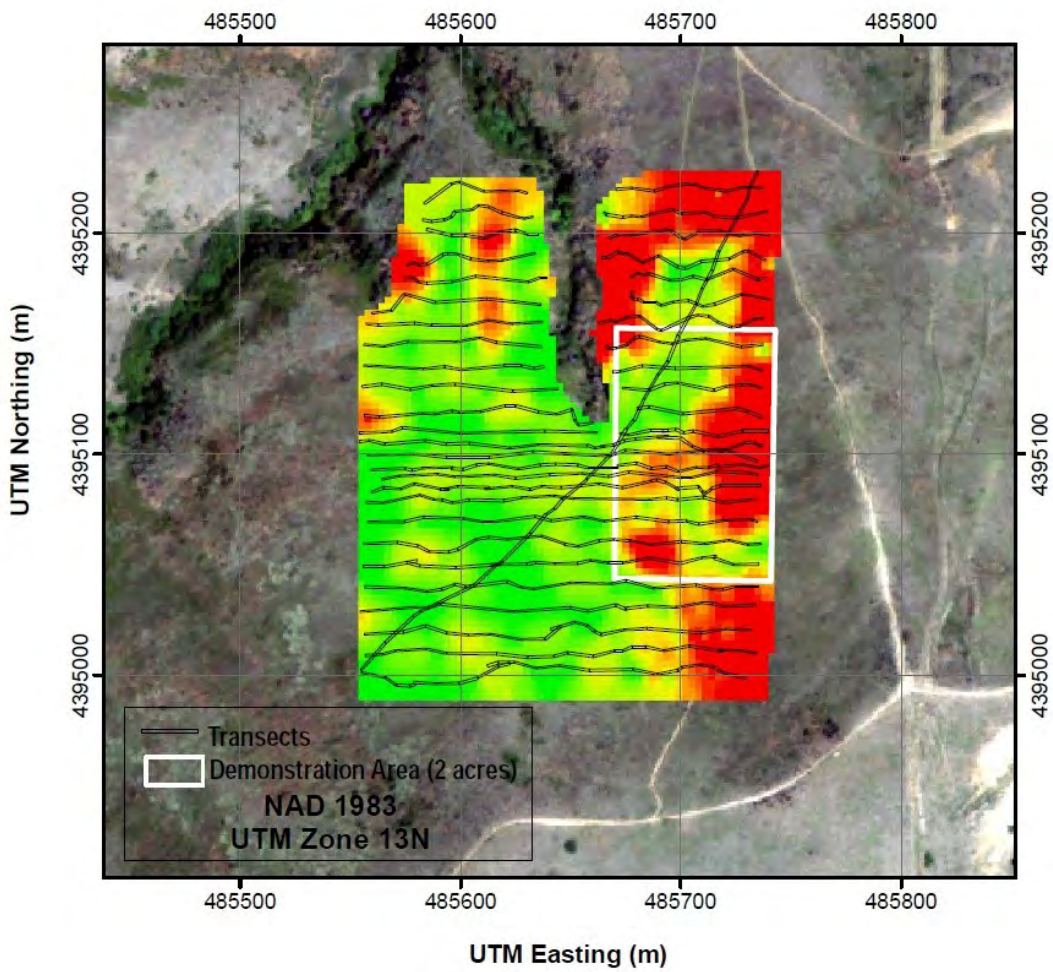

Figure 4: False color image of the anomaly density interpolated from the EM61 transect surveys over the ten-acre initial area and the two-acre area chosen for the Classification demonstration (red color suggests higher target density than green background level).

Figure 5: Cued interrogation of anomalies on the side of Green Mountain.

5.0 TEST DESIGN

The goal of the study is to demonstrate and characterize detection and discrimination with the MPV. Sensor classification performance is characterized as a function of the size and depth of the buried targets and the presence and effect of aggravating factors (nearby objects, magnetic soil and complex terrain).

5.1 DEMONSTRATION SCHEDULE

The field survey was completed in 10 days, including one day when wind conditions were such that the crew could not safely work on the exposed ridge (gusts up to 70 miles per hour). The first day was spent travelling to Denver, collecting the equipment and access key, assembling the sensor, visiting the site, presenting the technology to the two new field crew members and training on the IVS. The second day included more training on the IVS and training pit and delineation of the survey area in order to visualize the area boundaries and preprogram survey lines for easier navigation with the MPV and GPS. The technology was also presented to local residents with the ESTCP Program Office Manager and local state representatives. The third days was cancelled due to high wind. The detection survey took place between the fourth and sixth days, during which 0.1 acre was covered on average per hour. Three people were actively involved in the data collection, with two operating the MPV and one setting up ropes on the ground to mark the lines. The data were periodically downloaded for quality control, analysis and target picking by the PI. The detection list was submitted to the Program Office to verify detection of all seeded targets. Approximately 500 anomalies were selected for cued interrogation, which took four days with two field crew members. The data were pre-processed and inverted by the PI to control quality and verify adequate coverage while still in the field. Further analysis was done over the following weeks to locate all targets of interest and identify instances of multiple targets. This information was used to guide the digging crew. Data were distributed to other ESTCP partners for analysis. Dynamic and static data were inverted and used for classification over the following months. The following Gantt chart shows the schedule for each phase of testing and how the various phases are related.

Table 2: Demonstration steps

	Preparation Calibration			Field surveys			Post survey analysis		
Tasks and demonstration timeline	**1.1**	**1.2**	**1.3**	**2.1**	**2.2**	**2.3**	**3.1**	**3.2**	**3.3**
Mobilization – Demobilization	X					X			
CALIBRATION: Training pit		X							
CALIBRATION: Inversion and parameters stability analysis of training pit data		X							
CALIBRATION: Twice-daily test strip survey and data analysis			X	X	X				
DYNAMIC SURVEY: Detection in dynamic area				X					
DYNAMIC SURVEY: Target picking					X				
CUED SURVEY: Wooded area and dynamic area					X				

	Preparation Calibration			Field surveys			Post survey analysis		
Tasks and demonstration timeline	**1.1**	**1.2**	**1.3**	**2.1**	**2.2**	**2.3**	**3.1**	**3.2**	**3.3**
DATA PRE-PROCESSING: Cued data					X		X		
DATA ANALYSIS: Feature extraction								X	
DATA ANALYSIS: Classification ranked list								X	
RETROSPECTIVE ANALYSIS									X
REPORTING									X

5.2 SYSTEM SPECIFICATION

For cued interrogation mode the system is set for a 25 millisecond (ms) excitation and 25 ms recording of EMI transients. This is accomplished by using 0.9 seconds (s) data blocks that include 9 repeats (100 ms per cycle). Station time is set to 6.3 s by stacking 7 data blocks (effectively 9 x 7 = 63 cycles are averaged). Digital receivers use a 4 microsecond sampling rate. The data are recorded with 133 logarithm-spaced time gates (5% gate width) from 0-25 ms. The dynamic survey mode has a 2.7 ms time window and a short, 0.1 s data block so as to reduce smearing of the signal by sensor motion.

The open sky conditions were amenable to use of GPS for dynamic and cued surveys. The beacon system was also used in cued mode to verify the accuracy of the GPS. The GPS is a Trimble R8 that is mounted on the opposite end of the MPV handling boom. The GPS is also used to locate pre-programmed flag locations. Sensor orientation was measured with a XSens MTi orientation sensor that was mounted near the GPS. The three-axis sensor data was also used for verifying the pitch and roll inferred from the beacon measurements. The beacon boom was generally laid on the ground within 2 meters of the survey flag. Boom orientation was recorded with a secondary XSens orientation sensor that was affixed to the boom center. The boom was usually oriented across slope direction and on the left side of the target. After data processing, beacon-derived positions were located relative to the local flag and geographic North, and subsequently globally-referenced using the supplied GPS coordinates of each flag.

5.3 CALIBRATION ACTIVITIES

Calibration is designed to verify correct sensor operation and calibrate the recorded sensor response over known targets. It was expected that 75 mm and potentially 37 mm projectiles could be encountered at the site. We brought a sample of a 75 mm, 57 mm and a small ISO for test pit measurements. Each sample was successively placed inside a clutter-free training pit and surveyed in cued interrogation mode. Four different orientations and one depth per target were tested. Data were rapidly inverted to verify stability of the recovered target parameters.

Sensor drift was evaluated over an IVS where known targets were buried in a clutter-free environment. The strip was surveyed in dynamic and cued modes to test detection and classification. In-air and on-ground measurements were acquired after every twelfth target interrogation and before and after any battery change, so that variations in transmitter power and instrument noise could be verified. Geologic background measurements were acquired by identifying “quiet” areas, which can be recognized by examining the recorded decay curves in static mode. Data were analyzed to quantify the spatial and temporal variability in background

noise and detect potential soil magnetization. Beacon positions were compared with the GPS to validate location data.

5.4 DATA COLLECTION PROCEDURES

5.4.1 Sample density

The detection survey was carried out by walking along pre-defined survey lines and sweeping the sensor from side to side, while keeping the sensor head approximately parallel to the ground. Given an effective footprint of approximately 0.7 m, we adopted 1.2-m line spacing and surveyed by sweeping the sensor with 0.7-m amplitude and 0.7-m period. Station spacing depends on survey speed. Following an empirical rule that the sensor should not move more than the receiver length (8 cm) during acquisition of a data block (0.1 s), sensor-head speed should be between 0.5-1 m/s with station spacing of 0.05-0.1 m along each of the 5 receiver-cube tracks – this rule was generally well respected at George West (Figure 6). The resulting along-line speed is approximately 0.3 m/s. The lines were set to follow altitude contours along the sides of Green Mountain to minimize the amount of effort for the operator (Figure 7).

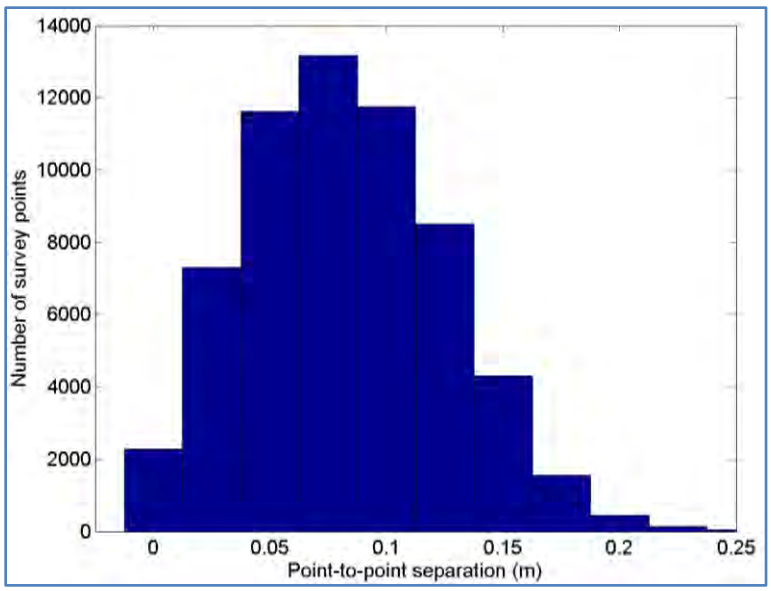

Figure 6: Station spacing in detection survey (spacing<0.1 m for 66% points and <0.15 m for 94%).

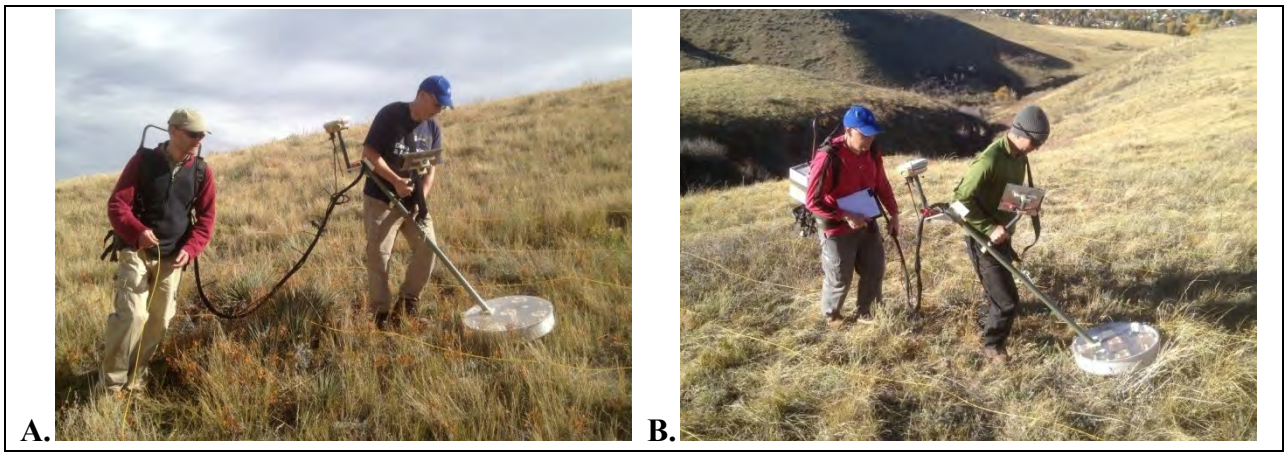

Figure 7: Detection survey across (A) and along (B) slope.

The process for cued interrogation is to collect data on top of and around the detected target location. The location is programmed into the MPV DAQ and located with the GPS (no ground paint or flags were used at this site). The first sounding is acquired at the picked location, followed with four soundings in a square pattern and a separation of 0.6-0.7 m (Figure 8). The resulting coverage is approximately uniform, with a receiver cube separation of 0.2 m. Additional points can be collected at the operator's discretion if the anomaly coverage is deemed insufficient.

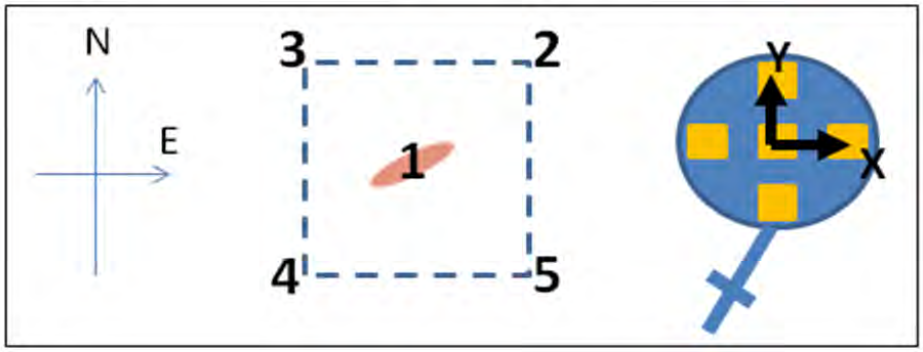

Figure 8: Cued survey pattern with five points centered on expected target location.

5.4.1 Quality checks

During a detection survey the sensor track is displayed on the field monitor. The operator regularly checked the monitor for possible gaps. The second operator watched the main operator to verify the survey speed, sweeping amplitude and to identify obvious gaps in coverage. For cued interrogation, each sounding is displayed immediately after acquisition. The operator can verify adequate anomaly sampling and data quality by examining data decay curves (Figure 9) and the arrows display. The first sounding requires particular attention to verify that the signal source originates directly below the marked location. Offsets can result from positional errors, differences in sensitivity between the detection sensor and the MPV, error in the picked location, or multiple targets. In such cases the operator is expected to apply close scrutiny to interpret all soundings, locate the signal source and acquire additional soundings if necessary. Anomaly coverage is verified by ensuring that the farthest receiver is measuring background. If residual signal from the target remains then additional soundings are collected to ensure full coverage of the anomaly. For instance, if the MPV front receivers show above-background signal when the MPV is placed in position 2 (Figure 8), then a sounding is to be collected North of the middle of positions 2-3. If a nearby, interfering target is detected while being un-flagged for cued interrogation, then supplementary soundings are acquired to improve characterization of the two sources.

Data quality checks are first done during the survey to verify that receivers are properly operating. Any abnormal sounding is tagged and a new sounding is acquired at same location. In case of receiver failure the survey is stopped until a solution is found. This did not occur at Camp George West. Data quality is also controlled post-survey, while still on site, to identify possible issues and re-acquisitions. Particular features to monitor are the spatial coverage of the anomalies(especially if the flag and anomaly peak are offset) beacon positions and signal to noise ratio.

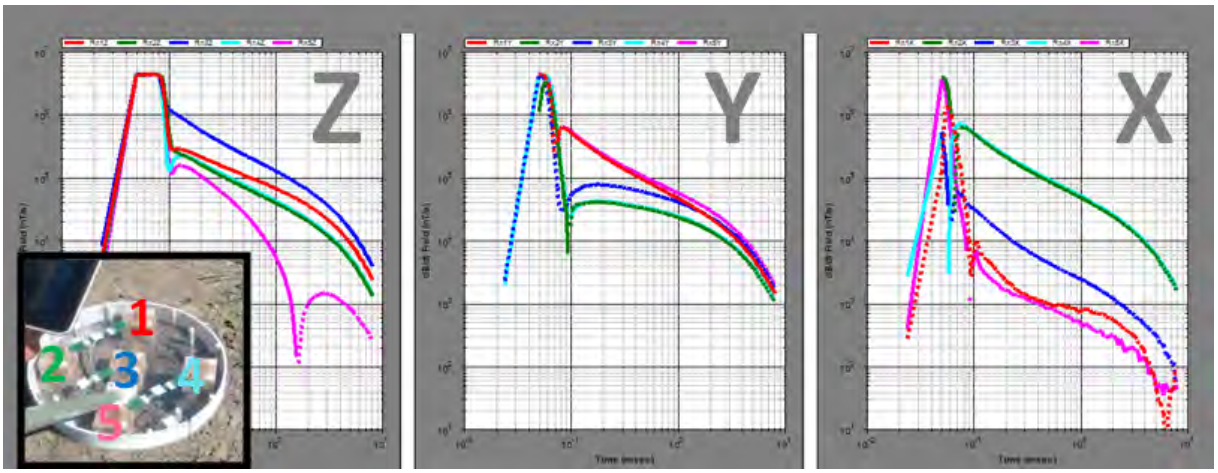

Figure 9: Typical target response when the MPV head is placed directly above a buried target. The Z-component data show that target is closest to center cube (#3) and equally distant from lateral cubes 2 and 4, while signal in cube 5 resembles background. The Y data confirm that target is buried between front and back cubes (1, 5) and X data confirm that target is located between side cubes 2 and 4.

We ensure that all anomalies are visited by pre-programming their GPS coordinates and displaying their location on the sensor display map. Despite occasional GPS signal drops under canopy, the GPS generally helps navigating between anomalies. Each visited anomaly is automatically marked on the map.

5.4.2 Data handling

Data are stored as .tem files on the DAQ and converted to .csv files before every battery change. Copies of all .tem and .csv files are stored on the DAQ, on a portable hard-disk drive and on the field laptops that is used for reviewing the data.

The DAQ carrier documents the survey by noting target names and file numbers in addition to any remarks made by the principal operator. Field notes are digitized every day by taking pictures of the notes and filling out a spreadsheet that is used for pre-processing.

6.0 DATA ANALYSIS

6.1 PREPROCESSING

The MPV computer DAQ records data streams from the sensor head, beacon receivers, attitude sensor and GPS with the GPS time stamp. The DAQ saves the data into a .tem binary file. Data from each sounding are converted to a .csv file without any data alteration. Several pre-processing stages are performed before delivery to the analysts.

The beacon receiver data, transmitter current and attitude measurement are combined to infer the MPV head location. When the GPS Q factor is equal to 4 the GPS and attitude can be combined to predict the sensor head location and compare to the beacon. In case of discrepancy we consider the field notes, the relative distance to the beacon boom and any possible disrupting factors to choose the most likely solution or discard the sounding. At Camp George West the beacon position was valid (i.e agreed with GPS measurements) 100% of the time.

The MPV EMI data is divided by the recorded transmitter current amplitude at turn off to normalize the response to a unit transmitter excitation, hence compensating for fluctuations in transmitter battery power. Background measurements are analyzed to define a background response that is subtracted from the cued data. A spatial parameterization of the background response can be utilized if significant spatial variability is observed. The resulting corrected data is visually validated.

Because each sounding generates an individual data file, files must be combined to a single record for each target. The merged file is composed of data blocks for each sounding with the sensor location and attitude, sounding number and field comment. Only validated soundings are included. The final file name is comprised of the sensor and target names following ESTCP naming conventions. Files are later posted on a ftp site for distribution to analysts.

6.2 TARGET SELECTION FOR DETECTION

Dynamic survey data were assimilated and interpreted to produce a digital map of the area and identify anomalies that required further investigation (Figure 10). A simple detection threshold was applied to the amplitude of the interpreted signal. Its value was derived from a formal, quantitative assessment based on numerical simulations of the worst case scenario for the expected targets and verification with experimental data from the site. The analytic process is illustrated in Figure 11.

A target is considered to be detectable if the amplitude of its response exceeds the background noise signal. To achieve detection of a given target at a given depth in 99% of cases, the signal amplitude should exceed the typical variability of the background signal by a certain margin. In mathematical terms, the signal should be larger than the median plus 2-3 standard deviations of the background response. The background noise statistics were analyzed on an initial subset of the field data and compared with the typical response of a 75 mm projectile at various depth, predicted using polarizabilities obtained at the Spencer Range demonstration. The detection objective was set to capture all 75 mm projectiles within 2 feet (or 61 cm) of the ground surface. Monte Carlo simulations were done to further quantify the worst case scenarios at that depth, varying the sensor and target offset, target azimuth and inclination, as well as introducing variations in ground clearance and in the sensor attitude. Test stand dynamic data were acquired with a sample 75 mm projectile to validate the method. The probability of detection was computed as a function of the target response and the threshold was chosen so as to ensure 99% detection of a 75 mm projectile at the specified maximum depth.

Note that the probability that a 75 mm could occur at this depth was not included in this analysis. The detection threshold would be significantly higher otherwise. Also note that a more elaborate, and recommended, method would combine the anomaly footprint and amplitude. This method would largely reduce the number of false detections caused by survey noise (e.g., noise anomalies associated with walking paths crossing the survey area in Figure 10).

A detection memorandum was submitted during the demonstration to validate the approach with the ESTCP Program Office.

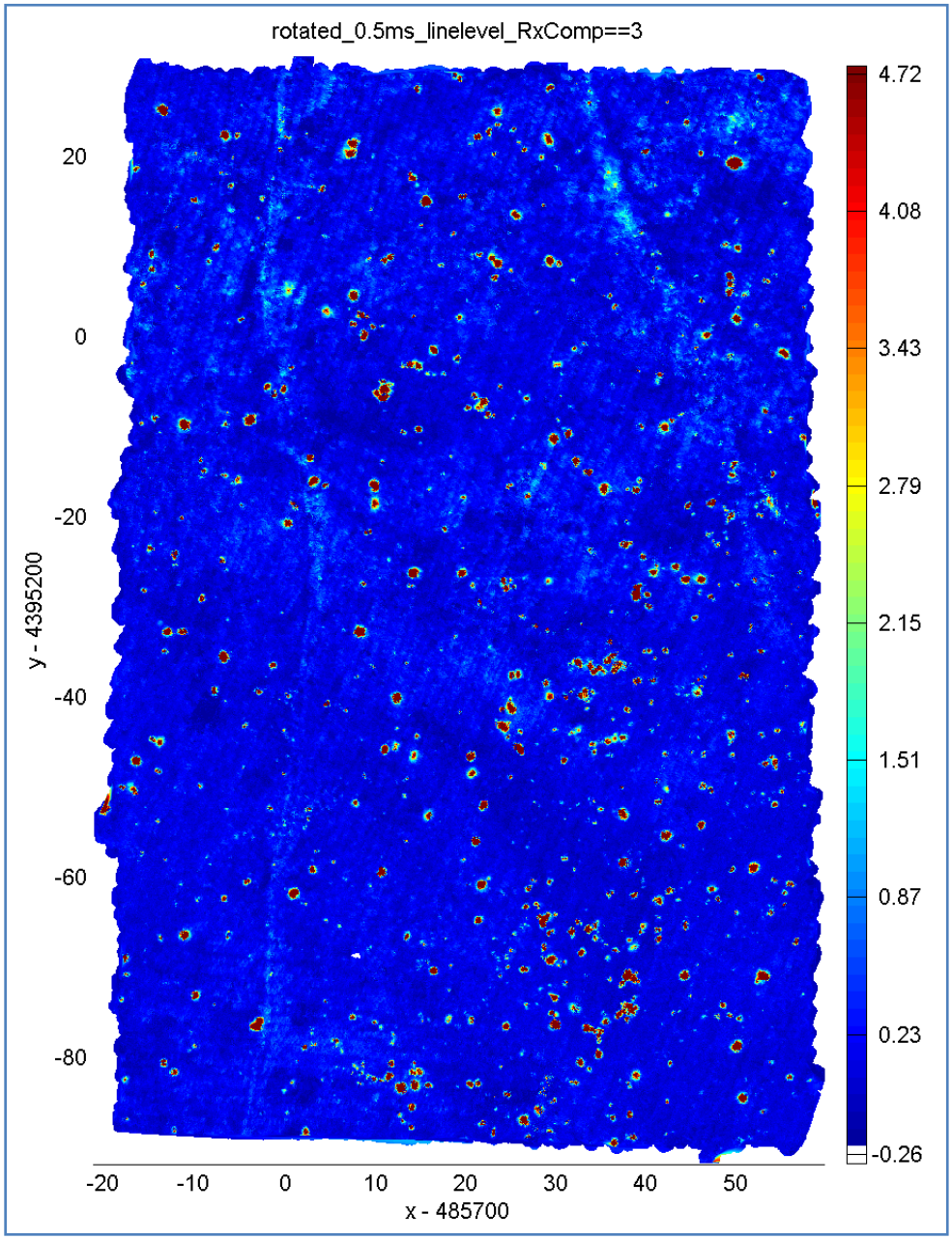

Figure 10: Detection map using the Z-component on all receiver cubes with the 0.5 ms time channel. Hiking paths running NS on W side and across NE corner remain visible in data.

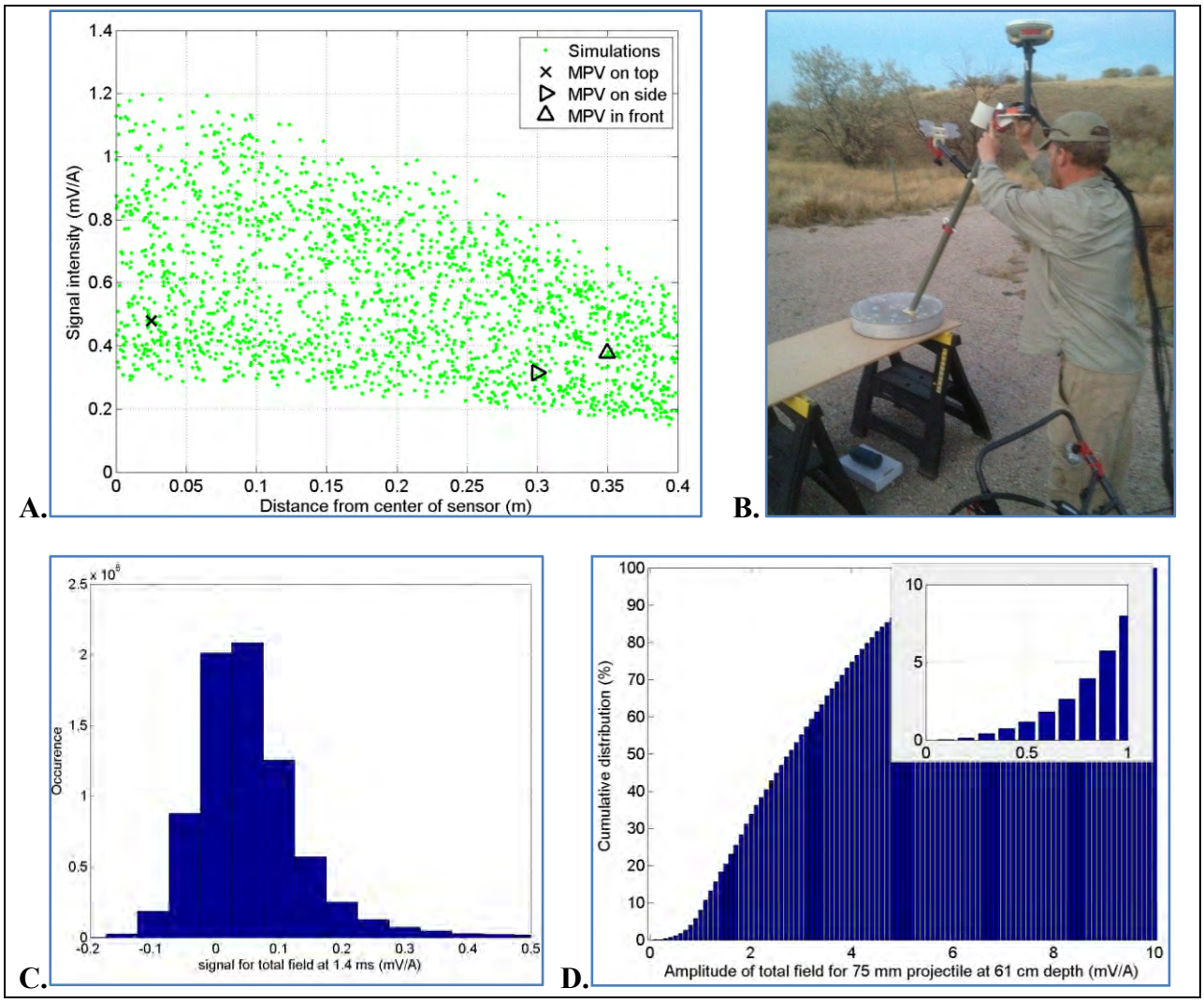

Figure 11: Target detection analytic process based on simulation and site-specific data. A: The response of 75 mm projectile buried at 61 cm depth is simulated for different sensor and target positions and orientations; markers indicate the amplitude of experimental dynamic data collected over a test stand for verification (panel B). C: Background noise is estimated from local field data. D: Probability of detection at 61 cm depth as a function of signal amplitude is derived from simulations.

6.3 PARAMETER ESTIMATION

Advanced data analysis is done with UXOLab, a MatLab-based software jointly developed with the University of British Columbia and tested in numerous ESTCP and SERDP projects. Data are inverted using a three-dipole instantaneous polarization model (Pasion and Oldenburg, 2001). The target polarizability decay parameters are the main features for input into the ensuing classification. Inversion setup parameters such as noise estimation are generally decided upon by examination of the training pit data. Solutions with one or multiple targets are generated for every selected target. Decisions regarding the number of targets at a given location are made through statistical classification by prioritizing the most munitions-like solutions. Inversion results are reviewed by an experienced geophysicist to identify any potential issues with the

inversion setup or with the data, and select data subsets as required for fitting all detected anomalies (masking).

6.4 TRAINING

Statistical classifiers are trained on a library of target features that has been accumulated during previous studies at YPG, Camp Beale and Spencer Range. The library was augmented with new features associated with local targets. Local information was incorporated by collecting data over a training pit in which munitions were placed in multiple orientations so that their parameter variance could be estimated.

Additional local information was included after analysis of the target features and comparison with the library. Training data were requested to the ESTCP to obtain information about particular targets. Targets may be remarkable because they belong to a cluster of unknown items with similar features. Targets may stand out for having particularly large inferred size. This process of requesting training data was iterated until sufficient confidence in the classifier was attained.

6.5 CLASSIFICATION

As with past ESTCP demonstration studies, the following guiding principles were applied:

- *Selection of features:* By analysis of the training data, those features that contribute to separation of the different classes (comprising UXO types and clutter) are selected. Our experience shows that the three sets of instant polarizability decays generally yield successful classification with the MPV (and other sensor data). The data are inverted in different manners, using single-target and multiple-target inversions and different noise parameters or mask sizes. Therefore multiple sets of features can be extracted from the same anomaly and the model that most likely resembles a TOI is automatically selected during classification;
- *Choice of classification algorithm:* Methods are elaborated through analysis of the training data. Past studies have been successful using a Library Fit method or a Support Vector Machine (SVM) classifier. These methods can be combined or applied multiple times with different parameters;
- *Classification:* Anomaly labels are placed in a prioritized dig-list by using the classifier to compute probabilities of class membership for unlabeled feature vectors. Targets deemed as most likely TOI are prioritized in the dig sheet;
- *Number of UXO-classes*: Statistical classifiers such as SVM can group multiple UXO types in a same class, while multiple classes can be used to represent a wide size range. The library fit uses a collection of polarizability decay curves. Multiple sets of curves may correspond to the same UXO type if some variability is found, for instance with large objects for which orientation may affect the recovered polarizabilities.

The classification approach was selected after examination of recovered target parameters and analysis of local conditions. Weak magnetic soil disturbance did not require any particular treatment and allowed use of standard classification protocols based on library misfit, similar to the preceding study at Spencer Range. The dynamic data and the static, cued interrogation were independently analyzed and led to two dig lists produced by different analysts.

The quality of the detection survey (dynamic) data was deemed sufficiently high to apply classification to 100% of the anomalies, as opposed to Spencer Range where some spatial gaps and less experience with the process fostered application of a hybrid classification analysis using

both dynamic and cued data. Each method is detailed in the classification memorandum (included in Appendix D). The TOI library was initially based on items found at previous sites. The library was modified after training, removing items that did not seem to be present, and adding TOI whose features differed from their typical reference class. A multi-stage classifier was applied. The first stage included all polarizabilities (L123) and the next stages only used a combination of two polarizabilities (L12, L13), and the final stage only the primary polarizability (L1). Targets for which training data were available were also included in the classifier to assess the effect of classification parameters on their ranking. The decision to switch from one classifier stage to the next was based on a decision statistic derived from the library misfit metric. For each stage, that metric shows a strong inflection when items strongly differ from library TOI (Figure 38 in Appendix D). The stage switch (or stop digging within this classifier stage) was automatically computed and further confirmed by visual inspection of the polarizabilities in ranked order (Figure 12) and comparison with ground truth data (obtained from training or earlier dig list stages).

The result of classification is a ranked anomaly list that can be formatted as in Figure 12. The first items on each anomaly list will be those targets for which reliable parameters cannot be extracted and therefore must be dug. Next will be the items that are considered as "high confidence' munitions. Items will be ranked according to decreasing confidence that the item is hazardous. Any items that were analyzed without reaching an unambiguous classification decision will be placed next on the anomaly list. Finally, all items that are confidently classified as non-hazardous will be ranked by their confidence.

Initial Ranked Anomaly List

Anomaly ID	Category	Dig on First Pass	Type	Comment
2498	-1	1		Training Data
247	-1	1		
1114	0	1		Can't extract reliable parameters
69	1	1	105	
811	1	1	48	High likelihood TOI
313	1	1	37	
883	2	1		
1642	2	1		Unable to classify
713	2	0		
406	3	0		
...	3	0		High likelihood not TOI
...	3	0		
...	3	0		
...	3	0		
...	3	0		
...	3	0		
...	3	0		

First Pass Threshold

Final Ranked Anomaly List

Anomaly ID	Category	Dig	Type
2498	-1	1	
247	-1	1	
1114	0	1	
69	1	1	105
811	1	1	48
313	1	1	37
883	1	1	
1642	1	1	
713	1	1	57
406	3	0	
...	3	0	
...	3	0	
...	3	0	
...	3	0	
...	3	0	
...	3	0	

Final Threshold

Figure 12: Format of prioritized anomaly list to be submitted to ESTCP Program Office.

7.0 PERFORMANCE ASSESSMENT

7.1 Repeatability on Instrument Verification Strip

The IVS was tested in dynamic mode during detection survey days. The goals were to detect the buried targets, achieve 100% spatial coverage through the detection sweep and collect training data for further analysis (noise characterization, dynamic inversion, classification feature extraction). Detection and coverage are illustrated in Figure 13 and Figure 14, where the detection data for six passes over the IVS lane are gridded and displayed. The Z-component data show strong responses over three targets (there is an empty hole between the first and second targets, starting from the South end). The presence of a metallic target is validated with the X and Y component data, which show a sign change as expected for a dipolar anomaly.

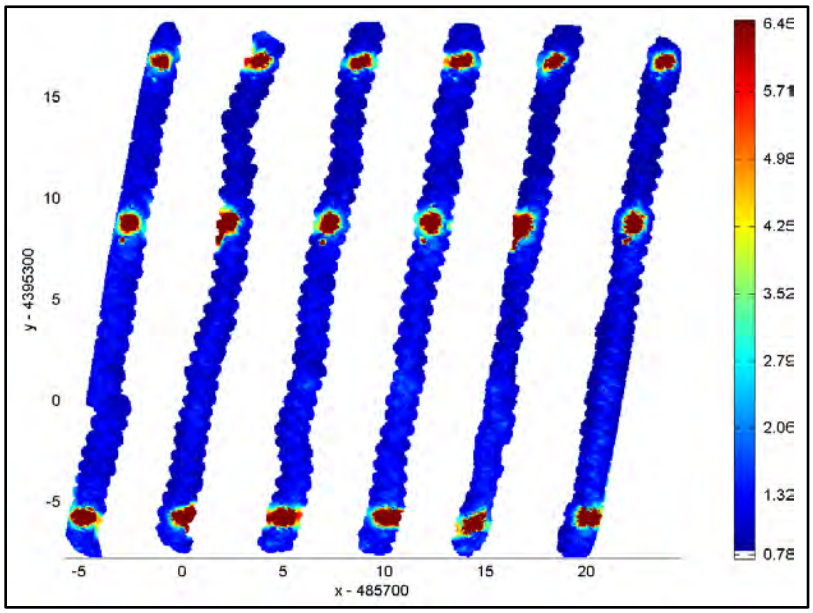

Figure 13: Detection on IVS lane for Z-component data at 0.5 ms.
Six passes are shown over 3 different days, (first day on left side). Each pass is displayed with a 5 m lateral offset for comparison. There are three buried items.

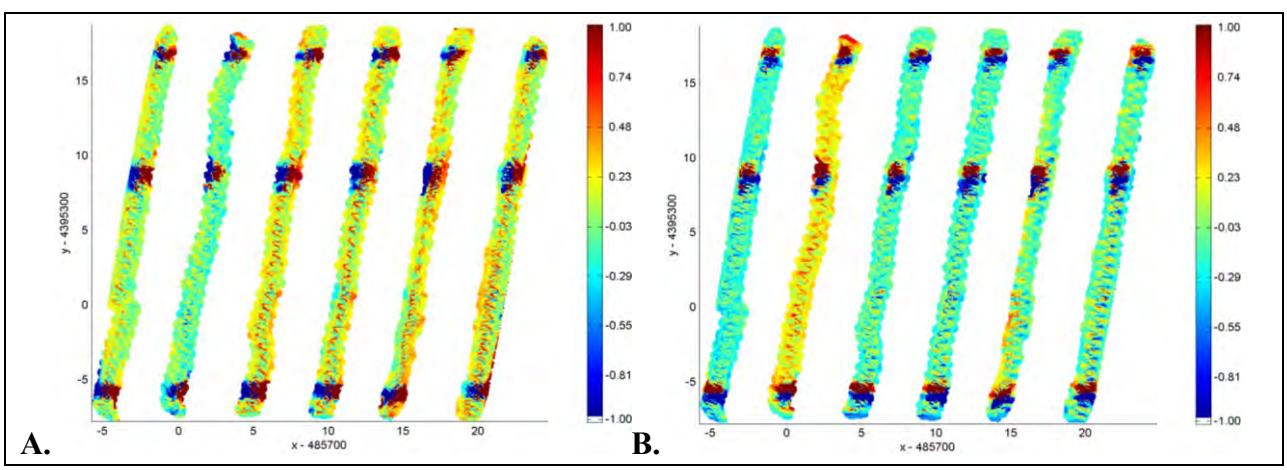

Figure 14: Detection on IVS lane for X-component (A) and Y-component (B) data.

The IVS targets were also interrogated in cued mode every day. The cued and dynamic data were inverted to verify the stability of the recovered target parameters as an indirect mean of verifying proper instrument operation. Predicted polarizabilities are shown in Figure 15 for both data types. The polarizabilities meet the stability criteria; the observed variability is greatest on the first day, due to some uncertainty on targets location and training of new crews. The polarizabilities were added as reference items to the classification library for the preparation of dig lists with the dynamic and cued data.

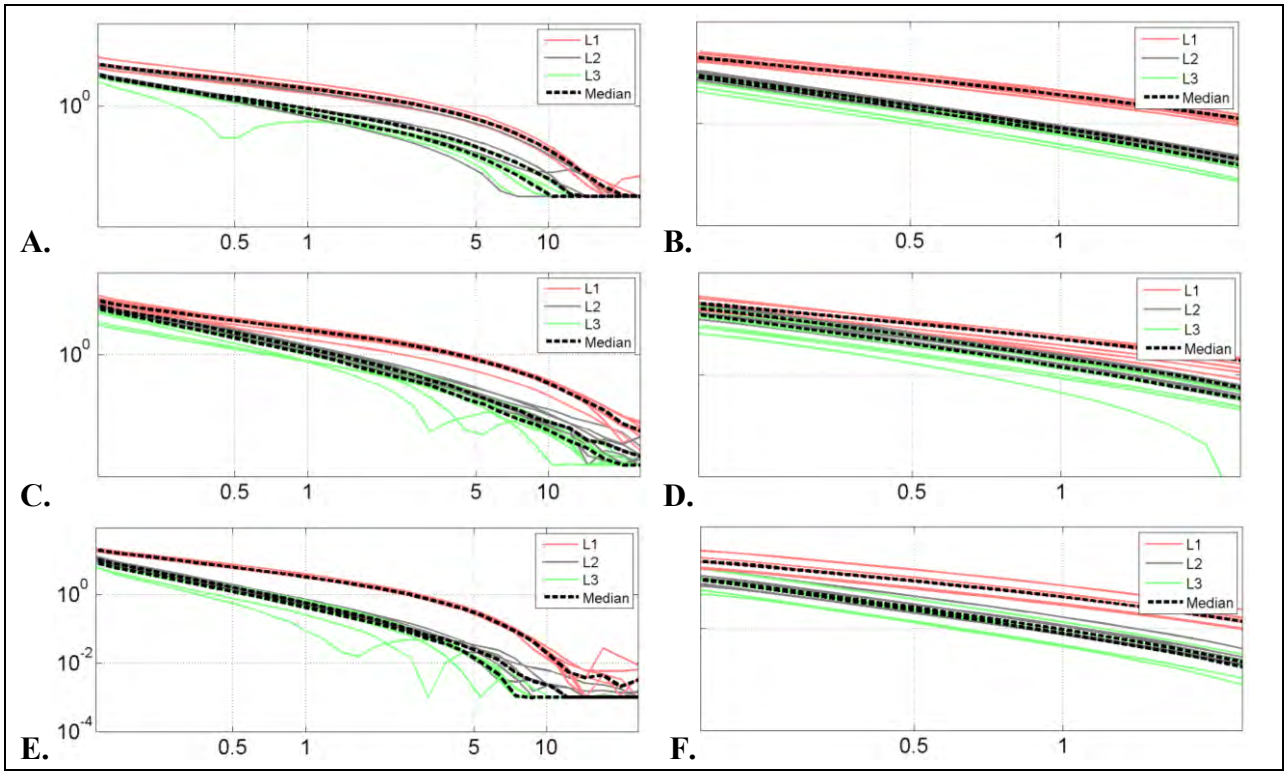

Figure 15: Polarizabilities on IVS lane for cued (A,C, E) and dynamic data (B,D, F). Target 1 (AB) and 4 (EF) are a medium ISO and target 3 (CD) is a 75 mm projectile. Note that Target 2 was an empty hole.

7.2 Acquisition of cued anomalies

One of the cued data collection objectives was to acquire all anomalies within 0.5 m of their detection pick. The data in Figure 16A show the difference in easting and northing coordinates between the picked target location and the first sounding for each cued interrogation event. Most interrogations fall within less than 0.2 m error. Three anomalies present a larger offset of 0.30-0.45 m. Their corresponding cued data are shown in Figure 16B-D. The gridded z-component data confirm full spatial coverage of these anomalies.

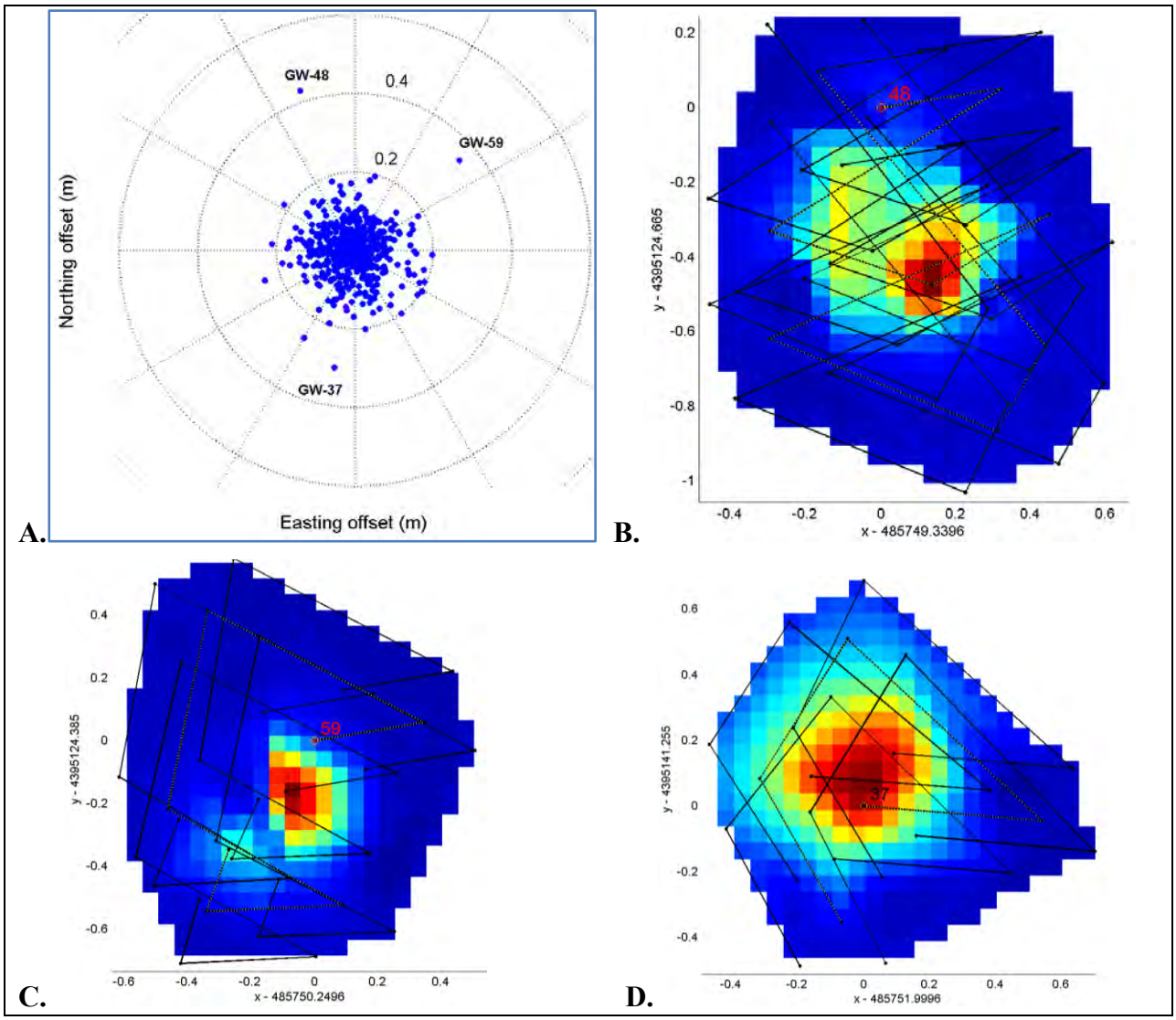

Figure 16: Positional accuracy of cued acquisition of field anomalies.
(A) Offset between first cued point and anomaly location; (B) Gridded Z-component data for target GW-48 with largest offset; (C) Target GW-59; (D) Target GW-37.

7.3 Detection of all targets of interest

The objective was to detect and locate all seeded targets within 0.5 m. The objective was attained, although one seeded ISO proved to be more difficult to locate because of the presence of a nearby piece of metal (75 mm base plate). The clutter was sufficiently large and close to the surface to generate a large response that overlapped with and dominated the response from the seed. This is shown in Figure 17A, where the base plate is target GW-2032 and the ISO target GW-12032 is located 0.55 m to the South-West. The two anomalies were difficult to isolate using our detection threshold method, as the lowest value between the two was ten times as large as the detection threshold (Figure 17B). However, the two separate targets were identifiable by inversion of the dynamic data. Detection algorithms could be improved to better account for multi-peak anomalies and take advantage of the wealth of information in multi-component data.

Practically, the presence of two separate targets was first revealed during cued interrogation of GW-2032, when the field operator detected the presence of a secondary source. The survey was extended to cover the footprint of the second anomaly, thereby following the standard operating procedure. The gridded data shown in Figure 17C-D illustrates coverage of the two anomalies. The Z-component data suggest the presence of two anomalies, though the second one has much weaker amplitude and could be due to noise. That second anomaly can be validated as a legitimate target by observing the typical sign change of a dipole source in the transverse component data (panel D for Y component). Inversion of the cued data unequivocally confirms the presence of a piece of scrap metal at GW-2032 and a medium-size ISO at GW-12032.

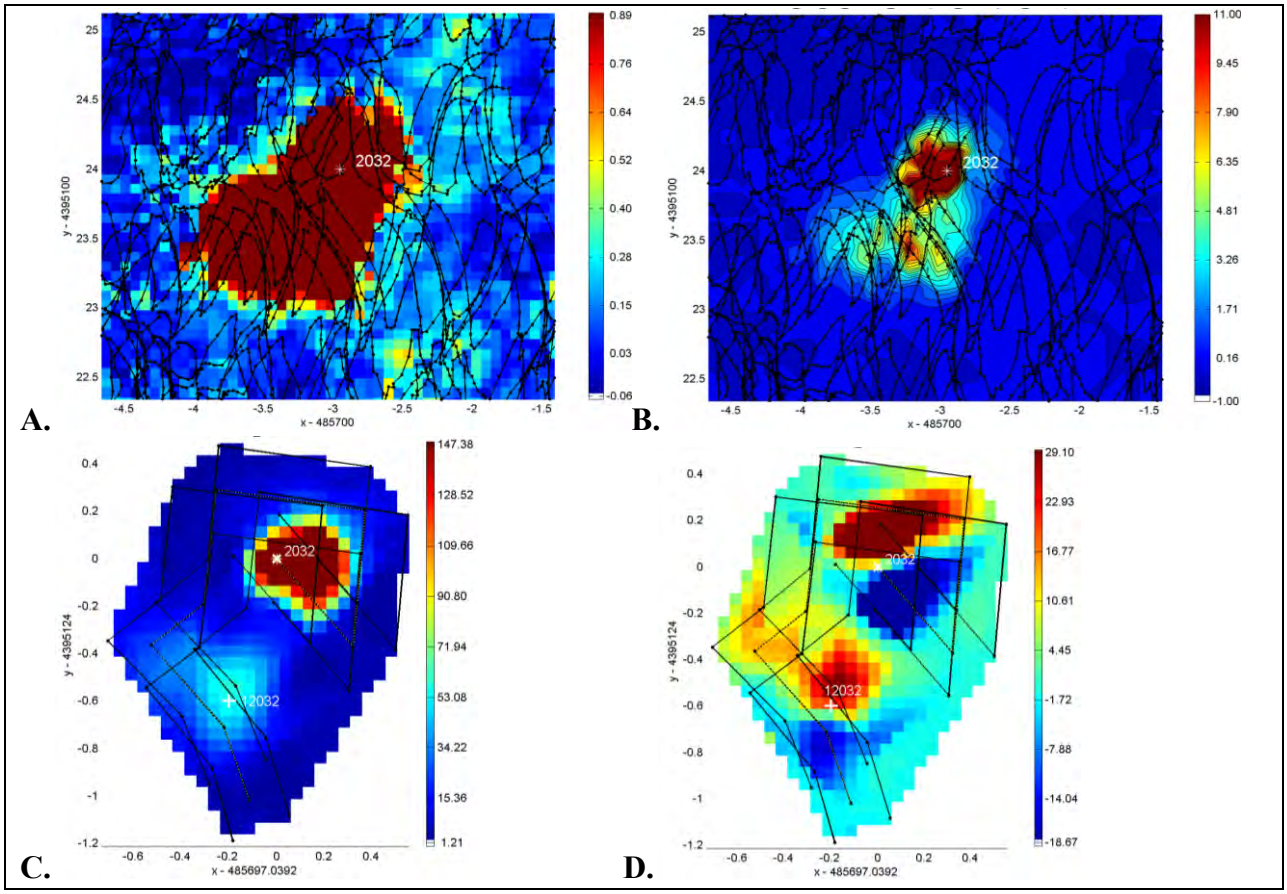

Figure 17: Detection and cued data around close targets GW-2032 and GW-12032. (A) Detection data: anomalies merge near threshold amplitude; (B) Detection data with extended color scale shows two anomalies; (C) Cued interrogation Z-component data; (D) Cued interrogation Y-component data.

7.4 False detections

The original picking was automatically executed using the calculated amplitude threshold for a 75 mm projectile at 61 cm depth. The threshold was close to two standard deviations of the background noise and some false detections occurred because of background variations. Our computation of threshold also indicated a minimum anomaly footprint size could have reduced the number of false detections. Applying the selected detection threshold to the automatic picking algorithm resulted in the selection of 567 anomalies.

Review of the selected anomalies indicated the presence of false detections caused by noisy late-time data. A composite detection channel was created by logarithmic integration of the decays between 0.5 and 1.65 ms as a means to smooth out noise variations in the received signal. Combining early and late time parts of the time decays also allows for some initial rejection of fast-decaying clutter from the target list. Applying the same logic for identifying the detection threshold as before, we combined the anomalies that were selected by both algorithms and reduced the number of picks to 483 high priority targets.

Cued interrogation was applied to 504 anomalies, retaining 21 low priority targets for quality control. The cued data were subsequently inverted and interpreted. We found that 68 anomalies could clearly be eliminated as false detections, while 30 anomalies were likely due to two or more close targets. The final anomaly list therefore included 466 items to characterize. The ordnance clearance team reacquired the 466 locations and cleared the holes. They found that 58 anomalies were not associated with any metallic material.

The largest number of false detections occurred in "zone 6" in the NW part of the site (Figure 18), with 34 empty holes out of 129 (including 19 false positives from the low priority quality control list). False detections were triggered by significant variations in the background signal that had not been filtered out. Most of these false detections (Figure 19) tend to concentrate along the hiking trail that runs across the area from the NNW to S. The path created a deep groove in the surface and prevented the operators from maintaining a constant ground clearance.

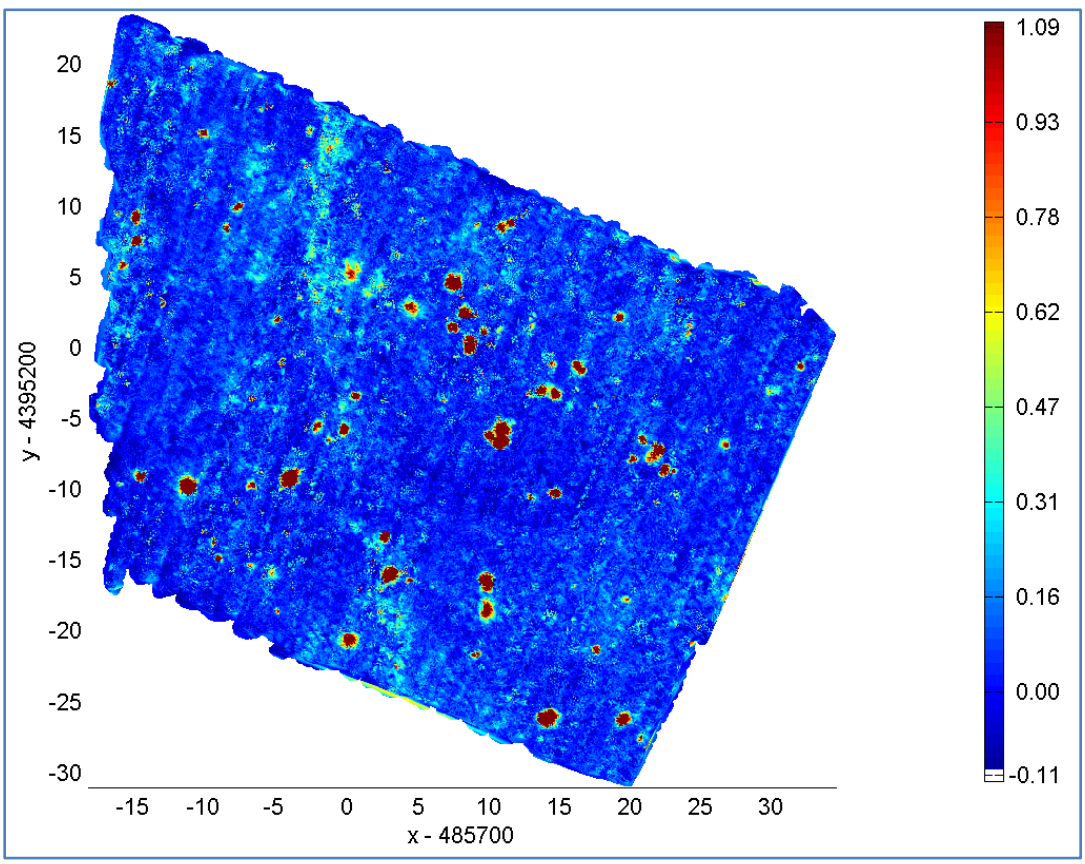

Figure 18: Detection map for zone 6, where many false alarms occurred along the hiking path (NNW to S).

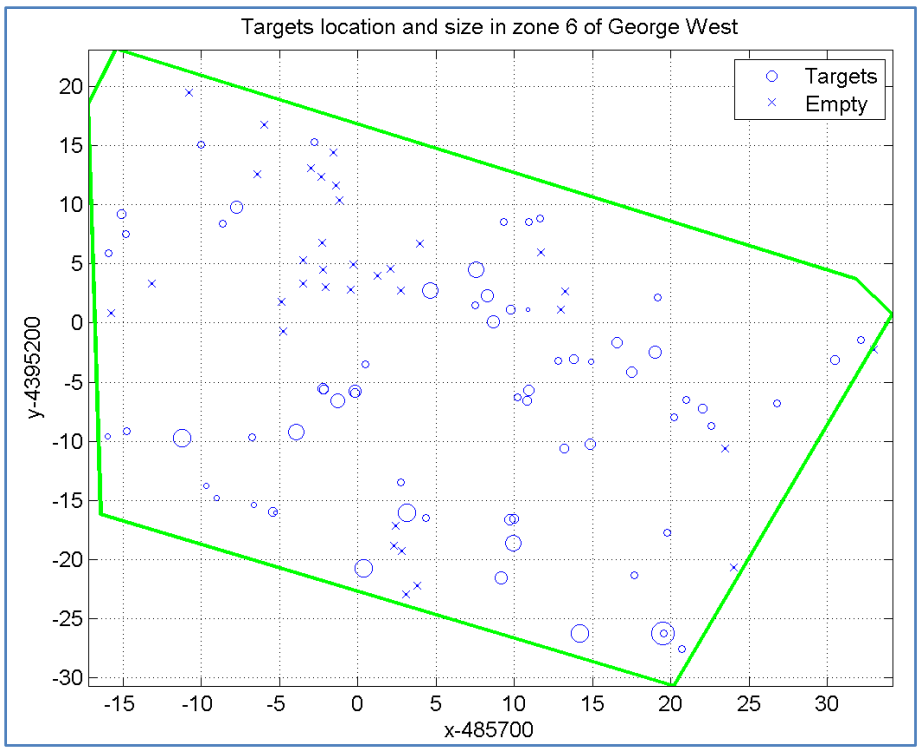

Figure 19: Location and size of excavated items in zone 6 of George West. Most of the empty holes (cross markers) are concentrated along the hiking path that crosses in the NNW to S direction in the W part.

Some false-detection anomalies were due to noise spikes, as shown in Figure 20, where the signal is abnormally high for the late time data of some receivers near target GW-6117. This type of noise was not recognized while picking targets, where, faced with limited time to analyze the data, we took the precautionary approach of not de-spiking or correcting data beyond leveling in order to capture all targets. This late time noise affected 13 of the 34 false detections.

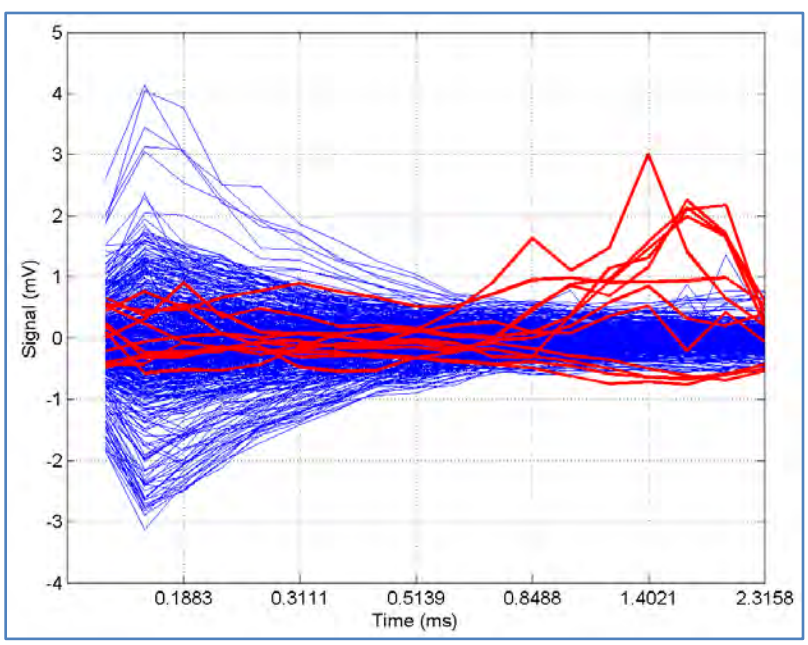

Figure 20: Noisy late-time data can cause false detections (GW-6117).

7.5 Classification with dynamic data

The dynamic data were inverted for single and multiple targets (write up in Appendix D). The data were analyzed independently of the cued data. Classification was attempted with the expectation that 75 mm, medium and small ISO and 37 mm projectiles could be encountered. Training data were requested accordingly. Although no small munitions were found in training, our approach remained conservative and included 37 mm and small ISO. Most targets were clearly identified through classification, leading to an efficient dig list (Figure 21).

Unfortunately, some data mismanagement on the PI part lead to confusion with target GW-3274 and its counterpart GW-13274, which had been created as a new label after inversion of cued data (both targets are clearly visible in Figure 22, which shows transverse component data). In the dynamic dataset both targets stem from the same anomaly and are therefore the result of a multi-target inversion. Training was requested to enquire about GW-3274, which resembled a medium ISO (Figure 23). The training data was mishandled by the PI and the target GW-13274 got pushed beyond the stop digging point. Being an obvious target in terms of its classification parameters, its decision statistic put it just after that stop digging point.

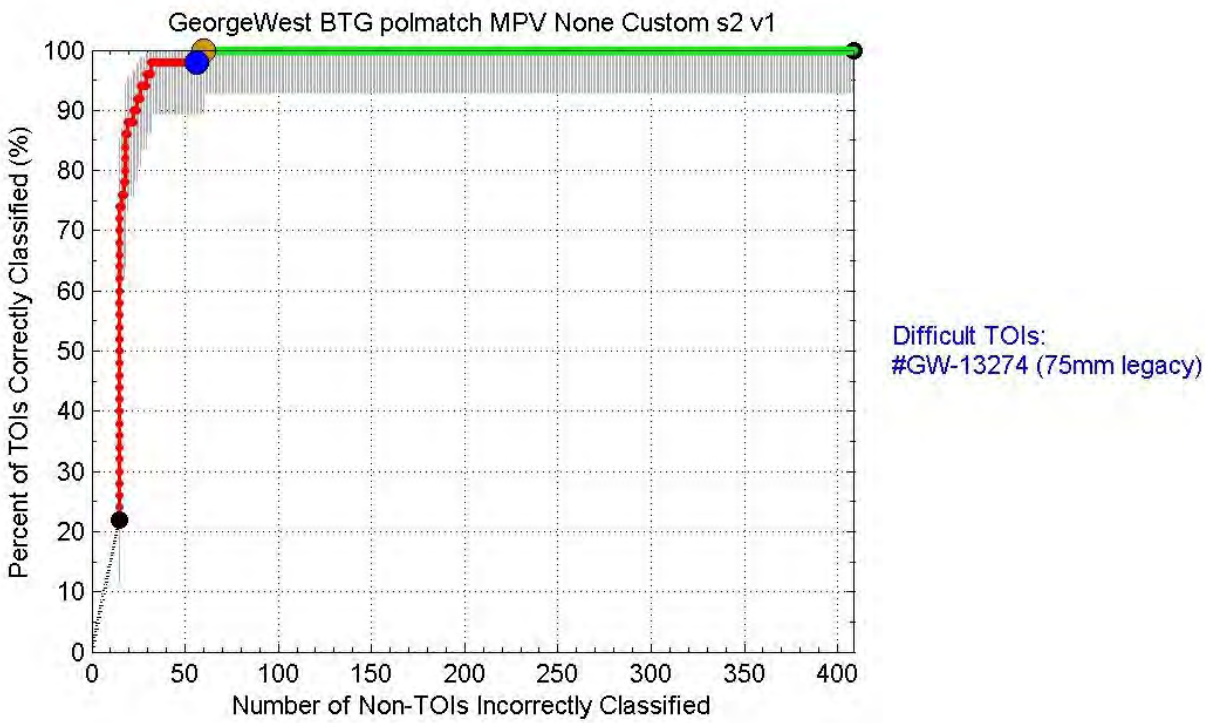

Figure 21: ROC curve for dynamic data analysis.

Besides the one missed target, we found that the dynamic data could generally constrain the target location parameters and at least two of the three polarizability components throughout the dynamic time range. The recovered target parameters proved to be reliable for classification at George West, where only large munitions were found.

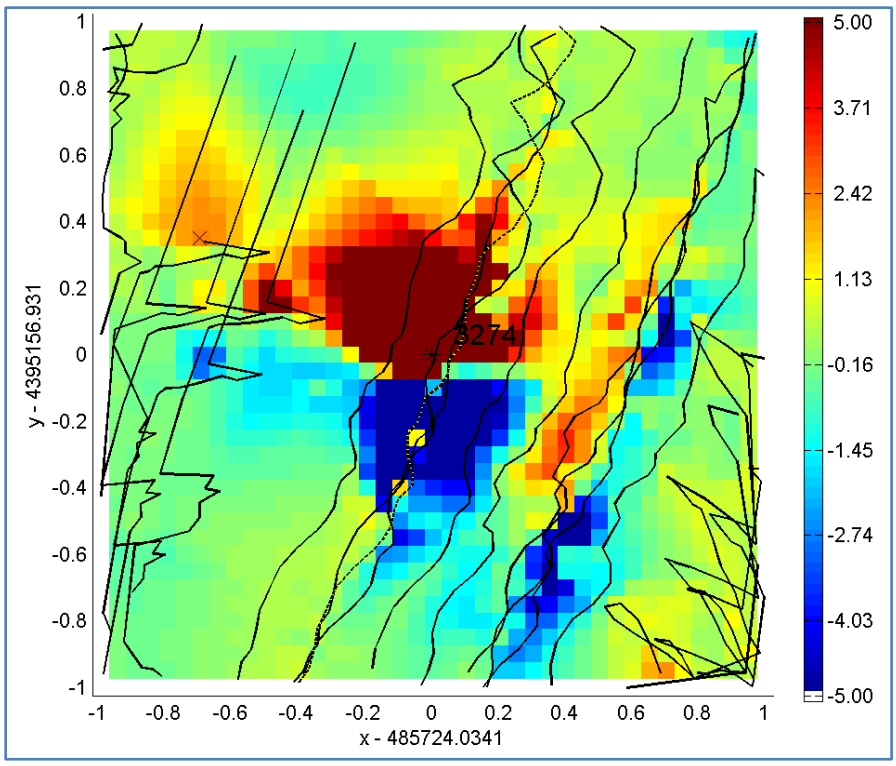

Figure 22: Gridded Y-component data reveals GW-3274 target and secondary GW-13274 at 0.4 m to SE. Transverse component data show a sign reversal near a dipolar target (Y-direction pointing North).

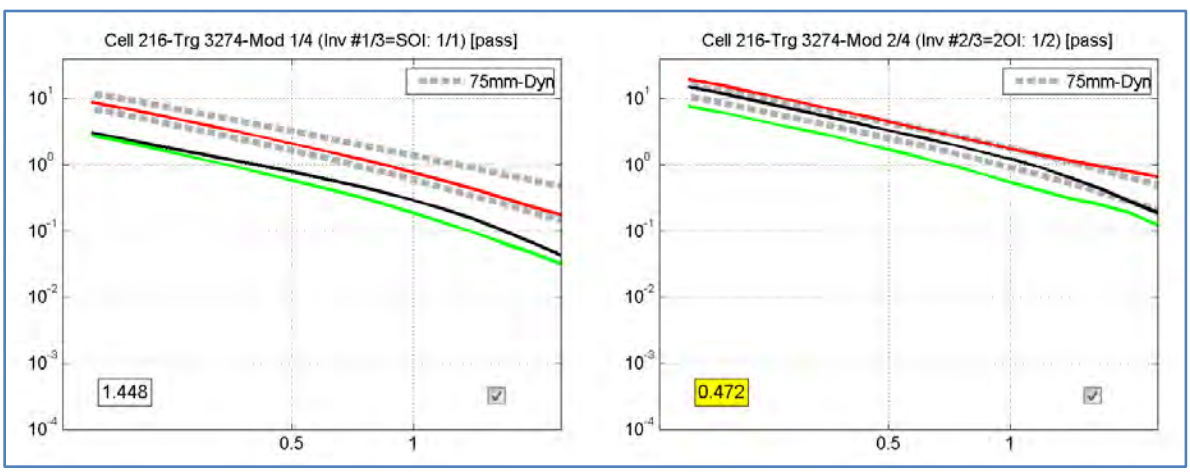

Figure 23: Polarizabilities for GW-3274 (left) and GW-13274 (right) as predicted by multi-target inversion. Training data indicated that GW-3274 was not a TOI. The lower left yellow box in the right panel indicates a low library misfit to a reference 75 mm projectile of 0.472 (lower than 0.6) that classifies the item as a TOI. Unfortunately the analyst made a bookkeeping error in assimilating the training data because both targets had been jointly analyzed. As a result the classification parameters for GW-13274 were pushed right after the dig point when the dig list was generated.

7.6 Classification with static data

The process is thoroughly described in Appendix E, as reported by the classification analyst. We defer the discussion to that section to preserve the integrity of that account. We found that the high data quality and large target size allowed for a clear parameter separation between TOI and scrap. Hence there was an obvious cut off point in the diglist, after which the remaining objects were clearly metallic scrap. The last item on the diglist was a TOI. Non-TOI items on that list were training items. As a result 100% correct classification of TOI was achieved with 92% clutter rejection.

7.7 Estimation of target location and depth

Inversion of cued, static data:

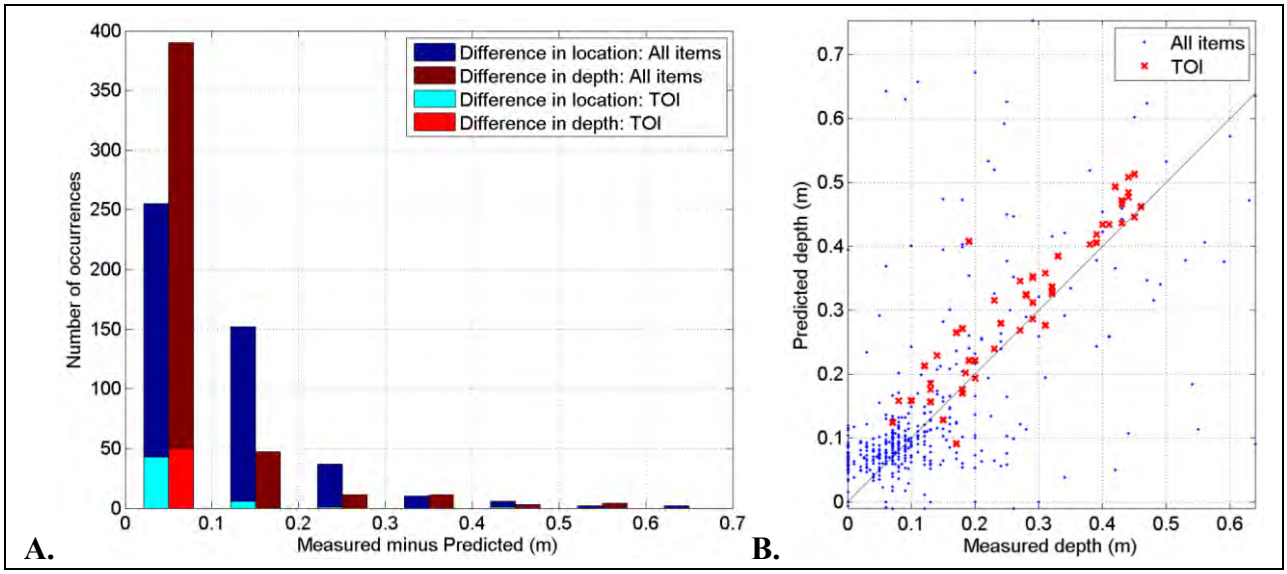

Figure 24: Predictability of target location and depth with cued data.

Results in Figure 24 show that inversion of cued data can predict with high accuracy the location and depth of TOI and clutter. The mean distance between observed and predicted location is 0.12 m and the standard deviation is 0.11 m. For depth prediction, the mean and standard deviation are 0.02 m and 0.10 m, respectively. The right panel details the depth distribution of field anomalies with cued data. Depth prediction of TOI is consistent at any depth. The one TOI outlier is target #12032, which was a secondary target to #2032 with 0.5 m offset. The apparent depth error is an artifact of the large offset and the steep slope because the survey was centered on target #2032. These results show that depth prediction is reliable with cued data.

Target location for detection and inversion:

Anomaly picking was based on a signal amplitude threshold, as usually practiced. In general the location of maximum signal amplitude or the center of the anomaly does not necessarily coincide with the actual target location, especially if the target is not vertical – for instance horizontal anomalies can generate two peaks located near each end of the target. Having inverted all dynamic and static data we can retrospectively compare the predicted target location with the detection pick and ground truth.

The difference between each target location method and the ground truth is shown in Figure 25. Cued inversion provides the best location prediction, as noted above. The anomaly picking method provides the worst prediction with a mean error of 0.20 m and standard deviation of 0.16 m. Locations derived from inverted dynamic data are more accurate than anomaly picking with a mean error of 0.14 m and standard deviation of 0.13 m. Practically, the two methods could be combined in a two stage process in which anomalies would first be picked on threshold and subsequently inverted to locate the underlying target. With high quality data some anomalies could readily be classified without need for re-acquisition for cued interrogation.

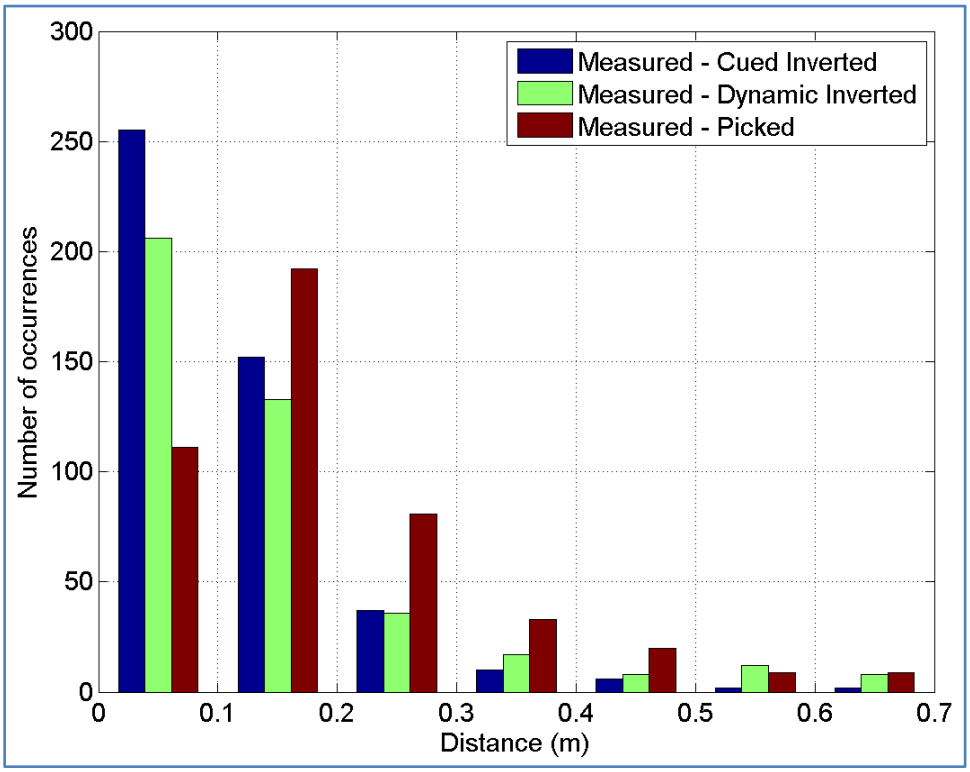

Figure 25: Target location for detection, cued and dynamic inversion and validation.

7.8 Production rate

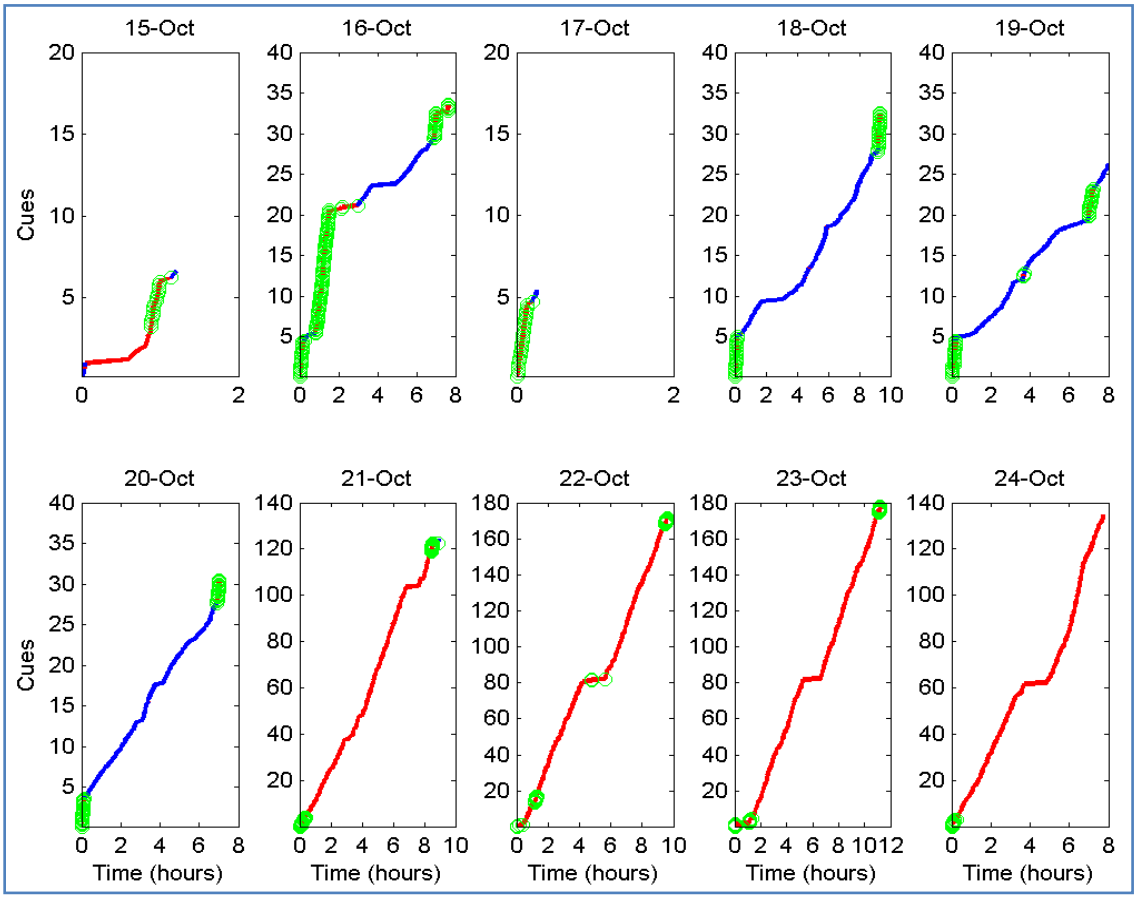

Figure 26: Graphical summary of the daily data-collection activities and production rate. Number of cued flags or group of lines is shown as a function of the time spent in the field each day: Cued interrogation (red), detection (blue), IVS (green circles) and interruptions (plateaus: daily lunch breaks and discussions with visitors). The first and third days only include testing and an IVS survey (travel day and windy day, respectively).

A graphical representation of the daily field activities is shown in Figure 26 as a function of time spent in the field. The field crew arrived at the site on the afternoon of October 15. After unpacking the equipment, assembling the MPV, setting up the GPS and verifying proper operation of the integrated systems, the crew visited the site and started collecting some data on the IVS. The IVS and test pit were studied on the second day. Survey ropes were laid for dynamic detection survey and detection was tested for less than 2 hours. The survey was interrupted for a meeting with local stakeholders and residents. Survey was cancelled on the third day due to extreme winds. The following three days were dedicated to dynamic data collection over 2 acres, with interruptions for moving survey ropes and resting. The next four days were spent on cued interrogation of 530 anomalies, with a peak of 150 targets on October 23. On the last day, 15 targets were reacquired after QC to extend the spatial coverage of their anomalies. The weather conditions had turned to drizzling rain and a jacket was placed on the MPV DAQ. Snow rolled in shortly after.

8.0 COST ASSESSMENT

Time and resources were tracked for each task to assess the cost of deploying the technology at future live sites. Some of the reported costs do not represent those of a completely mature technology for production work yet. For instance, the cued data classification costs include training of geophysicists at appraising MPV inversion results and classification parameters. Cued data pre-processing includes analysis to characterize the new attitude sensors (AHRS) and characterize their stability. Interpretation of dynamic data and target picking were also in developmental stage, in which optimal choice of receivers and channels were being studied for this novel data type. Data processing costs are therefore higher than expected for production-type surveys.

8.1 COST MODEL

A cost model for the George West Demonstration is proposed in Table 3. It is based on a burdened hourly rate of $100 for any of the personnel involved. The field study was conducted with four people for dynamic survey and three people for cued interrogations. The MPV was generally operated with one field technician and one field geophysicist with MPV experience, and one geophysicist who managed the study, provided training, occasionally helped with data collection and handled all data processing tasks. For the dynamic survey a third field person helped with laying out survey lines and taking turns at operating the MPV. Eight days were spent on site.

Table 3: Cost model for MPV demonstration at Camp George West.

Cost Element	Data to be Tracked	Estimated Unit Time	Estimated Total Hours	Estimated Total Cost
Survey preparation				
Sensor maintenance	Unit: $ Cost • MPV maintenance			$5,000
Pre-survey activities	Personnel: Geophysicist • Demonstration plan and coordination • Preparation of survey data		80 h 40 h	$8,000 $4,000
Development time	Personnel required: Geophysicist Time to prepare assimilation of detection data Time to test target picking algorithms Time to review AHRS integration for beacon		10 h 10 h 40 h	$1,000 $1,000 $4,000
Field survey				
Mobilization and demobilization	Cost to mobilize to site: 3 people • Flight, car, hotel, per diem • Shipping • Daily travel	8 h 2 h 0.5 h	48 h 4 h 12 h	$13,000 $3,000 $1,200
Rentals, materials and miscellaneous	Survey equipment rental (GPS) Material supplies Miscellaneous tasks and interruptions	8 h	3 h 24 h	$3,000 $1,000 $2,400

Instrument setup	Typical field crew: 1 geophysicist + 2 tech. • First/last day: unpack/pack, assemble, set up and test pit • Typical day (GPS set up and IVS surveys) • Analyze IVS data (Geophysicist)	12 h 1 h 0.5 h	36 h 14 h 4 h	$3,600 $1,400 $400
Data collection for detection	Field personnel : Field crew of 3 QC personnel : Geophysicist Crew: Time to collect & record data per acre (total 2 acres)	4 h 15 h	6 h 90 h	$9,600
Data collection for cued survey	Personnel : Field crew of 2 Personnel : Geophysicist Crew: Acquire, collect and record data per flag (total 500 flags)	3.6 min	15 h 60 h	$7,500
Pre-processing and QC	Personnel required: Geophysicist Detection: Cost per acre Cued data: Cost per flag Cued data: Additional processing, post survey (review accuracy of beacon positioning)	5 h 2.5 min	10 h 25 h 40 h	$1,000 $2,500 $4,000
Data extraction	Personnel required: Geophysicist Time to built detection map per acre	5 h	10 h	$1,000
Anomaly selection	Personnel required: Geophysicist Time to establish anomaly selection threshold and pick anomalies in dynamic data (per acre)	8 h	16 h	$1,600
Classification of dynamic data (500 anomalies)				
Data extraction	Personnel required: Geophysicist Time to extract and mask dynamic data	2 min	17 h	$1,700
Parameter extraction	Personnel required: Geophysicist Time for inversion & QC	3 min	25 h	$2,500
Classifier training	Personnel required: Geophysicist Time to build feature library for dynamic data	2 min	17h	$1,700
Classification and dig list generation	Personnel required: Geophysicist Time required	2 min	17 h	$1,700
Classification of cued interrogation data (500 anomalies)				
Data extraction	Personnel: Geophysicist in training + expert Time to extract and analyze cued data	3 min	25 h	$2,500
Parameter extraction	Personnel: Geophysicist in training + expert Time for inversion & QC	4 min	34 h	$3,400
Classifier training	Personnel: Geophysicist in training Time to identify features and potential TOI	2.5 min	21 h	$2,100
Classification and dig list production	Personnel: Geophysicist in training + expert Time to prepare memo, apply classifier and assimilate ground truth	2 min	20 h	$2,000

8.2 COST DRIVERS

The MPV was developed to provide a portable sensor with advanced discrimination capabilities that can operate at sites with challenging surveying conditions. As a portable system, deployment logistics and costs for transport and operation are relatively lower than those of towed arrays or other vehicular-based systems. The primary costs are incurred for labor and travel for the operators, and the primary cost driver becomes the duration of deployment, directly related to the acreage to be surveyed as well as the difficulty of the terrain (steep, rocky, very uneven, and wooded terrain can take somewhat longer to survey because it is more difficult to hike across these areas).

8.3 COST BENEFIT

The primary driver for developing the MPV is to make discrimination feasible at a wide range of sites where field conditions prohibit the use of cart-based systems, and for small-scale deployment where a small area needs to be surveyed or where anomalies need to be resurveyed at a lower cost than a cart-based system.

9.0 MANAGEMENT AND STAFFING

A flow chart showing the managerial hierarchy and the relationship between the principal investigator (PI) and other personnel is shown in Figure 27.

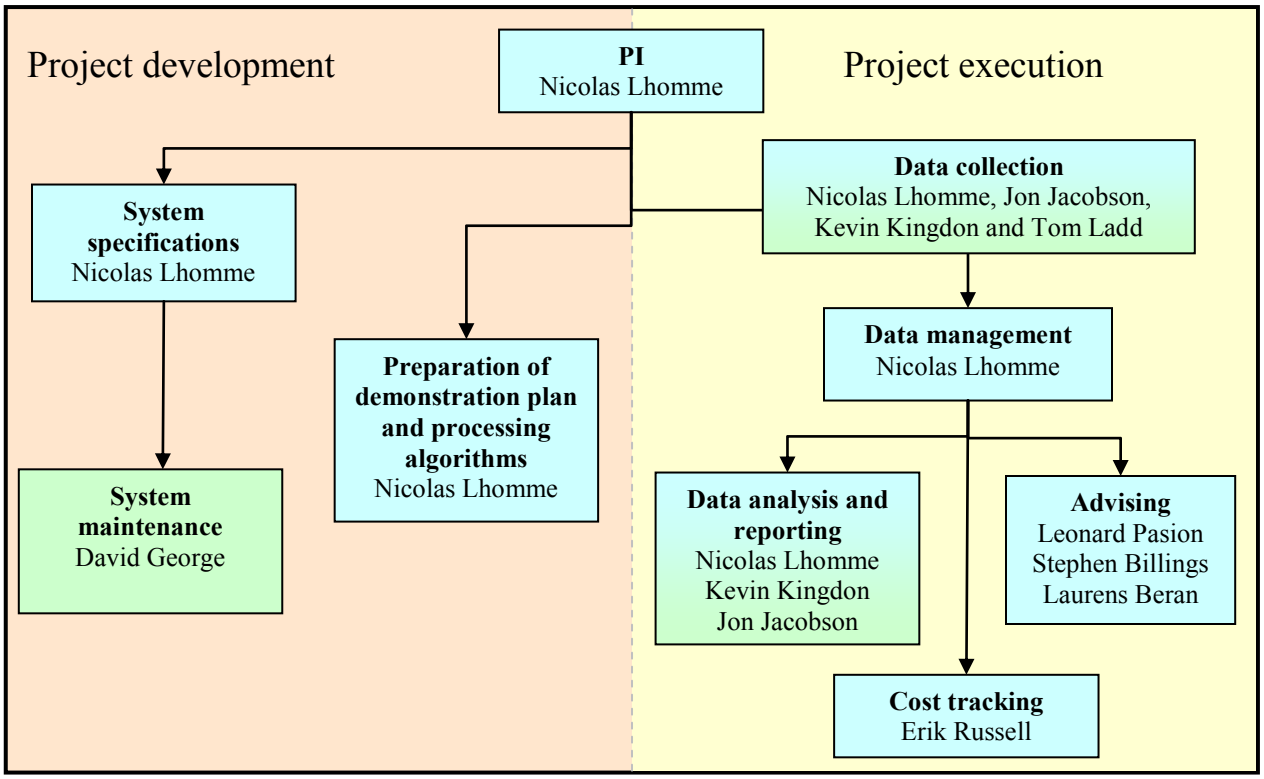

Figure 27: Project management hierarchy for Camp George West demonstration.

Field survey preparation and operation was performed under the direction of the PI Nicolas Lhomme. The PI explained the SOP for data collection and actively participated in the early stages of data collection to ensure adequate survey operation and to verify data quality. Jon Jacobson, who participated in all previous field deployments, led the data collection and trained the crews to operate the MPV for dynamic surveying and cued interrogation. The PI reviewed all collected data, analyzed the dynamic data, picked targets and pre-processed the data. Inversion and classification was done in Vancouver by PI and colleagues. The PI is in charge of communication with ESTCP and reporting.

10.0 REFERENCES

Barrowes, B.E., O'Neill K, George, D.C., Snyder, S., Shubitidze, F. and Fernandez, J. P., Man-Portable Vector Time Domain EMI Sensor and Discrimination Processing. SERDP 1443 FY07 Annual Report, 2007.

Bell, T., Geo-location Requirements for UXO Discrimination. SERDP Geo-location Workshop, 2005.

Billings, S., Pasion, L., Lhomme, N. and Oldenburg, D., Discrimination at Camp Sibert using Time-Domain EM. SERDP/ESTCP Partners in Environmental Technology Symposium, Wash., DC, Dec. 2007.

Gasperikova, E., Smith, J. T., Morrison, H. F. and Becker, A., BUD results from the ESTCP Demonstration sites. SERDP/ESTCP Partners in Environmental Technology Symposium, Wash., DC, Dec. 2007

Lhomme, N., Barrowes, B. E. and George, D. C., EMI sensor positioning using a beacon approach. Proceedings of SPIE Defense, Security+Sensing, Orlando, Florida, April 2011.

Lhomme, N., Demonstration of MPV Sensor at Yuma Proving Ground, Arizona. Demonstration Report. ESTCP Project MR-201005, 2011b.

Pasion, L. & Oldenburg, D., A Discrimination Algorithm for UXO Using Time Domain Electromagnetics. Journal of Engineering and Environmental Geophysics, 28, 91-102, 2001.

San Filippo, B., Norton, S. and Won, I. J., Precision Local Positioning of an EMI Sensor Using the Transmitter as a Beacon, SERDP/ESTCP Partners Symposium, 2007.

Stakeholder Review Draft, Colorado Site Inspection Report, Army National Guard Munitions Response Sites, Site Inspection Phase, CH2M HILL, March, 2012.

APPENDICES

Appendix A: Health and Safety Plan (HASP)

Health and safety procedures will be followed as indicated below, and will also comply with the ESTCP guidance for this demonstration.

- **Applicable local, state, and federal health and safety laws and regulations**

  On-site staff will comply with health and safety requirements in accordance with Code of Federal Regulations (CFR), Part 29, Section 1910.120 and any site-specific requirements as noted during site orientation or other direction provided by ESTCP and Colorado Parks representatives. Although 29 CFR 1910.120 pertains to personnel conducting activities at known or suspected hazardous waste sites and may not be directly applicable to the planned activities, the code provides a reasonable framework safe work practices.
- **Potential for worker exposure to hazardous materials and/or other hazards**: None or minimal. Any site-specific hazards also will be briefed during orientation.
- **Physical requirements are expected of workers**: Basic fitness, heat resilience.
- **Number of people required to operate the technology:** Two field operators and one QC person (PI)
- **Technology's history of breakdowns or accidents:** No issues to date.
- **Potential effects from the transporting of equipment, samples, wastes, or other materials associated with the technology:** All components of the technology are inert, to the exception of Li-ion batteries that must be shipped by ground according to federal regulation.
- **Impact of technology on surrounding environment:** None. Technology is non destructive and man portable.
- **Closest medical facility:** St.-Anthony Hospital
  11600 West 2nd Place
  Lakewood, CO 80228, United States

Driving directions from study site:

1. Head **southeast** on **W Exposition Dr** toward **S Gardenia St**	443 ft
2. Take the 1st left onto **S Gardenia St**	289 ft
3. Take the 1st right onto **W Center Dr**	1.0 mi
4. Turn right onto **W Alaska Pl**	269 ft
5. Turn left onto **S Alkire St**	0.2 mi
6. S Alkire St turns right and becomes **W Cedar Dr**	0.8 mi
7. Turn left onto **S Union Blvd**	0.4 mi
8. Turn right onto **W 2nd Pl**	486 ft
9. Turn right onto **Healing Way**	0.1 mi

The facilities are indicated on the map of Figure 28 relative to the test area.

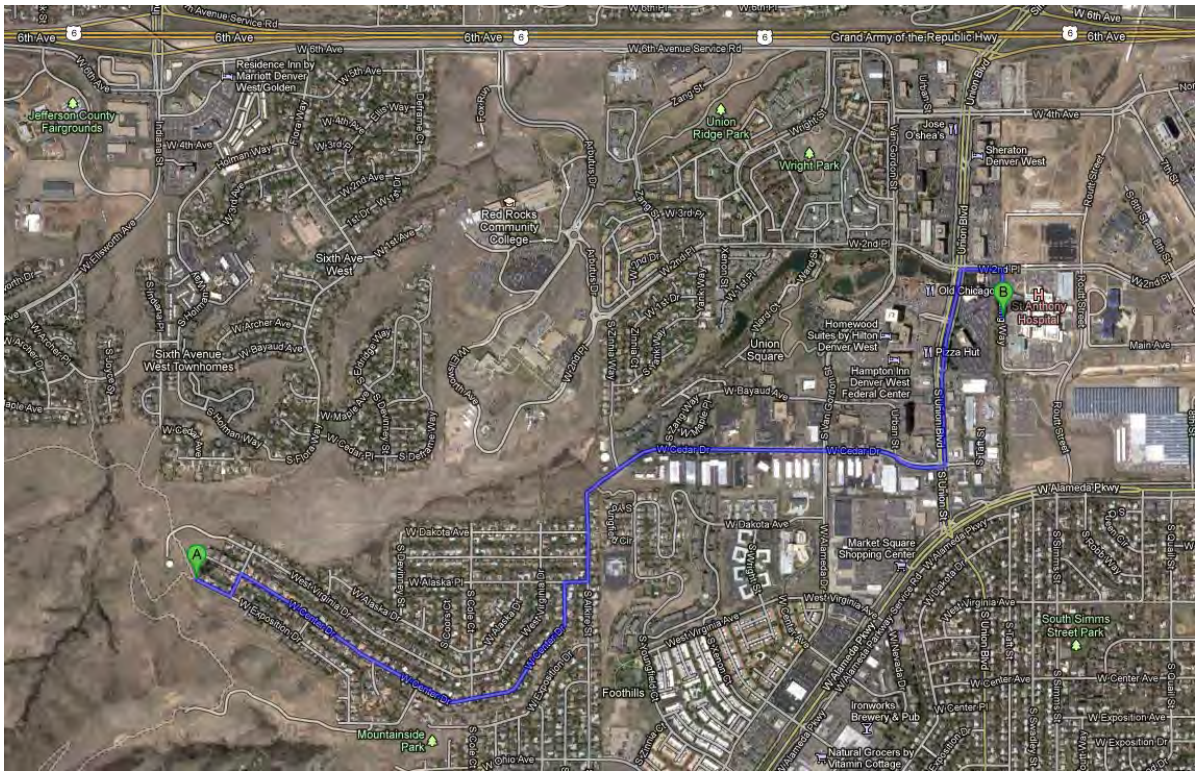

Figure 28: Location of medical facilities: St. Anthony Hospital in Lakewood, CO.

Appendix B: Points of Contact

Points of contact (POCs) involved in the demonstration and their contact information are presented in Table 4.

Table 4: Points of Contact for the MPV Demonstration.

POINT OF CONTACT Name	ORGANIZATION Name Address	Phone Fax E-mail	Role in Project
Dr. Nicolas Lhomme	Black Tusk Geophysics, Inc. 112 A, 2386 East Mall, Vancouver, BC V6T 1Z3, Canada	Tel: 604-428-3382 Nicolas.Lhomme@btgeophysics.com	PI
David George	G&G Sciences, Inc. 873 23 Rd Grand Junction, CO 81505	Tel: (970) 263-9714 Fax: (970) 263-9714 dgeorge@ggsciences.com	Sensor manufacturer
Dr. Herb Nelson	ESTCP Program Office 4800 Mark Center Drive Suite 17D08 Alexandria, VA 22350-3605	Tel: 571-372-6400 Herbert.Nelson@osd.mil	ESTCP Munitions Management Program Manager
Tracie White	Colorado Department of Public Health & Environment Hazardous Materials & Waste Management Division 4300 Cherry Ck Drive South Denver, CO 80246-1530	Tel: 303.692.3452 Fax: 303.691.7878 tracie.white@state.co.us	Project Manager and Local Stakeholder

Appendix C: Detection range with MPV survey

This appendix material was included in the original demonstration plan. The analysis was revised on site once the detection depth was decided and experimental data were acquired.

C.1. Spatial coverage requirement and detection depth

The MPV footprint in a detection survey can be assessed by studying the amplitude of the signal on a side receiver as a function of the target offset. We simulate a projectile placed at various horizontal offsets and depths in horizontal position (weakest signal) and vertical orientation (shortest spatial decay) and compare with strong background signal (Beale soil). Model polarizabilities are extracted from static data (proven to have similar decay as dynamic one in 0-2.7 ms excitation range); background measurements come from Camp Beale.

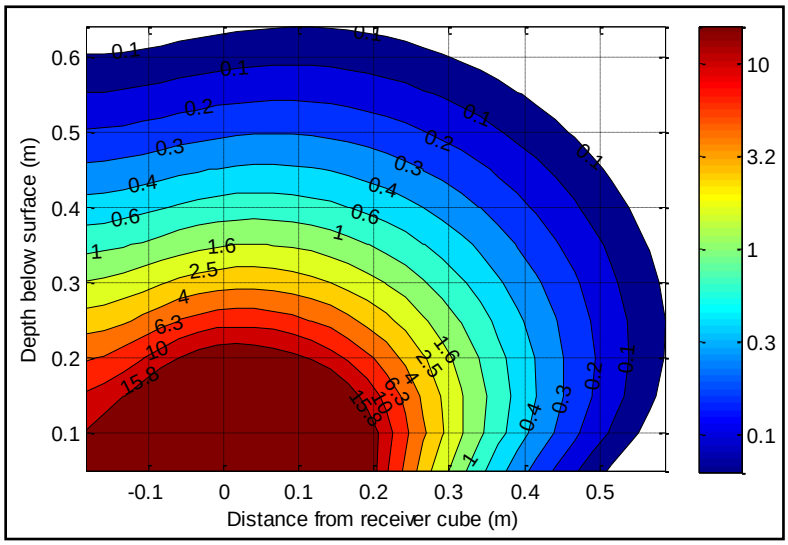

Figure 29: SNR cross section map for different target offset and depth relative to MPV receiver. A 37 mm projectile is placed in horizontal orientation. Noise is based on Camp Beale magnetic soil. Reference receiver is MPV side cube #2. Negative coordinates correspond to points closer to the center of the sensor than cube #2. SNR=1 when signal and background have equal amplitude; target are detectable when SNR>1.6 (signal is 60% larger than noise).

The relative amplitude of target signal and background noise (Signal to Noise Ratio or SNR) is illustrated in Figure 29 for a typical 37 mm in a horizontal orientation. The figure shows the SNR for different positions and depths of the target relative to a side receiver on the MPV. When the target is below the receiver (Distance=0), it is detectable at 35 cm depth as signal exceeds noise by 60% (SNR=1.6 contour). Similar detection signal would be observed with 10 cm lateral offset. At 20 cm offset, the target would be detected at up to 30 cm depth. If the target was vertical it would be clearly detected at 35 cm depth with a lateral offset of up to 15 cm (Figure 30). Therefore we assume that a 10 cm target offset would maintain detection of a 37 mm target.

Simulations for a 105mm projectile suggest detection in Camp-Beale-type conditions at 70 cm with 10 cm offset (Figure 31). Detection depth would increase by 20-30 cm at a site with low background response, for instance at the Beale IVS (Figure 32). Overall detection depth is generally unaffected when the target is up to 10 cm away from the sensor head and therefore the sensor footprint is approximately 70 cm (50 cm diameter sensor head plus 10 cm on either side).

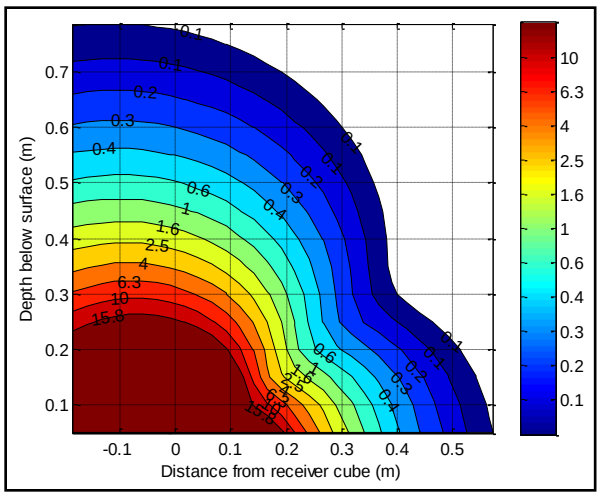

Figure 30: SNR contour lines for 37 mm target in vertical orientation.

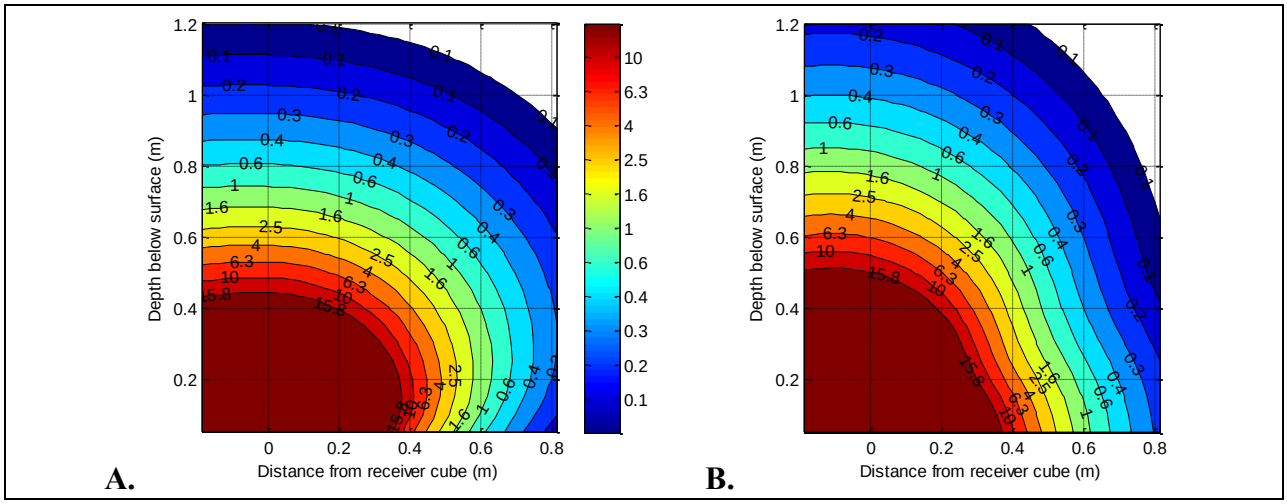

Figure 31: Detection contour for 105 mm projectile in horizontal (A) and vertical (B) position.

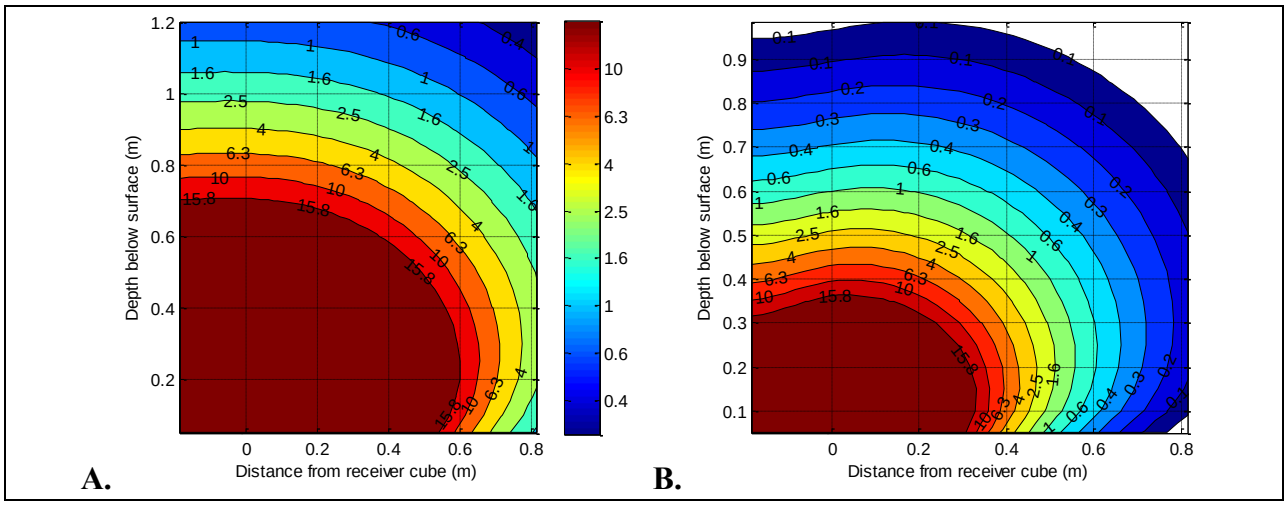

Figure 32: Detection contour in quiet background for 105mm (A) and 37 mm (B) in horizontal position. Depth of investigation is increased.

C.2. Detection threshold for 75 mm projectile

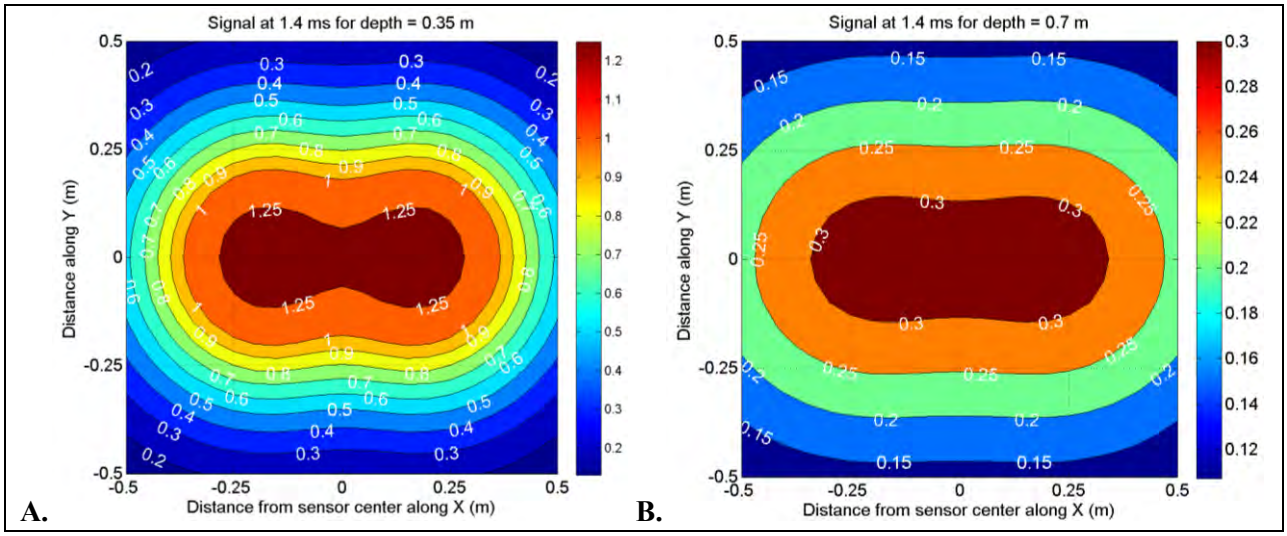

Figure 33: Predicted total response for 37 mm (A) and 75 mm (B) projectiles placed in horizontal position. Here the total response is the sum of the signal amplitude on all receivers at 1.4 ms.

The predicted response for a dynamic survey with the MPV over a 75 mm projectile can be simulated by utilizing the target polarizabilities inferred from the detection survey on the IVS at Spencer Range. As shown in Figure 33, the target response of a 75 mm projectile at 0.7 m depth is significantly weaker than that of a 37 mm at 0.35 m (the objective at Spencer).

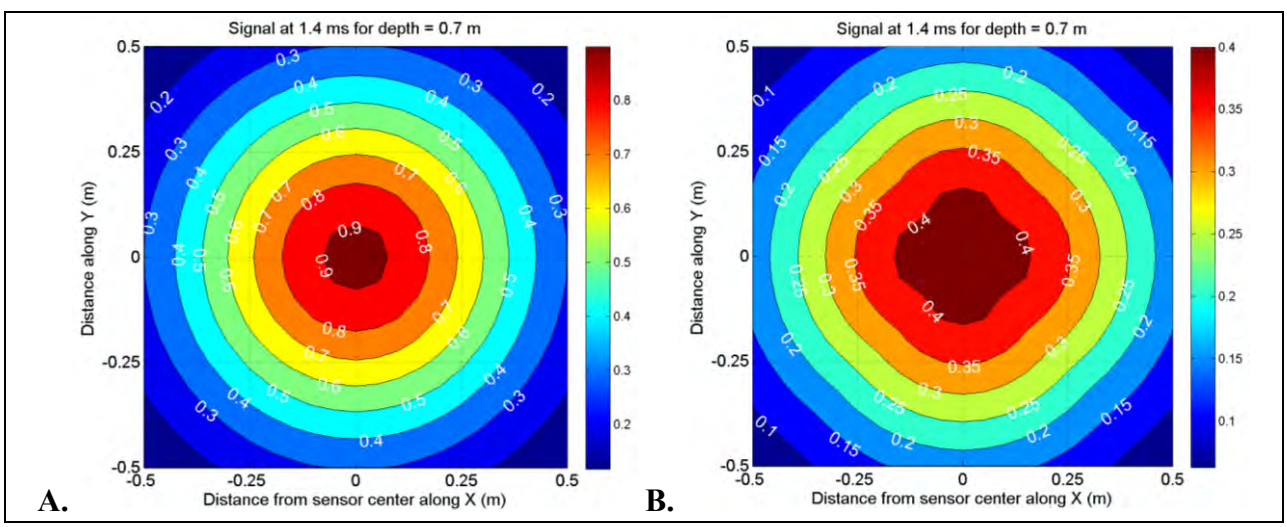

Figure 34: Surface anomaly for a dynamic survey above a 75 mm target at 0.7 m depth in vertical position using the sensor total response (A) or the maximum total field (B) (detection map based on 1.4 ms simulated response).

In contrast with the Spencer study, we propose to base our analysis here on the total response, defined as the square root of the sum of the squared amplitude over all the receivers (5 cubes with 3 receivers each), as opposed to the maximum value among cubes of the total field (norm of the 3 orthogonal receiver coils). The amplitude of the former is twice as large (Figure 34) while

the associated background noise response variability is approximately 40% larger (Figure 35), which improves detection.

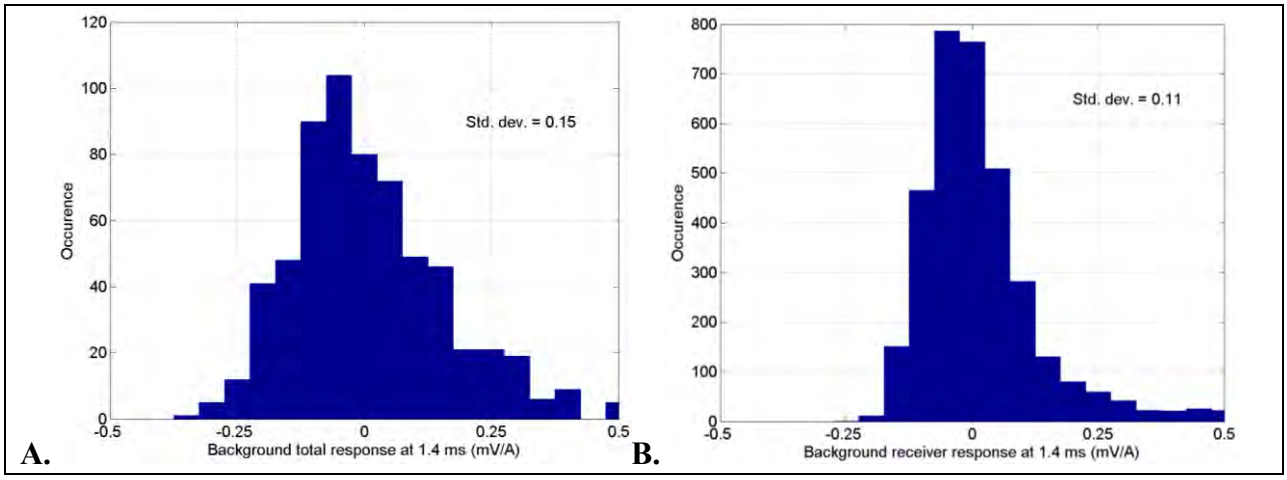

Figure 35: Variability of background response using sensor total response (A) or maximum total field (B).

Background noise in detection data varies as a function of intrinsic sensor noise, environmental noise and sensor motion (ground clearance). This variability is characterized in Figure 35. After leveling of the background noise, the data keep some variability and one can expect that a target would be detectable when its anomaly consistently exceeds 2 standard deviations – e.g., 0.3 mV/A for the total response. At 0.70 m the target is clearly detectable in vertical position (Figure 34), whereas it is close to detection sensitivity in horizontal position (Figure 33B). The depth of investigation at Camp George West could be reduced if surface obstacles such as vegetation and boulders force large variations in sensor height or large horizontal offsets. The total response as a function of target depth and offset is shown in Figure 36. If the detection objective was to detect a 75 mm projectile at 0.70 m depth, an additional 0.05 m of ground clearance (or 0.75 m equivalent target depth) would require a lower threshold of 0.22 mV/A.

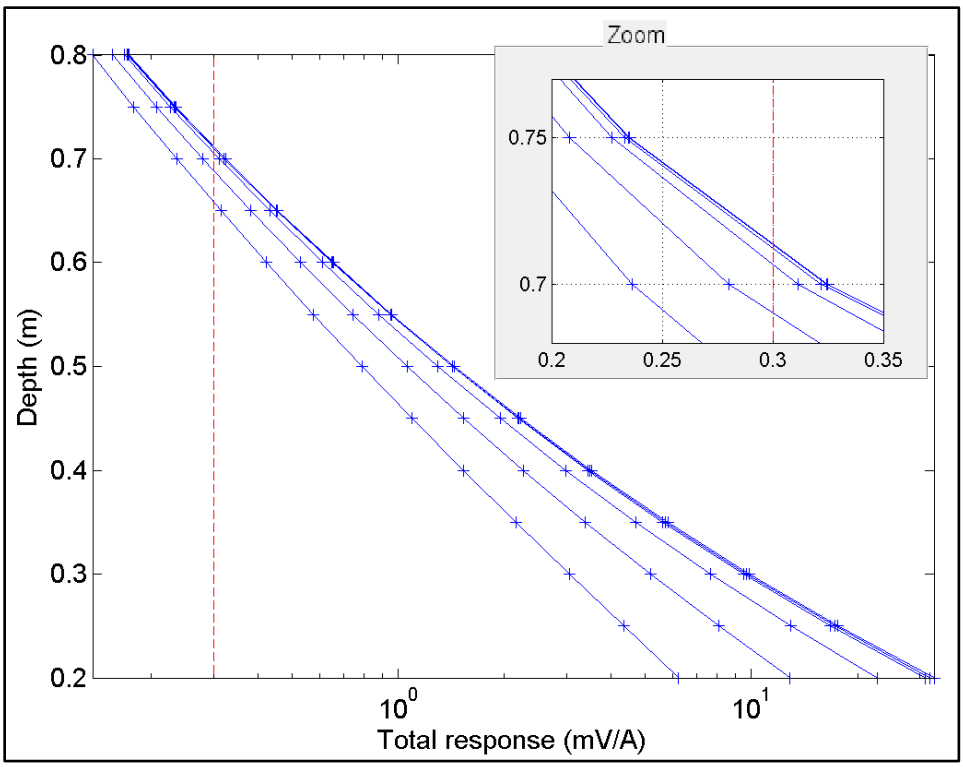

Figure 36: Signal amplitude as a function of depth for a 75 mm projectile in horizontal orientation. The blue curves represent signal amplitude for different horizontal offset between sensor head and target, with 0.10 m increments from 0 to the left. The red line indicates the 0.3 mV/A threshold. Zoom in inset.

The probability of detecting a 75 mm target at a given depth can be explored through Monte Carlo simulations. Assuming that there is a uniform probability for the target position, depth and orientation and for the sensor attitude, and that the target is within 0.40 m of the sensor head, we find that the probability of a target among other similar targets at the same depth would be below the 0.3 mV/A threshold is 2% at a depth of 0.55 m, 5% at 0.60 m, 9% at 0.65 m, 11% at 0.70 m and 16% at 0.75m. Increasing that threshold to 0.5 mV/A, the probabilities are 7, 11, 15, 19 and 26%, respectively. The probability that a 75 mm reaches a depth of 0.70 m is small. The resulting probability that we miss that target is 10 times as small with a 0.3 mV/A threshold and 5 times as small with 0.5 mV/A.

If we assume that the distribution of depth for a 75 mm matches the positive side of a normal distribution with zero mean and 0.5 m standard deviation (this puts 16% of targets below 0.70 m, which seems unrealistically high), then the probability of a target with a detection signal below 0.3 mV/A is 0.8% and below 0.5 mV/A is 1.8%.

Appendix D: Classification memorandum for dynamic data

The following section was submitted as an independent document to the ESTCP Program Office after analysis of the training data and prior to submitting a ranked anomaly list.

1. Methodology

Classification is performed using the standard UXOLab software. The dynamically acquired data were inverted using standard inversion parameters as proposed in the demonstration plan. Results were reviewed to verify that the recovered models fit the observed data. When necessary, inversions were redone after altering model-search bounds or masking out some data in order to improve the fits. Models that did not fit the data of interest were rejected while all other plausible models were kept for classification. A spatial representation of the recovered models is shown in Figure 37, for which size and decay parameters were derived from inverted polarizabilities.

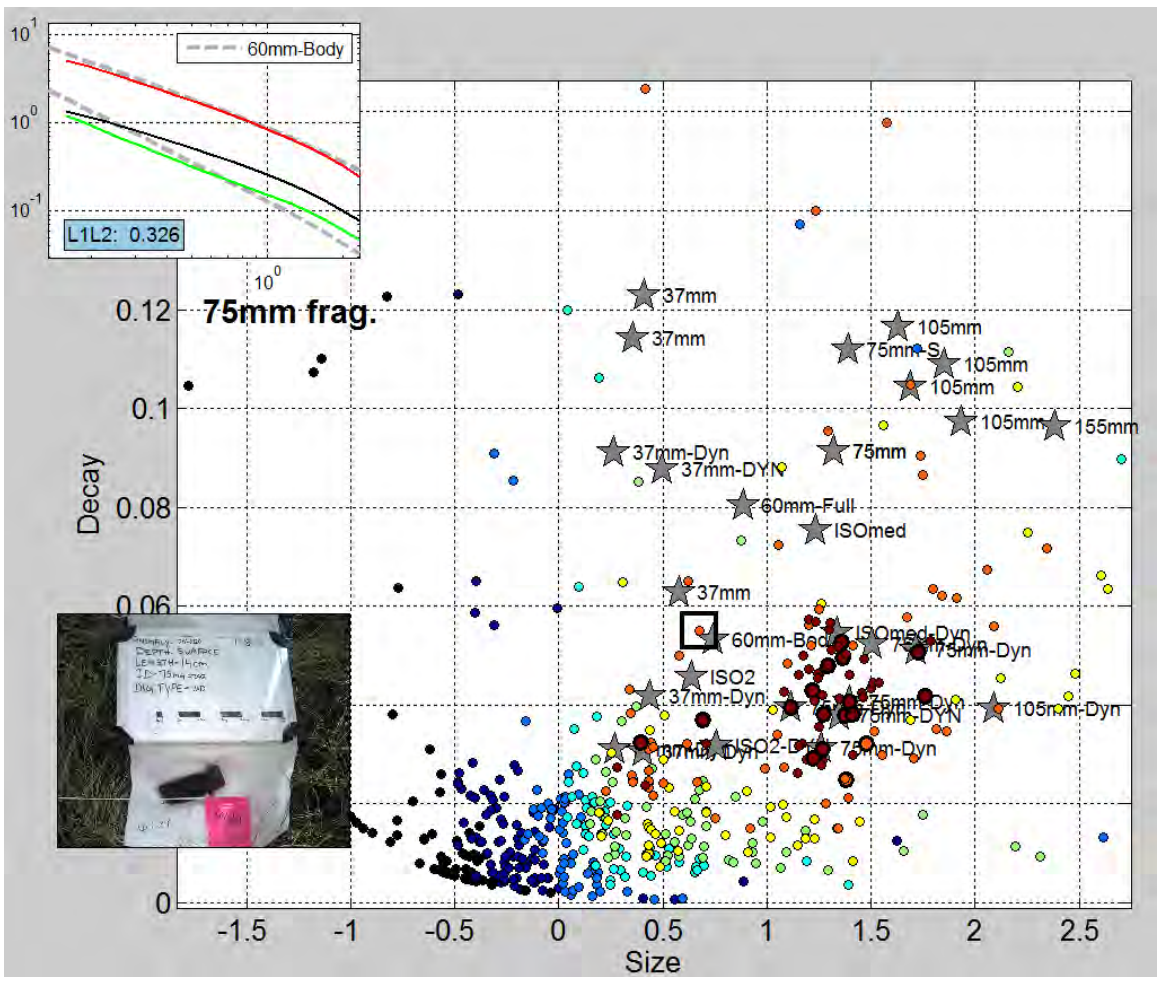

Figure 37: Distribution of target size and decay parameters relative to reference UXOs. Symbol colors (from red to yellow then blue) reflect the likelyhood that anomalies are potential UXO (based on default library misfit metrics). The reference library here includes statistically-inferred polarizabilities to compensate for the small sample set of targets surveyed in dynamic mode.

2. Unclassifiable anomalies

Every field anomaly was fit with a model that either described a metallic object or a background response from the soil (which has low magnetic viscous remanence at the site).

3. Classification approach and features

Classification is based the recognition of typical UXO features. Potential UXO are identified because their recovered target parameters – or signature – resemble known UXO, or there are multiple occurrences of metallic objects with highly similar features. The classification features are the three time-varying, orthogonal polarizabilities that are derived from the geophysical inversion of field data.

4. Training data selection

Training data were requested in order to establish the degree of confidence with which inverted polarizabilities could be trusted for classification, similar to a sensitivity analysis. The anomalies of interest were selected because either the amplitude or decay rate of one of the polarizabilities was deviating from a library item. The results are summarized in Table 5. We found that, for the selected anomalies, an increase in decay rate after 1.5 ms relative to library items is a sign of clutter and that the amplitudes of all three polarizabilities were informative, though slight shifts in amplitude could occur (probably from leveling the data).

Table 5: Training data request.

Anomaly	Reason for training	Depth (cm)	Identification	Dig Type	Interpretation
GW-10	75mm	7	75mm Frag	MD	no match with L3
GW-10		6.5	75mm Base	MD	2nde target possible but not guaranteed
GW-2028	37mm for L13 or L12	15	75mm Frag	MD	Trust all of L123
GW-2038	75mm, lower L1	20	TOI, 75mm partial with filler (base).	TOI	Attention to amplitude shift from leveling
GW-3014	75mm for 2Ls	15	75mm.	TOI	Trust L123
GW-3268	60mm body at early time	7	75mm Frag	MD	Trust late time and L123
GW-3271	75mm or ISO2	38	75mm.	TOI	lower amplitude than ref
GW-3274	ISO2 early time, mediocre coverage	7	Frag	MD	Trust late time
GW-37	75mm w larger L23	27	75mm.	TOI	Shift on amplitude depending on mask size
GW-4039	ISO2	0	Frag	MD	Slightly faster decay
GW-4043	75mm for L1L3	29	75mm.	TOI	L2 or L3 slightly off
GW-50	75mm at early time	30	75mm Frag	MD	Decay faster than 75mm: Trust late time

GW-50	mediocre coverage	31	75mm Frag	MD	
GW-50		31.5	75mm Frag	MD	
GW-5005	37mm or ISO2	8	75mm frag.	MD	Slightly faster decay
GW-5014	105mm	44	75mm.	TOI	Amplitude shift from leveling
GW-5015	75mm	44	75mm.	TOI	TOI solution has 75mm looking like plate with loglin decay
GW-5080	37mm for L12, slight decay diff	7.5	Frag	MD	Decay rate and L123
GW-5091	37mm for L12	7	Frag	MD	Yes for multi
GW-5091	Multi	18	Frag	MD	Trust L123 and decay rate
GW-6071	Deep 105mm?	15	Hot rock @ 8	NC	Unstable L123 for 105 - only L1 for 75mm
GW-6081	75mm for L1	39	Hot Rock Layer 8	NC	Risk to confuse with 75mm-multi
GW-6120	60mm body for L1, different decay L23	0	75mm frag.	MD	Trust L123 and decay rate
GW-6144	37mm for L13 but faster decay	1	Frag	MD	Trust L123 and decay rate
GW-7001	ISO2 for L13 perfect - mediocre coverage	1	75mm frag.	MD	Trust L123
GW-86	37mm for L13	26	75mm Frag	MD	Trust all of L123 to reject

5. Parameters and thresholds

We propose to apply a multi-stage classifier using the same standard methods as those applied to other sensor data as part of ESTCP MR-201159. The classifier is primarily based on polarizability library misfits. The first stage uses all three polarizabilities (L1L2L3), the second L1L2, the third L1L3 and the fourth just L1. Transitions from one stage to the next are selected by applying the classifier to the entire dataset and using the fact that some items were marked as UXO either during the inversion QC or from training data. For each stage the decision statistic resembles an L-shaped curve in which the elbow marks a transition in the statistic – stage thresholds are chosen near the elbow (Figure 38).

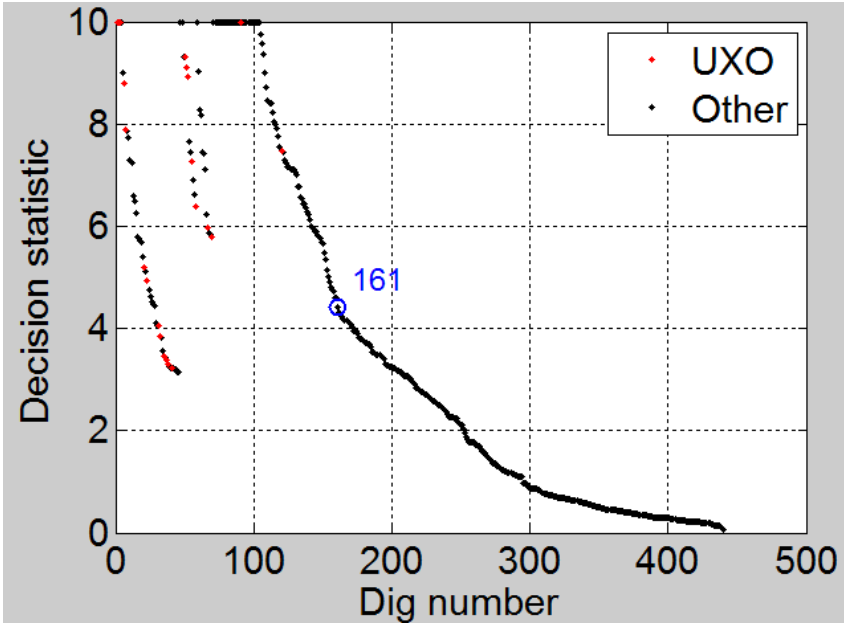

Figure 38: Decision statistic based on "recognized UXO" (red dots).

6. Stop-dig decision

A dig list is generated with the multi-stage classifier. The corresponding polarizabilities are visually inspected to verify that the classifier performs as expected and to gauge the relevance of the selected parameters – for instance obvious soil-like models may be selected by the classifier because they resemble a UXO more than their nearby clutter, in which case the model can be manually rejected. Training data are left among other anomalies to relate their associated polarizabilities to similar-ranked anomalies. The operator manually selects a stop dig point after which UXO are less likely to appear.

7. Stage 1 list: analysis of missed targets

Four targets of interest were missed in the first stage of classification. A summary of target parameters and data fits is shown for each target in Figure 39 to Figure 44. These targets could have been identified if a higher tolerance to library misfit had been applied. In particular, all four items could have been selected with moderate relaxation of the misfit to the first two polarizabilities.

Target GW-6021 would not immediately pass this criteria due to the inversion QC, in which an inversion with lower fit to the data was failed while its associated target parameters L1L2 would fit a 75mm projectile. Because there is an element of subjectivity in the inversion QC process in which the operator may decide to pass or fail some inversions based on a combination of metrics, we shall not alter the inversion QC conclusions at this stage. Instead we adapt the classifier to work with the validated models. Target GW-6021 does not clearly match a 75mm with L1L2, we introduce an intermediate classification stage in which we automatically search with the classification software for the best combination of L1, L2+L3 and size and decay parameters so as to capture all four items. As shown with the decision statistic of Figure 45 this classification stage is particularly efficient. We apply these classification parameters and combine with the other classification parameters to build and submit the Stage 2 dig list.

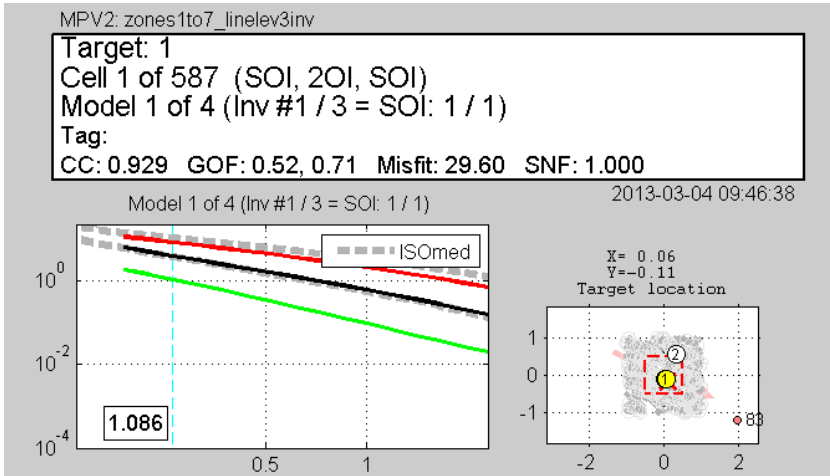

Figure 39: Classification of target GW-1. The first two polarizability curves L1-L2 match with medium ISO. Details on the data fit are shown in Figure 40 below.

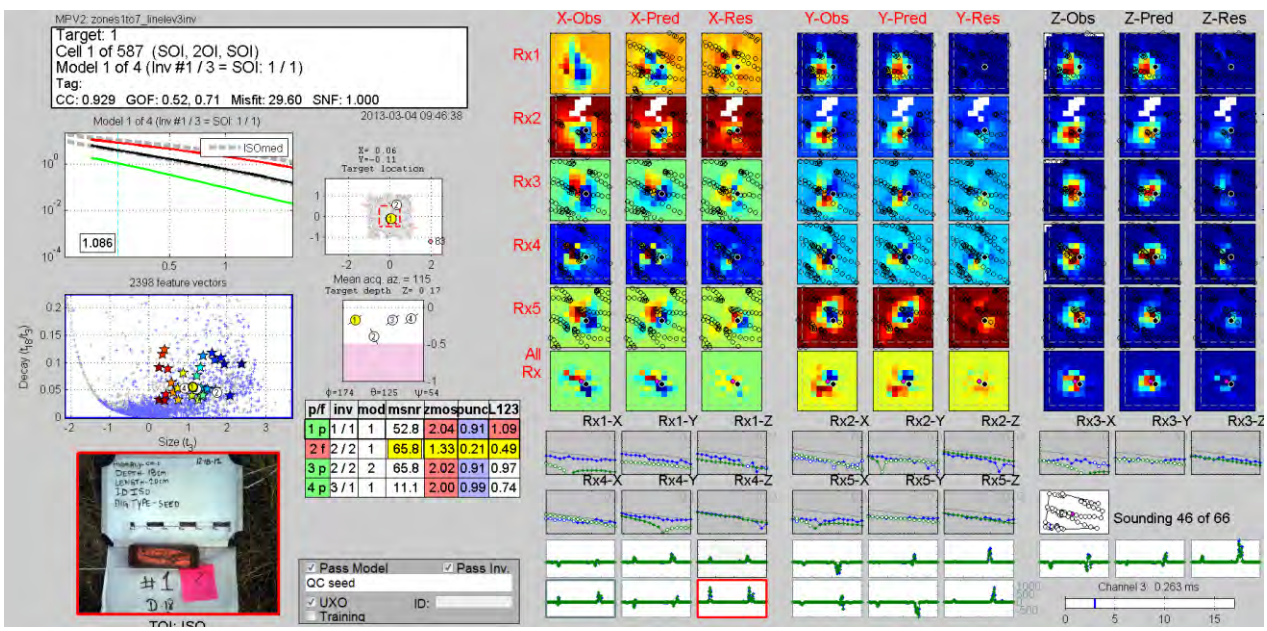

Figure 40: Full inversion QC display for Target GW-1

The left side displays the target parameters of Figure 39, including polarizability decay curves (top left), location map, feature plot for size and decay (stars show reference items), predicted depth for different models, ground truth picture, data quality metrics and QC comments. Here the first two recovered polarizabilities do match those of a medium ISO.

The right side panels detail the data fits. In the upper part there are 3 groups with 3 columns each of gridded data. Each group corresponds to a data component (X, Y and Z); within each group the first column shows observed data, the second one predicted data and the third one residual. Each row corresponds to a receiver cube (Rx1-5) and the sixth row aggregates all cubes. The gridded images show close fit to observed data.

The lower part includes a series of profiles: the top two rows have the time decay at one point; the bottom two rows show all points at a given time channel (0.263 ms).

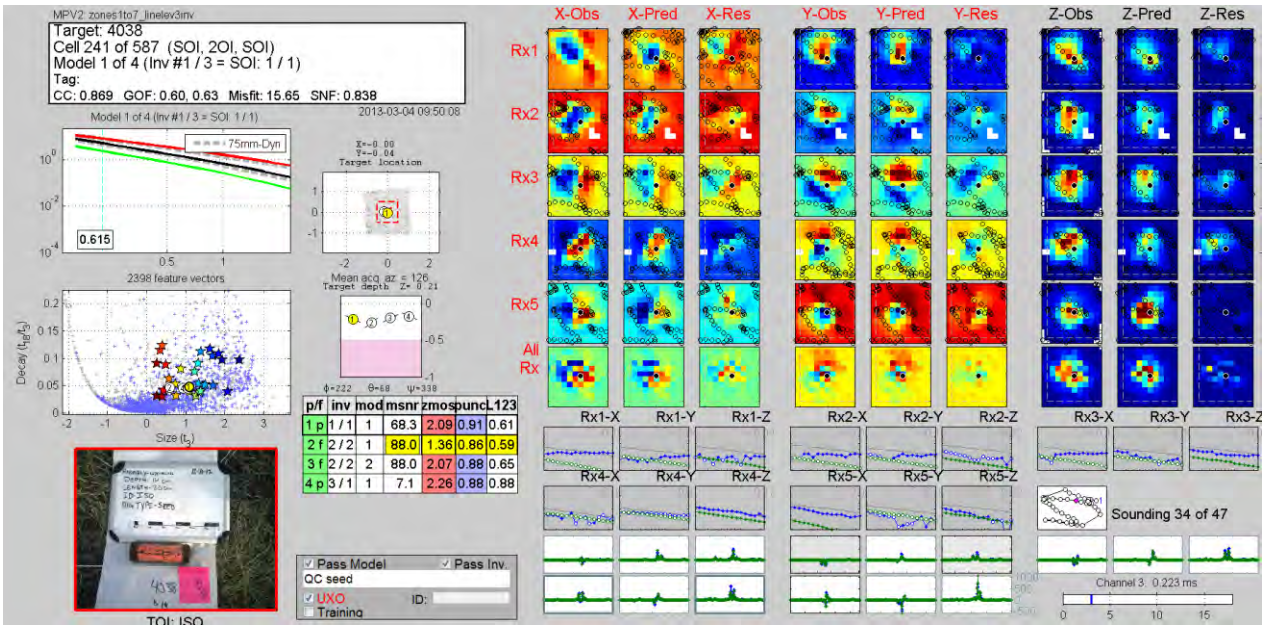

Figure 41: Target GW-4038 would relate to a 75 mm projectile according to the L1 and L2 parameters for the single-target inversion (it would also fit a medium ISO with larger tolerance).

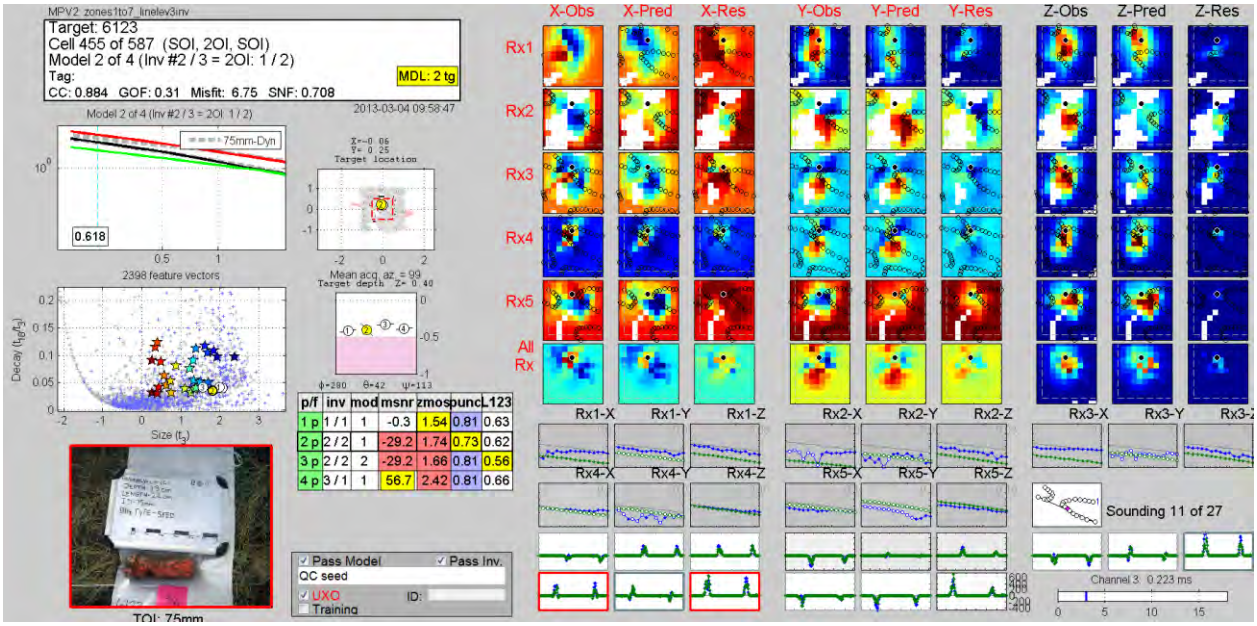

Figure 42: Target GW-6123 does fit a 75 mm projectile using the L1 and L2 parameters.

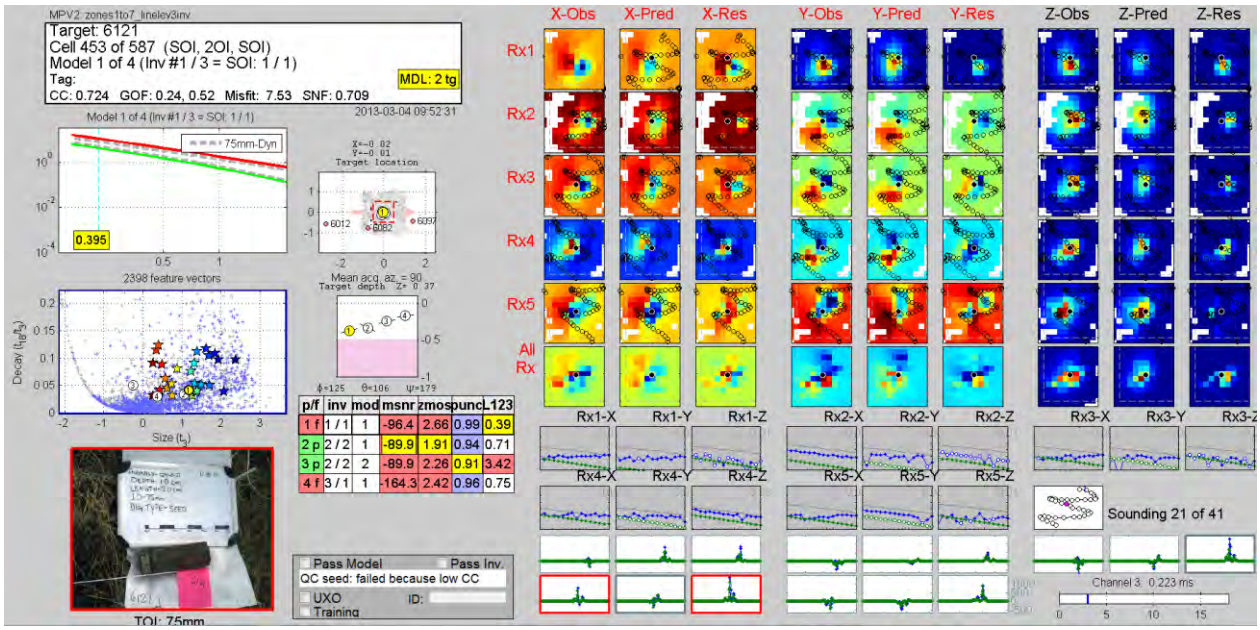

p/f	inv	mod	msnr	zmos	punc	L123
1 f	1 / 1	1	-96.4	2.66	0.99	0.39
2 p	2 / 2	1	-89.9	1.91	0.94	0.71
3 p	2 / 2	2	-89.9	2.26	0.91	3.42
4 f	3 / 1	1	-164.3	2.42	0.96	0.75

Figure 43: Inversion and classification parameters for target GW-6121.

The first model stemming from a single target inversion was failed because the fit was not optimal (first line in table), although its derived target parameters most resemble a 75 mm projectile (see Figure 44, top left, best match to 75 mm). The two-source inversion yields a better fit but its derived parameters require a more lax L1L2 threshold to be matched to a TOI.

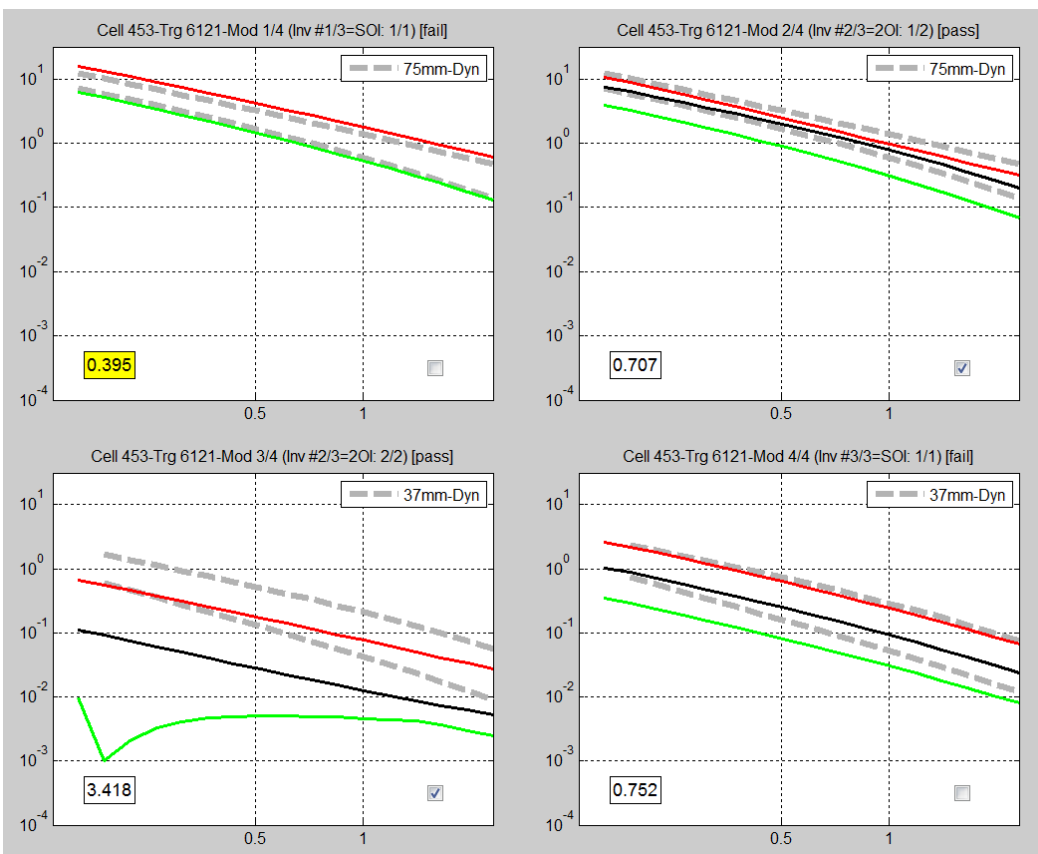

Figure 44: Model parameters for GW-6121.

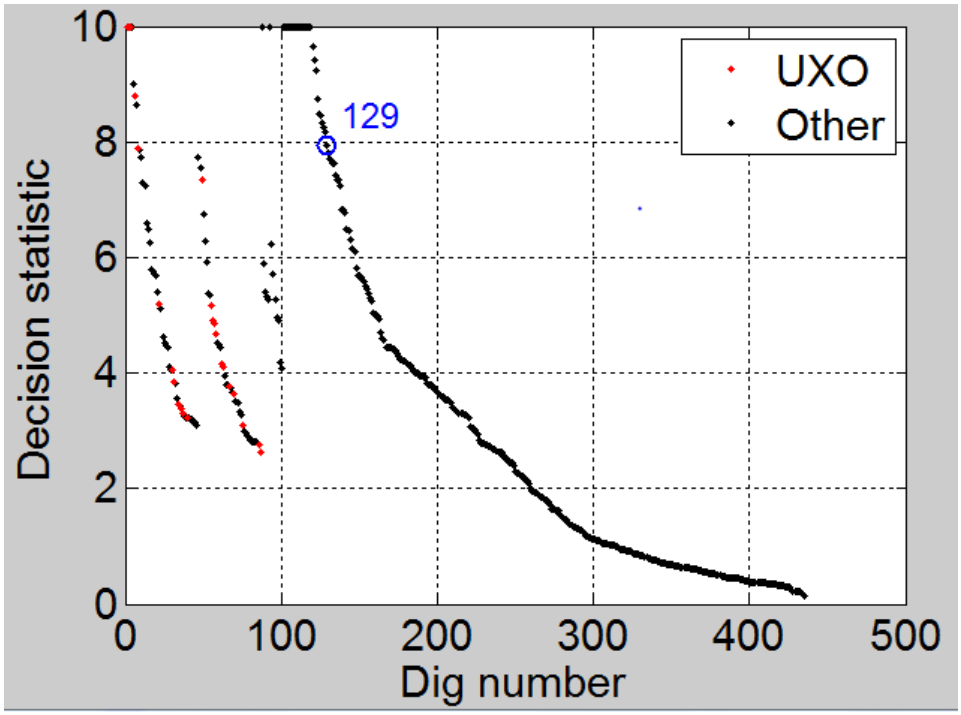

Figure 45: Decision statistic for dynamic stage 2.

Appendix E: Classification with cued interrogation data

The following is a write up from the analyst who applied classification to the cued data. The analyst had extensive experience at classification though no direct experience with MPV data. The data had already been inverted and verified by another geophysicist and the PI in order to prepare a list of target locations for ground validation by the excavation crew.

1. Background

The MPV cued dataset consisted of three sets of single and two object inversions using three unique methods for positioning:

1. Geographic coordinates inferred from beacon
2. Geographic coordinates inferred from RTK GPS
3. Slope corrected geographic coordinates inferred from beacon (in horizontal plane)

Careful attention was required to achieve accurate positioning at the George West site because of the significant slope on which the survey data was acquired. Inversion results were verified and valid models were selected prior to delivery to the analyst for classification. One of the focuses of model selection was ensuring that for closely spaced targets, only models corresponding to the intended centered target were passed and models fitting nearby adjacent targets were failed.

2. Training Data Selection

A large library of 19 reference polarizabilities obtained from data collected at previous sites was the starting point for training data selection. The library contained 7 ordnance families as shown in table 1. Some items had multiple entries representing small variations in the response due to target orientation or target type (e.g. 37 mm with and without rotating band, etc).

Table 6: Targets included in the initial reference library.

Target type	Number of variations in library
155mm	1
105mm	4
75mm	4
Medium ISO	1
60mm	2
Small ISO	2
37mm	5

The BTG *QCZilla* software was used to search for polarizabilities within the dataset that matched the items in the reference library. No matches were found to either of the larger two items (155mm and 105mm) and those items were therefore removed from the reference library to be used at Camp George West. There were multiple excellent matches to the 75mm reference

item. All polarizabilities identified by the QC tool as matching the user specified misfit threshold for the 75mm are shown in Figure 46. Three different targets matching the 75mm polarizabilities were chosen for training data. One excellent match to the reference polarizabilities as well as two targets that produced deeper recovered models and slightly worse matches to the reference 75mm were selected for training data. All three were confirmed to be 75mm as illustrated in Figure 46.

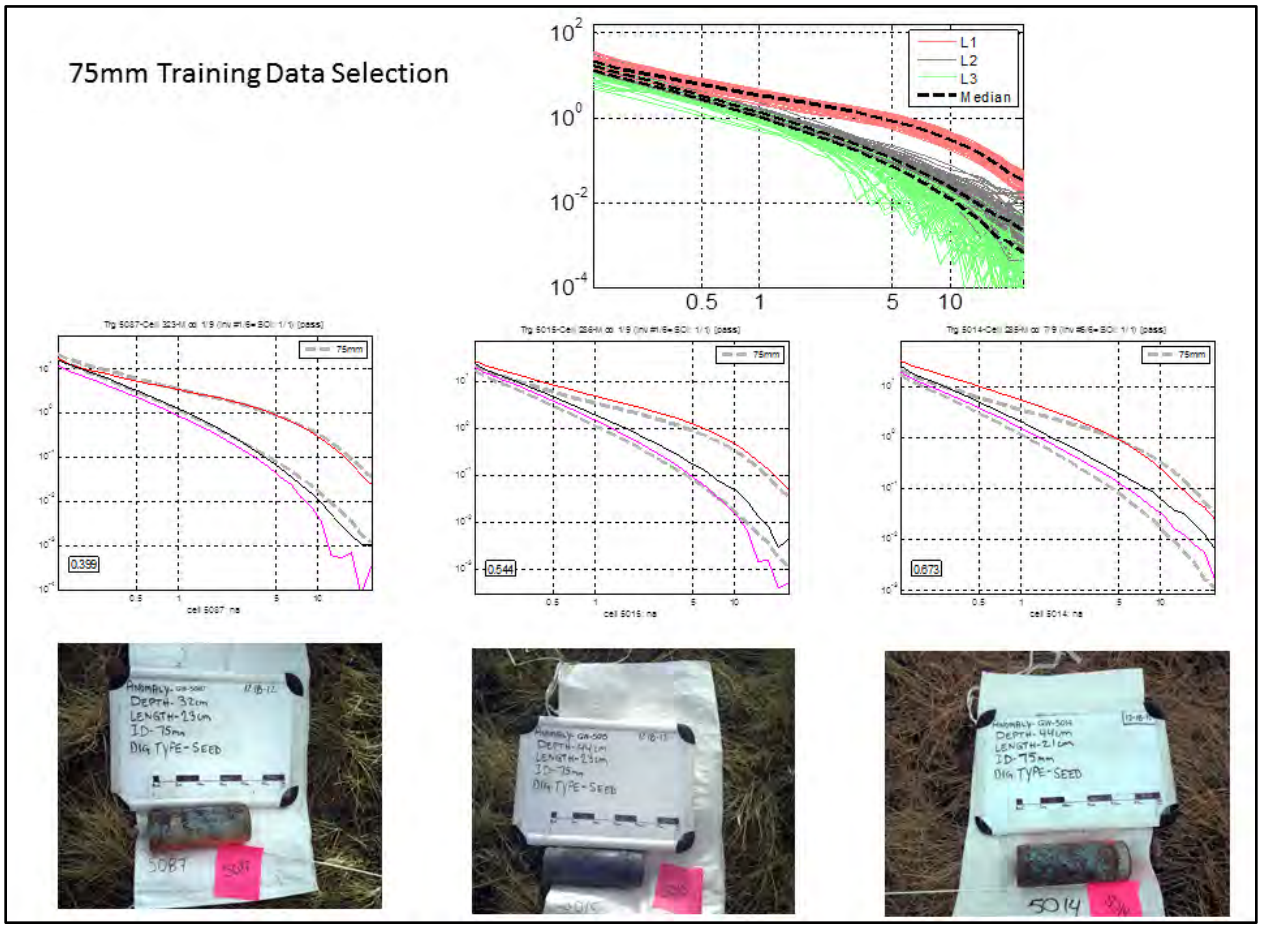

Figure 46: Cued data classification - Training data requests for potential 75mm projectiles. Top plot shows all polarizabilities matching the reference 75mm projectile. Middle 3 plots show polarizabilities for 3 training data requests and the reference library polarizability (grey dashed line) . The bottom row of 3 photos indicate all 3 items were confirmed as 75mm projectiles.

The other item which appeared to have multiple high quality matches to the reference library polarizabilities was the medium ISO. Figure 47 shows all models which were identified as matching the reference item. One of these items was requested in the training data request and was confirmed to be a medium ISO and was therefore retained in the reference library.

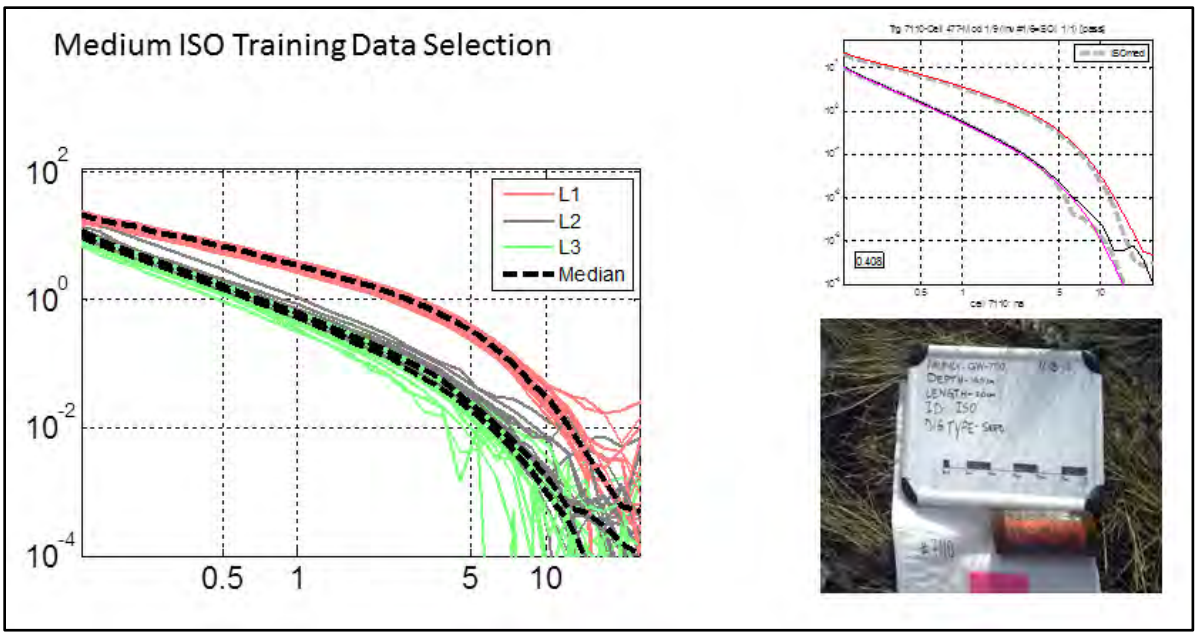

Figure 47: Cued data classification - Training data requests for potential medium ISOs. Plot on left shows all polarizabilities matching the reference medium ISO. The top plot on the right shows polarizabilities for a training data request and the bottom right photo confirms a medium ISO.

Identifying matches to smaller items in the reference library (60mm, 37mm, small ISO) did not result in any additional confirmed TOIs in spite of aggressive attempts. There were not nearly as many matches to the smaller reference library items as observed for the 75mm projectile and the medium ISO even as the user defined misfit values for these smaller items were relaxed. For example, the results in searching for polarizability matches to the reference library 60mm mortar are shown in Figure 48. Of the eleven identified models, three were confirmed to have excellent matches to two of the confirmed TOIs (either 75mm projectile or medium ISO) and therefore not requested as training data. Of the remaining four items, three were requested as training data, all three of these were confirmed to be non TOI. This analysis led to the decision to remove the 60mm mortar from the reference library. Similar aggressive searches for matches to 37mm and small ISO items in the reference library were also unsuccessful in discovering confirmed TOI via training data requests. These items were similarly removed from the reference library.

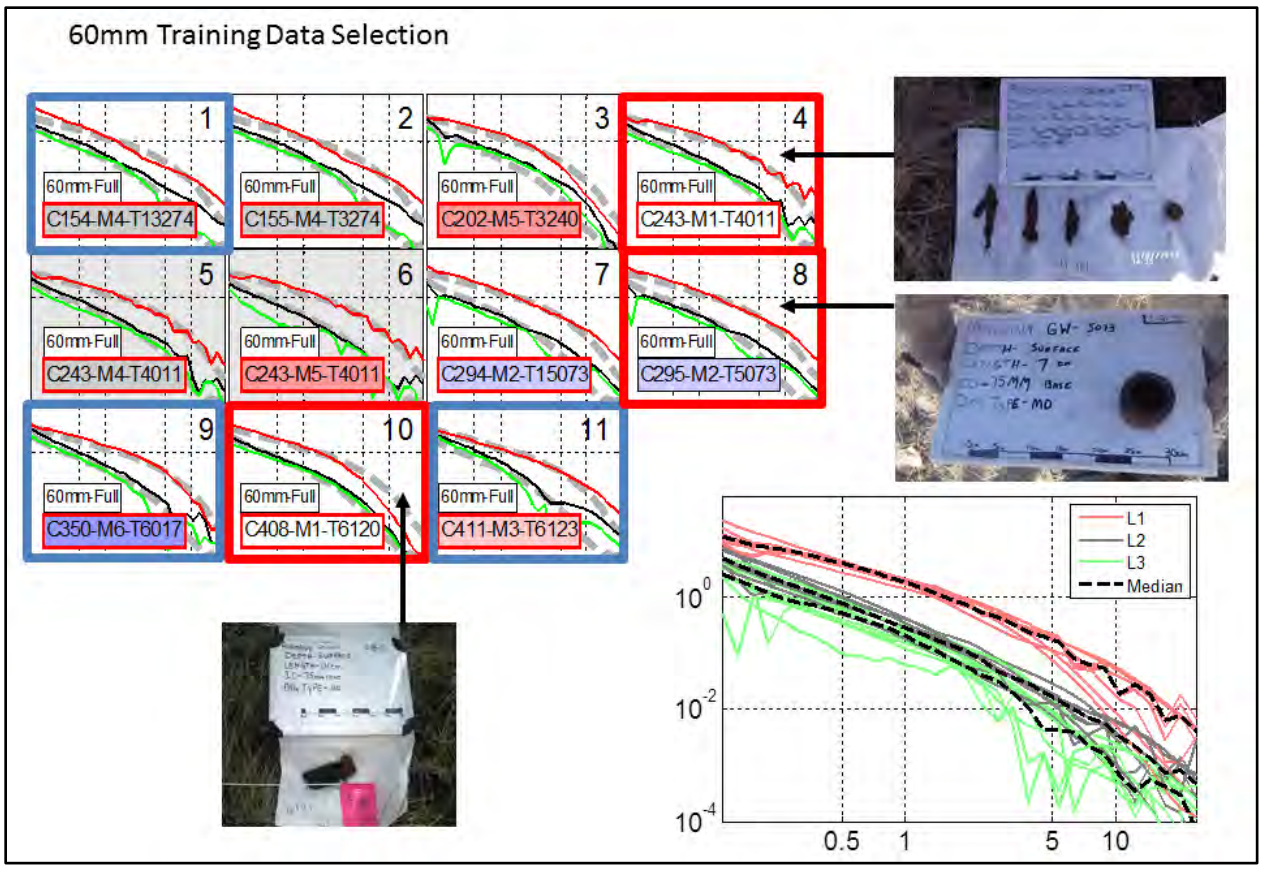

Figure 48: Cued data classification - Training data requests for potential 60mm mortar. Plot on bottom right shows all polarizabilities matching the reference 60mm. The plot in the upper left shows all polarizabilities matching the user defined misfit to the reference 60mm. Polarizabilities chosen for training data requests are outlined in red and accompanying groundtruth photos indicate items are not 60mm mortars. The models outlined in blue indicate that those targets had an alternate model which was an excellent match to items retained in the reference library (either a 75mm projectile or medium ISO).

3. Self-Similar Polarizabilities

Having eliminated items from the reference library that do not match any of the recovered polarizabilities in the dataset, we next want to ensure that there are no TOI at the site which are outside of the reference library and add any new TOI found to the library. To search for these items, we perform cluster analysis in the size-decay feature space, looking for self-similar polarizabilities. This was done using the BTG *TrainZilla* software: the user can draw a polygon in feature space and specify misfit parameters that will be used to look for self-similar polarizabilities within the defined polygon. Figure 49 shows an example for an unknown cluster of targets which was determined to be non-TOI (pusher plates) via training data requests. The full feature space was examined for clusters of self-similar polarizabilities representing new TOI classes but none were identified. Training data requests were also made for a few one-off axi-symmetric targets, none of which turned out to be TOI.

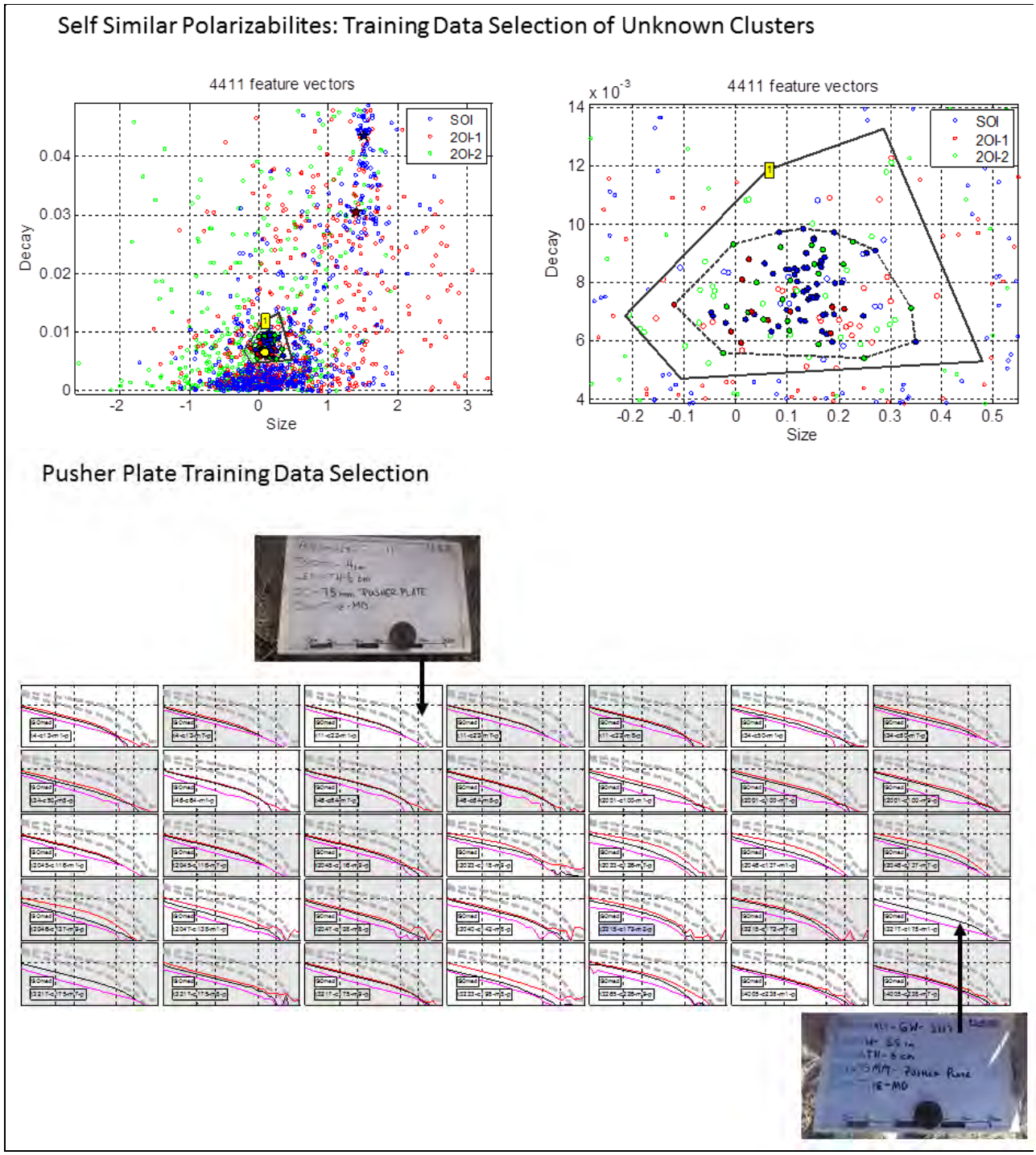

Figure 49: Training data requests for an unknown cluster.
Plot on upper left shows size decay feature space and user defined polygon surrounding a visually identified cluster that does not correspond to any items in reference library. Upper right plot shows a zoomed-in view of that same feature space. The bottom plot shows all of the self-similar polarizabilities identified in the polygon. Many small, plate-like polarizabilities were observed. Multiple targets were chosen for training data requests and all were identified as non-TOI pusher plates, identifying the target dominating the cluster.

4. Dig List Generation

A total of 27 items were requested for training data. Of those items, only 75mm and medium ISO were identified as TOI. Training data also revealed partial 75mm items that were classified as TOI. In both cases, the recovered polarizabilities of the partial 75mm items had at least 1 model which was still a reasonably good match to the intact 75mm reference library items (see Figure 50). The existence of partial 75mm was important when producing the dig list as they produce slightly worse fits to the reference model. Because aggressive searching for smaller TOI did not reveal any targets, the decision was made to proceed with classification using a reference library comprised of only the 75mm projectile and the medium ISO.

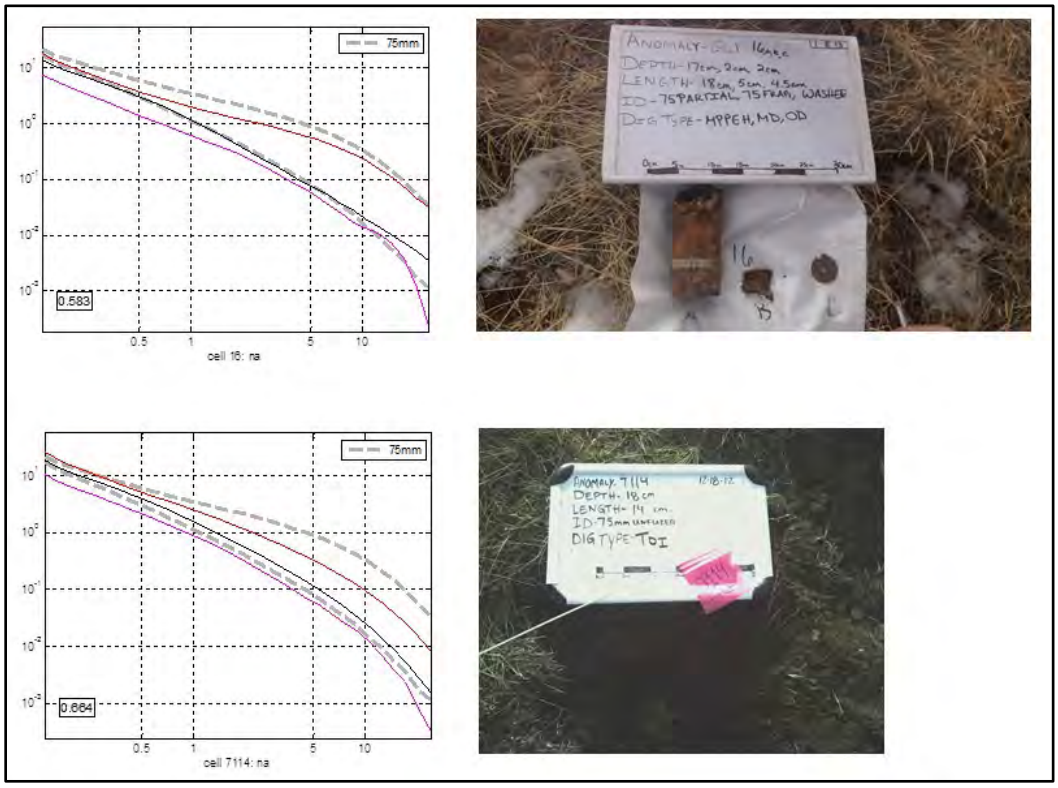

Figure 50: Analysis of training data requests revealed two partial 75mm TOI. Both items produced at least one model that was a reasonable match to the 75mm library reference.

A dig list was generated using 3 stages:

1. Rank targets based on a misfit of all 3 polarizabilities over all time channels
2. Rank targets based on a misfit of all 3 polarizabilities using only time channels 1:23 (0.1 ms to 5.23 ms).
3. Rank targets based on L1 polarizability.

The polarizabilities used to rank the dig list are illustrated in Figure 51 which shows the boundaries between the three stages (blue background on dig number in upper right corner). Because the reference library consisted of only 2 relatively large items (75mm projectile and medium ISO), Stage 1 was used to identify large items that have excellent agreement with the reference library. Training data indicated that these relatively large items produced well recovered polarizabilities out to late times. Reviewing the ranking of these targets based on stage

1, it was determined visually that after 69 digs, the matches to the library items had fallen off beyond likely TOI (this point was selected somewhat conservatively because of the training data results observed for partial 75mm TOI in Figure 50). Stage 2 was chosen based on training data results that indicated some of the deeper targets had difficulty constraining the polarizabilities at times later than 5ms. This identified 3 additional items (digs 70-72) that produced very good matches to the reference library. After these three additional digs, the match to reference items was significantly worse so at dig 73 ranking was switched to stage 3 using the L1 polarizability. Note the drop off in quality of polarizability matches starting at stage 3 (beginning at dig 73). Objects tend to be plate-like and are immediately a poor match to the two items in the reference library. As a result, the stop dig point was set at the end of stage 2 (dig 72).

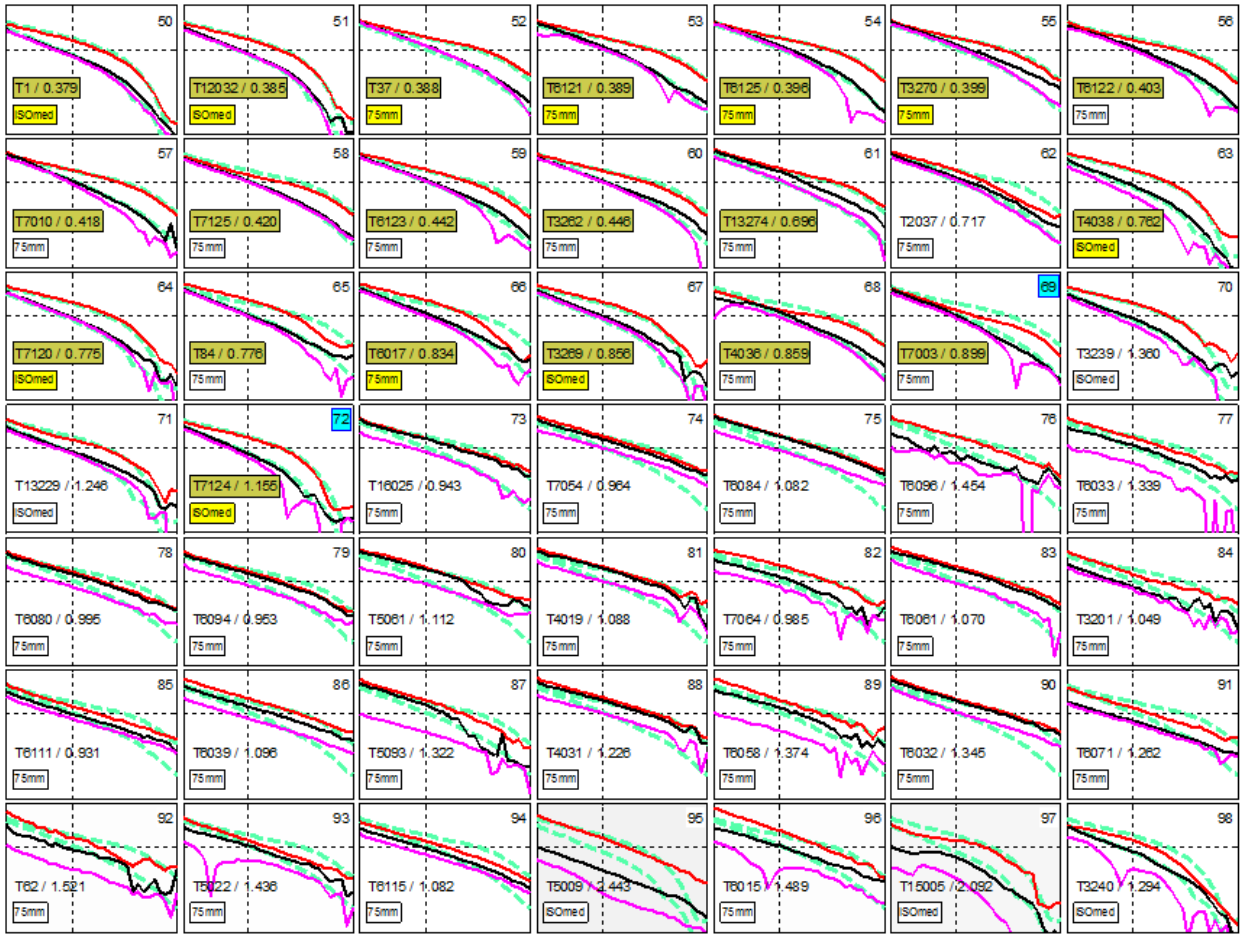

Figure 51: Polarizability decay curves in ranked dig list for digs 50-98.
Stage 1 using all 3 polarizabilities over all time channels is used to rank digs up to dig 69; stage 2 uses all 3 polarizabilities over time channels 1:23 to ranks digs 70-72 and stage 3 ranks the remaining digs using main polarizability (L1). Stop dig point was set at dig 72, where a large drop off in polarizability fits is observed.

5. Partial and Final ROC Curves

Ground truth results up to the stop dig point were provided along with the partial ROC curve shown in the top panel of Figure 52. No new TOI were identified from review of the partial ground truth results. This, in conjunction with the aggressive search for additional TOI in the training data requests led to the decision to not make further changes to the submitted dig list.

Final scoring for the complete dataset is shown in the bottom panel of Figure 52. Only one non-TOI was excavated after training. All TOI for the site were identified in the first 72 digs leading to an 85% reduction in the total number of digs and a 93% reduction in the number of unnecessary digs.

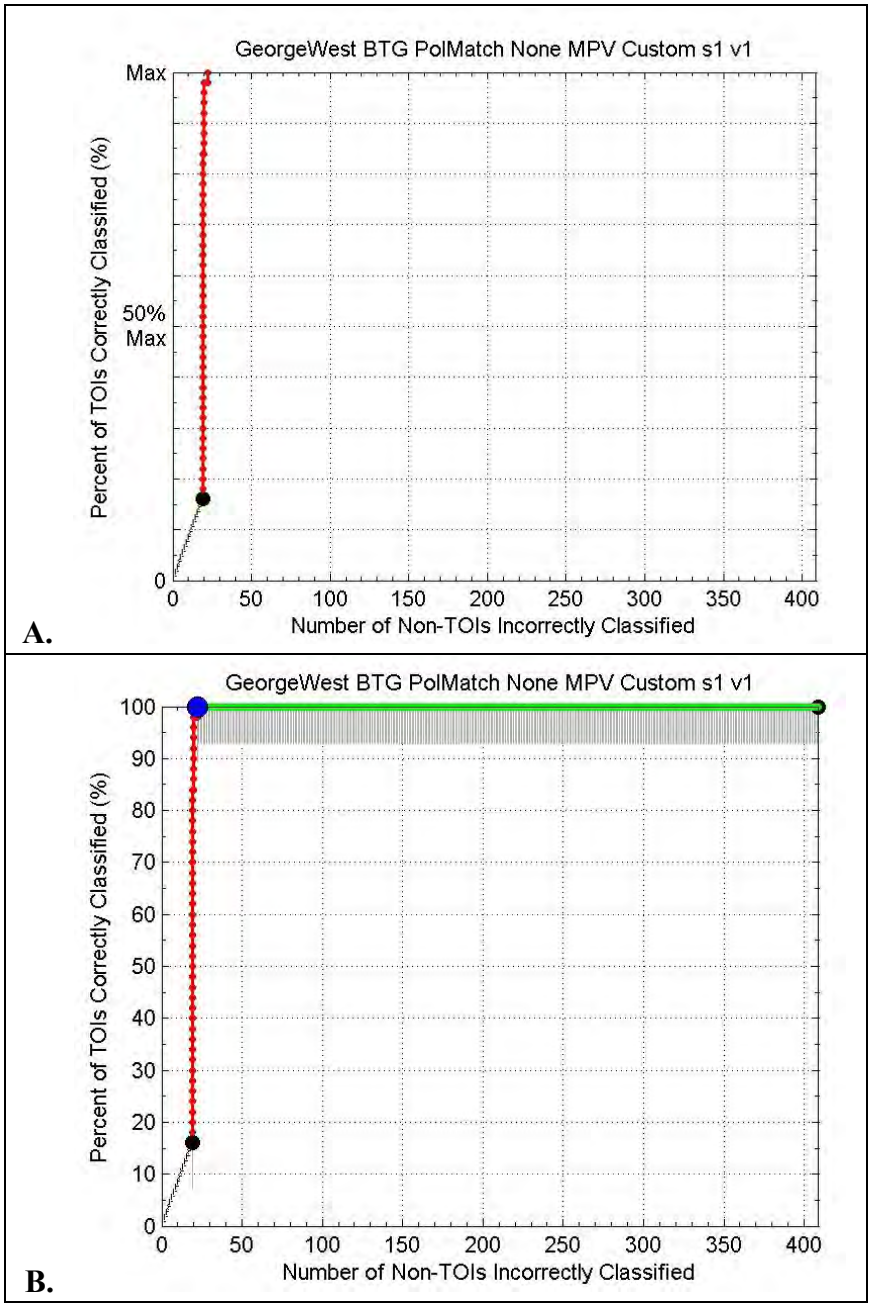

Figure 52: Partial (A) and final (B) ROC curve for classification with cued data.